

PROCESSING, MECHANICAL, AND ENVIRONMENTAL  
PERFORMANCE OF ENGINEERING POLYMER  
WOOD-PLASTIC COMPOSITES

By

MARK CHRISTOPHER HATCH

A dissertation completed in partial fulfillment of  
the requirements for the degree of

MASTER OF SCIENCE IN CIVIL ENGINEERING

WASHINGTON STATE UNIVERSITY  
Department of Civil and Environmental Engineering

AUGUST 2008

To the Faculty of Washington State University:

The members of the Committee appointed to examine the thesis of MARK CHRISTOPHER HATCH find it satisfactory and recommend that it be accepted.

---

Chair

---

---

## ACKNOWLEDGEMENTS

I would like to thank the faculty and staff of WSU for your assistance and support the last two years. Special thanks to my advisor and committee chair Dr. Michael Wolcott for the constructive input and support. There are so many people at the Wood Materials and Engineering Laboratory to thank, but I will try to give as much credit as possible. To Dr. Don Bender thanks for providing me the opportunity to come to WSU and work in a world class laboratory devoted to structural engineering utilizing wood and timber. I would not have been able to complete this thesis without the technical assistance of wood lab personnel such as Bob Duncan, Scott Lewis, Brent Olson, Dr. Long Jiang, and Dr. Karl Englund. Thanks also to Judy Edmister, Pat Smith, and Janet Duncan for answering administrative questions and going the extra mile to ensure that project needs were met. A very special sign of appreciation goes out to my loving wife Michaela, who has been their side by side with me and an inspiration the last two years.

PROCESSING, MECHANICAL, AND ENVIRONMENTAL  
PERFORMANCE OF ENGINEERING POLYMER  
WOOD-PLASTIC COMPOSITES

Abstract

by Mark Christopher Hatch, M.S.  
Washington State University  
August 2008

Chair: Michael P. Wolcott

Interest in expanding the scope of wood-plastic composites (WPCs) to structural applications has extended current composites containing polypropylene (PP), polyethylene (PE), and polyvinylchloride (PVC) to their mechanical limits. This study examines new, innovative WPCs composed of two engineering thermoplastics, nylon 12 and thermoplastic epoxy resin (TPER), which are superior to PP, PVC and PE in mechanical strength and stiffness. Our evaluation of TPER and nylon 12 WPCs included: 1) development of an extrusion processing methodology, 2) mechanical characterization and modeling of the elastic modulus with respect to formulation design, and 3) assessment of moisture and temperature impact on performance. We also developed a model based on shear-lag theory to accurately predict the stiffness of WPCs. Preliminary mechanical properties of nylon 12 and TPER WPCs indicate excellent potential for structural applications; due in part to their reduced moisture absorption and superior strength and stiffness compared to traditional high density PE composites.

# TABLE OF CONTENTS

	page
ACKNOWLEDGEMENTS.....	iii
ABSTRACT.....	iv
TABLE OF CONTENTS.....	v
LIST OF TABLES.....	x
LIST OF FIGURES.....	xii
CHAPTER 1 – INTRODUCTION.....	1
1.1 Background.....	1
1.2 Incentive.....	2
1.3 Research Development.....	2
1.4 Objectives.....	4
1.5 References.....	4
CHAPTER 2 - PROCESSING OF ENGINEERING POLYMER WOOD PLASTIC COMPOSITES: THERMOPLASTIC EPOXY RESIN (TPER) AND NYLON 12.....	7
2.1 Abstract.....	7
2.2 Introduction.....	7
2.3 Materials and Methods.....	9
2.3.1 <i>Material</i> .....	9
2.3.2 <i>Torque Rheometry</i> .....	10
2.3.3 <i>Extrusion</i> .....	10
2.3.4 <i>Injection Molding</i> .....	11
2.3.5 <i>Mechanical Testing</i> .....	12



3.4.3 <i>Moisture Content and Mechanical Properties</i> .....	35
3.5 Conclusions.....	37
3.6 Acknowledgements.....	38
3.7 References.....	38
3.8 Tables.....	40
3.9 Figures.....	41
 CHAPTER 4 – APPLICATION OF ELASTICITY SHEAR-LAG MODELS TO WOOD- PLASTIC COMPOSITES.....	
4.1 Abstract.....	46
4.2 Introduction.....	46
4.3 Analytical Models.....	47
4.3.1 <i>Cox Shear Lag Model (CSLM)</i> .....	47
4.3.2 <i>Previous Refinements for Applying CSLM to WPC</i> .....	49
4.3.3 <i>Double Shear Lag (DSL) Model</i> .....	50
4.3.4 <i>Modulus Fiber Orientation Modification</i> .....	53
4.4 Experimental Material and Methods.....	54
4.4.1 <i>Experimental Materials</i> .....	54
4.4.2 <i>Methods</i> .....	55
4.5 Results and Discussion.....	56
4.6 Conclusions.....	59
4.7 References.....	60
4.8 Tables.....	62
4.9 Figures.....	63

CHAPTER 5 – CONCLUSIONS AND FUTURE WORK.....	71
5.1 Conclusions.....	71
5.2 Future Work.....	73
APPENDIX A – PROCESSING INFLUENCES ON THERMAL DEGRADATION OF EXTRUDED NYLON 12 COMPOSITES.....	75
A.1 Introduction.....	75
A.2 Materials and Methods.....	76
A.3 Results and Discussion.....	76
A.4 Conclusions.....	78
A.5 References.....	79
A.6 Tables.....	79
A.7 Figures.....	80
APPENDIX B –POST EXTRUSION COOLING OF NYLON 12 COMPOSITES.....	81
B.1 Introduction.....	81
B.2 Materials and Methods.....	81
B.3 Results and Discussion.....	82
B.4 Conclusions.....	82
B.5 References.....	82
B.6 Tables.....	83
B.7 Figures.....	83
APPENDIX C – DYNAMIC MECHANICAL ANALYSIS (DMA) OF THERMOPLASTIC EPOXY RESIN (TPER) COMPOSITES.....	84
C.1 Introduction.....	84

C.2 Materials and Methods.....	84
C.3 Results and Discussion.....	85
C.4 Conclusions.....	85
C.5 References.....	85
C.6 Figures.....	86
APPENDIX D – PHASE TRANSITION BEHAVIOR OF NYLON 12 COMPOSITES.....	88
D.1 Introduction.....	88
D.2 Materials and Methods.....	88
D.3 Results and Discussion.....	88
D.4 Conclusions.....	89
D.5 References.....	89
D.6 Tables.....	89
D.7 Figures.....	90
APPENDIX E – DERIVATION OF DOUBLE SHEAR LAG (DSL) MODEL.....	91
D.1 Derivation.....	91
D.2 References.....	95

## LIST OF TABLES

Table 2.1 Mechanical properties, density, and processing melt pressures of extruded TPER/WF and nylon 12/WF composite formulations at various die temperatures and lubricant contents...	20
Table 2.2 Extrusion temperature profile for a TPER/WF and nylon 12/WF composites.....	20
Table 2.3 Mechanical properties, density, and processing melt pressures of TPER/WF and nylon 12/WF composites at various initial wood fiber moisture contents (MC).....	21
Table 2.4 Mechanical properties, density, and processing melt pressures of extruded TPER/WF and nylon 12/WF composites at various wood fiber loadings.....	21
Table 2.5 Mechanical properties and density of injection molded TPER/WF and nylon 12/WF composites at various wood fiber loadings.....	22
Table 3.1 Formulation for each WPC polymer system.....	40
Table 3.2 Extrusion profile for each WPC polymer system.....	40
Table 4.1 Data input for shear-lag models.....	62
Table 4.2 DSL model ( $\theta = 12.5^\circ$ ) error for TPER, Nylon 12, and HDPE WPCs.....	62
Table A.1 Mechanical properties, density, and processing melt pressures of extruded nylon 12/WF formulations at 10 rpms, 20 rpms, and with pre-processed wood flour.....	79
Table B.1 Mechanical properties and density of extruded nylon 12/WF formulations at various distances from extruder die exit to cooling chamber.....	83

Table D.1 Thermal Properties of nylon 12 and nylon 12/WF composites. Heat is measured in J/g  
of nylon 12.....89

## LIST OF FIGURES

Figure 2.1 Primary chemical structure of TPER (Top) and nylon 12 (Bottom) polymers (TPER adapted from Constantin et al., 2004).....	23
Figure 2.2 Variation of torque with respect to time of 40% TPER/ 60% WF and 40% nylon 12/ 60% WF composites (no lube) at various chamber temperatures.....	24
Figure 2.3 MOR and density of TPER/WF and nylon 12/WF composites at various extrusion die temperatures.....	24
Figure 2.4 Variation of torque with respect to time of various formulations of 37-40% TPER/ 60% WF and 37-40% nylon 12/ 60% WF.....	25
Figure 2.5 Extruded TPER/WF composites containing 2% OPE629A, 1% OPE629A, and 3% WP2200 from left to right, respectively.....	25
Figure 2.6 Flexural modulus of elasticity (MOE) of TPER/WF and nylon 12/WF composites with various wood flour contents .....	26
Figure 2.7 Strain to failure of TPER/WF and nylon 12/WF composites with various wood flour contents .....	26
Figure 2.8 Flexural modulus of rupture (MOR) of TPER/WF and nylon 12/WF composites with various wood flour contents.....	27
Figure 2.9 Stress-strain curves for injection molded TPER, nylon 12, and HDPE WF composites with 40% wood fiber. (HDPE curve adapted from Gacitua, 2008).....	27
Figure 2.10 Density of TPER/WF and nylon 12/WF composites with various wood flour contents.....	28

Figure 3.1 Modulus of rupture (MOR) of WPCs at various temperatures.....	41
Figure 3.2 Strain to failure of WPCs at various temperatures.....	42
Figure 3.3 Temperature modification factor, $C_t$ , from ambient (21.1°C) for MOR ( $C_{t,R}$ ) and MOE ( $C_{t,E}$ ) of WPCs.....	43
Figure 3.4 Moisture absorption and volumetric strain of WPCs from 0 to 121 days of water soaking.....	44
Figure 3.5 Moisture content vs. volumetric strain of WPCs from 0 to 121 days of water soaking.....	44
Figure 3.6 Moisture Content modification factor, $C_m$ , for MOR ( $C_{m,R}$ ) and MOE ( $C_{m,E}$ ) of WPCs.....	45
Figure 4.1 Cylindrical fiber embedded in polymer matrix with tension stress applied to the polymer matrix @ $x = L/2$ (fiber end) according to a) Cox Shear Lag Theory (Cox, 1952) and b) Double Shear Lag (DSL) model.....	63
Figure 4.2 Scanning electron microscope (SEM) image of TPER WPC.....	64
Figure 4.3 Comparison of MOE vs. fiber volume fraction for injection molded TPER and nylon 12 WPCs using shear lag and DSL models (Data adapted from Hatch, 2008).....	65
Figure 4.4 Comparison of predicted MOE vs. fiber volume fraction for compression molded 20 mesh oak WF/ HDPE and 40 mesh oak WF/HDPE using DSL and shear lag models (Data adapted from Facca, 2006).....	66
Figure 4.5 DSL model ( $\theta = 12.5^\circ$ ) curve predictions for varying fiber aspect ratios ( $L/R_o$ ) from 6 to $\infty$ for nylon 12 and TPER WPCs (Data adapted from Hatch, 2008).....	67

Figure 4.6 DSL model ( $\theta = 12.5^\circ$ ) curve predictions for varying fiber bulk specific gravities ( $G_B$ ) from 0.3 to 0.7 for nylon 12 and TPER WPCs (Data adapted from Hatch, 2008).....	68
Figure 4.7 DSL model ( $\theta = 12.5^\circ$ ) curve predictions for varying matrix moduli ( $E_m$ ) and wood fiber moduli ( $E_f$ ) for TPER WPCs (Data adapted from Hatch, 2008a).....	69
Figure 4.8 DSL model curve predictions for $\theta$ from 0 to $90^\circ$ for nylon 12 and TPER WPCs (Data adapted from Hatch, 2008).....	70
Figure A.1 Thermogravimetric curves for nylon 12/WF components, composite, and prediction curve based on rule of mixtures.....	80
Figure A.2 Thermogravimetric curves for nylon 12/WF composites and prediction curve based on rule of mixtures.....	80
Figure B.1 Flexural modulus of rupture and elasticity, and density of nylon 12/WF composite with delayed cooling after die exit: 0, 7.6, and 15.2 cm.....	83
Figure C.1 Log $E'$ , log $E''$ , and $\tan \delta$ from dynamic mechanical analysis (DMA) of TPER WPCs.....	86
Figure C.2 Log $E'$ , log $E''$ , and $\tan \delta$ from dynamic mechanical analysis (DMA) of TPER WPCs.....	87
Figure D.1 DSC thermograph of cooling for nylon 12 WPCs. Heat is measured in J/g of nylon 12.....	90

Figure D.2 DSC thermograph of second heating for nylon 12 WPCs. Heat is measured in J/g of nylon 12.....90

## **Dedication**

This thesis is dedicated to my wife, parents, and grandparents  
for all their support throughout the years.

# CHAPTER 1 – INTRODUCTION

## 1.1 Background

Many innovative composites have been developed in the last century, but few have the potential of wood/natural fiber-plastic composites (WPCs) to revolutionize a potential 5.85 billion dollar structural material market (Smith and Wolcott, 2006). These composites are rapidly being applied for use in residential decking, and are projected to obtain a 20% decking market share by 2010 (Winandy et al., 2004). This has been fueled by WPCs' benefits in terms of life-cycle costs, reduced maintenance, decay resistance, and environmental friendliness compared to chemically treated timber decking. Projections predict that WPCs will eventually cross over into other commercial structural markets including industrial decking, fencing, and other structural construction components that currently utilize wood, plastic, and in some cases, metal as the primary load resisting system.

WPCs are typically composed of three components, each with specific purposes in the final composite. The primary component of WPCs is a wood or natural fiber filler, which adds stiffness and strength to the composite when processed with a polymer component. Thermoplastic polymer systems commonly used in WPCs are polyethylene (PE), polypropylene (PP), and polyvinylchloride (PVC). These polymers act as a matrix encasing the fiber filler, thus providing stress transfer between fibers and increasing decay resistance. Lubricants are added to increase processability. WPCs for timber replacement products are typically produced through extrusion processing at temperatures over 100°C. This involves dry mixing the components and feeding them into the extruder, where they are melt blended and consolidated. The final step involves extrusion of the material through a die that has been cut to produce the specified shape required for the final WPC application. Other production processes are available (i.e., injection

and compression molding), but only extrusion allows for continuous production, given that the required cross section is two-dimensional.

## **1.2 Incentive**

Currently, WPCs consisting of PE, PP, and PVC are primarily used in non-structural or low-load applications with little restriction on mechanical properties. However, their decay and moisture resistance may prove beneficial for use in high-strength structural applications. A U.S. Navy report suggests their use in industrial decking and other materials for waterfront facilities (Wolcott et al., 2007). High-strength WPCs also have potential use in sill plates and other connection elements where concrete foundations contact structural wood members in both residential and commercial construction (Duchateau, 2005).

In previous attempts to improve the performance properties of WPCs, composites have been enhanced with chemical agents to improve polymer and wood fiber interaction (Anderson, 2007). However, these chemicals can pose health hazards such as handling and storage problems, and difficulties associated with composite production. To prevent these problems, this study proposes a new high strength engineering polymer system to improve WPC performance.

## **1.3 Research Development**

Two high-strength engineering thermoplastics have been identified as potential candidates for extruded WPCs. The first was poly(hydroxyaminoether), commonly called thermoplastic epoxy resin (TPER). Although it was first developed in the early 1950's as a branch of thermosetting technology, its barrier, coating, paint-ability, and thermoplastic properties propelled it into such markets as packaging and auto parts in the 1990s (White et al., 2000; Chmielewski, 2008; Constantin et al., 2004). A preliminary study by White et al. (2000)

on compression-molded TPER WPCs showed that at roughly 30% wood fiber tension, capacity improved from 43 MPa to approximately 75 MPa. The hydrophilic nature of wood fiber and TPER was found to facilitate adhesion between the two components.

Another group of thermoplastic engineering polymers, polyamides (nylon 6, 6-6, 10, and 12), have been investigated for use in WPCs, but high melt temperatures at or above degradation temperatures of wood/natural fiber fillers have limited investigation into extrusion processing of these composites (Klason et al., 1984). Therefore, research has focused on nylon 12 ( $T_m$ : 178°C), due to its lower melt temperature (Lu et al., 2007). While not as prevalent as nylon 6, nylon 12 has been utilized for moisture-sensitive products such as packaging, food processing, clothing, marine products, and piping because of its lower sorption rate. It also bonds well with wood, which improves its strength and stiffness (Klason et al., 1984; Lu et al., 2007). Nylons in general are known for their toughness, strength, scratch and wear resistance.

In 1952, Cox developed one of the first mechanics-based models to predict stiffness of composite systems for the paper industry. Cox's shear-lag theory and its application has been modified throughout literature for use in geology, paper, WPCs, and carbon fiber composites (Zhao, 1997; Nairn, 1997; Facca, 2006; Nardon & Prewo, 1986). Facca (2006) proposed two modifications for use with WPCs, adjusting the fiber modulus based on cell wall density to bulk fiber density, as well as the pre-processed moisture content of the wood fiber. However, Facca's results suggested that further modification to the model was necessary for accurate prediction of WPC stiffness.

A common feature of engineering WPCs is mechanical performance sensitivity to temperature and moisture changes (Marcovich et al., 1997; Huang et al., 2006; Stark, 2001, Schildmeyer, 2006; Anderson, 2007). Similar behavior is expected for nylon 12 and TPER

WPCs, although specific magnitudes are expected to vary significantly. Moisture sensitivity is a primary concern in TPER WPCs due to their hydrophilic nature, which could increase moisture absorption of the composite. For applications that are sensitive to outdoor temperature and moisture fluctuations, performance expectations must be adjusted to reduce the likelihood of WPC failure (Schildmeyer, 2006).

#### **1.4 Objectives**

Although previous studies have addressed nylon 12 and TPER WPCs, no research has been published to date that adequately analyzes extruded composites for these polymer systems. The primary goal of this research is to evaluate processing and mechanical performance of nylon 12 and TPER WPCs. Specific objectives are outlined below:

- 1) Develop extrusion processing profile recommendations for nylon 12 and TPER WPCs.
- 2) Evaluate WPC formulations with varying fractions of polymer, wood flour, and lubricant to characterize mechanical performance.
- 3) Apply shear-lag theory to accurately model the stiffness behavior of WPCs.
- 4) Examine temperature influences on the mechanical properties of extruded nylon 12 and TPER WPCs.
- 5) Determine the moisture absorption rate and mechanical performance of nylon 12 and TPER WPCs subjected to wet environments.

#### **1.5 References**

Anderson, S., "Wood Fiber Reinforced Bacterial Biocomposites: Effects of Interfacial Modifiers and Processing on Mechanical and Physical Properties." Master's Thesis, Washington State Univ., Pullman, WA, Dec. 2007.

- Chmielewski, C., Personal Communication. 06 March, 2008.
- Constantin, F., Fenouillot, F., Pascault, J., Williams, R. J., "Post-Crosslinkable Blends: Reactions Between a Linear Poly(hydroxyl-amino ether) and a Diepoxy." *Macromolecular Materials Engineering*, Vol. 289, pp. 1027-1032, 2004.
- Cox, H.L., "The elasticity and strength of paper and other fibrous materials." *British Journal of Applied Physics*, Vol. 3, pp. 72-79, 1952.
- Duchateau, K. A., "Structural Design and Performance of Composite Wall-Foundation Connector Elements". Master's Thesis, Washington State Univ., Pullman, WA, 2005.
- Facca, A.G., Kortschot, M.T., Yan, N. "Predicting the Elastic Modulus of Natural Fibre Reinforced Thermoplastics." *Composites Part A*, Vol. 37, pp. 1660-1671, 2006.
- Huang, S.H., Cortes, P., Cantwell, W.J., "The influence of moisture on the mechanical properties of wood polymer composites." *Journal of Material Science*, Vol. 41, pp. 5386-5390, 2006.
- Klason, C., Kubat, J., Stromvall, H. E., "The Efficiency of Cellulosic Fillers in Common Thermoplastics. Part 1. Filling without Processing Aids or Coupling Agents." *International Journal of Polymeric Materials*, Vol. 10, Issue 3, pp. 159-187, 1984.
- Lu, J.Z., Doyle, T.W., Li, K., "Preparation and Characterization of Wood-(Nylon 12) Composites." *Journal of Applied Polymer Science*, Vol. 103, 270-276, 2007.
- Marcovich, N. E., Reboredo, M. M., Aranguren, M. I., "Dependence of the Mechanical Properties of Woodflour-Polymer Composites on the Moisture Content." *Journal of Applied Polymer Science*, Vol. 68, pp. 2069-2076, 1998.
- Nairn, J.A., "On the use of shear-lag methods for analysis of stress transfer in unidirectional composites." *Mechanics of Materials*, Vol. 26, pp.63-80, 1997.
- Nardone, V.C., Prewo, K.M., "The Strength of Discontinuous Silicon Carbide Reinforced Aluminum Composites." *Scripta Metallurgica*, Vol. 20, pp. 43-48, 1986.
- Schildmeyer, A.J., "Temperature and Time Dependent Behaviors of a Wood-Polypropylene Composite. Master's Thesis, Washington State Univ., Pullman, WA, 2006.
- Smith, P.M., Wolcott, M.P., "Opportunities for Wood/Natural Fiber-Plastic Composites in Residential and Industrial Applications." *Forest Products Journal*, Vol. 56, Issue 3, pp. 4-11, March 2006.
- Stark, N., "Influence of Moisture Absorption on Mechanical Properties of Wood Flour-Polypropylene Composites." *Journal of Thermoplastic Composite Materials*, Vol. 14, 2001.

- Windandy, J.E., Stark, N.M., Clemons, C.M., "Considerations in Recycling of Wood-Plastic Composites." 5<sup>th</sup> Global Wood and Natural Fibre Composites Symposium, Kassel, Germany, April 27-28, 2004.
- White, J. E., Silvis, H. C., Winkler, M.S., Glass, T. W., Kirkpatrick, D. E., "Poly(hydroxyaminoethers): A New Family of Epoxy-Based Thermoplastics". Journal of Advanced Materials, Vol.12, No. 23, pp. 1791-1800, 2000.
- Wolcott, M. P., Pierre-Laborie, M., Smith, P., Damohapatra, S., McDonald, A., Yang, H., Chowdhury, S., Yadama, V., McGraw, D., Smith, T. Navy Report. "Durable Wood Composites for Naval Low-Rise Buildings." Jan. 2007.
- Zhao, P., Ji, S., "Refinements of shear-lag model and its applications." Tectonophysics, Vol. 279, pp 37-53, 1997.

**CHAPTER 2 -  
PROCESSING OF ENGINEERING POLYMER WOOD  
PLASTIC COMPOSITES: THERMOPLASTIC  
EPOXY RESIN (TPER) AND NYLON 12**

**2.1 Abstract**

Natural fiber composites are commonly used in residential decking, siding, and fencing applications, but their use in high-load structural applications has been limited by their low strength performance. However, wood-plastic composites (WPCs) consisting of nylon 12 and thermoplastic epoxy resin (TPER) exhibit excellent mechanical performance. This study evaluated the extrusion parameters for each composite including: barrel/die temperature profile, lubricant compatibility, wood flour (WF) content, and WF moisture content (MC). Increases in strength and modulus of both composites indicated significant adhesion between polymer and wood components. These composites show promise for use in structural applications currently lacking WPC presence.

**2.2 Introduction**

Over the past two decades, wood-plastic composites (WPCs) have become widely accepted as a viable substitution for wood members in non-structural or low-load applications (Smith and Wolcott, 2006; Clemons, 2002). WPCs are commonly used in residential decking, siding, and fencing, which are applications sensitive to decay and moisture damage. The limited strength of existing WPCs has limited their impact on structural materials requiring higher-strength properties, although other applications such as industrial decking and transportation materials could benefit from WPCs natural durability and processing capabilities. However, this would require superior strength performance to traditional WPC systems. Commercial WPCs

currently utilize polypropylene (PP), polyvinylchloride (PVC), and polyethylene (PE) as the base polymer. Previous research has identified two engineering polymers, poly(hydroxyaminoethers) (e.g. thermoplastic epoxy resin, TPER) and nylon 12 (Figure 2.1), as having significant potential in high strength WPCs (White et al., 2000; Lu et. al., 2007).

TPER is commercially used in automotive frames and packaging applications (White et al., 2000; Constantin et al., 2004; Chmielewski, 2008). Analogous to their thermosetting cousins, thermoplastic epoxy resins exhibit vastly improved mechanical characteristics compared to commodity thermoplastics. In addition, intermolecular hydrogen bonding afforded by the TPER structure promotes excellent adhesion gas barrier properties. White et al. (2000) found that compression-molded TPER WPCs increased tension capacity from 43 MPa to 75 MPa with the addition of 30 % wood flour. Unlike many polyolefin WPCs, this was attributed to the adhesion potential of TPER.

Previous research has also identified nylon 12 as having significant potential in WPCs due to its high strength properties, low melt temperature and water sorption rate relative to other nylons. Like TPER, nylon 12 is widely used in many commercial applications such as food processing, packaging, marine products, clothing, tubing, and piping (Lu et. al., 2007). The challenge for commercial use of nylon 12 in WPCs is its relatively high melt temperature (ca. 178°C), which requires processing temperatures over 200°C.

The development of nylon 6 WPCs ( $T_m$ : 215°C) has been widely studied, especially for injection and compression molding processes with both wood and high purity cellulose (Klason et al., 1984; Sears et al., 2001). However, few studies have been conducted on the use of nylon extrusion processes in WPCs because processing wood flour at temperatures over 200°C leads to the production of volatiles from decomposition. In this process, entrapped gases and degraded

wood polymers reduce the mechanical properties of the wood flour and polymer systems (Saheb and Jog, 1999).

To avoid the high processing temperature requirements of nylon 6, Lu et al. (2007) characterized several formulations of nylon 12 WPCs processed with various wood flour loadings. In this research, material was processed at or below 200°C using a torque rheometer to melt blend the formulation followed by compression molding to form a plaque. It was found that increasing the wood content significantly improved the modulus of elasticity (MOE) and modulus of rupture (MOR) in nylon 12 wood composites. Lu et al. (2007) hypothesized that strong interfacial adhesion between wood and nylon 12 improved the mechanical properties.

However, little research has been conducted on the extrusion processing of TPER and nylon 12 WPCs. The goals of this research are to explore formulation and process parameters towards development of extruded TPER and nylon 12 wood flour (WF) composites. In some experiments, injection molding was used to facilitate a larger range of wood flour content. The primary objectives of this study are to:

1. Define a suitable temperature profile for the extrusion process,
2. Determine a compatible lubricant system for an extruded composite,
3. Evaluate the influence of wood fiber moisture content on mechanical and physical properties of the final extruded composites, and
4. Experimentally relate wood fiber loading to mechanical performance for each composite.

## **2.3 Materials and Methods**

### *2.3.1 Material*

The WPC formulations evaluated were composed of wood flour, lubricant, and one of two engineering polymers: a commercial TPER polymer (L-TE05-10, MFI: 10, T<sub>g</sub>: 81°C),

provided by L&L Products (Romeo, MI), or nylon 12 (Grilamid L 20 G,  $T_m$ : 178°C, MFI: 20, density: 1.01g/cm<sup>3</sup>), supplied by EMS-Chemie (Sumter, SC). The wood flour component used was 60-mesh pine (*Pinus spp*) flour (American Wood Fibers, Schofield, WI) with a moisture content (as received) of 9-10%. Commercial lubricants evaluated were: OPE629A oxidized polyethylene homopolymers (Honeywell, Morristown, NJ), Glycolube® WP2200 (Lonza Inc., Allendale, NJ), and a 2:1 blend of zinc stearate (Lubrazinc® WDG) and EBS wax (Kemamide® EBS) (Chemtura, Middlebury, CT).

Prior to extrusion, the wood flour was dried to a moisture content of < 2% by total mass (oven dry weight) using a steam tube dryer. Wood flour, polymer, and lubricants were then mixed in a low intensity blender for 5-10 minutes to form a dry blend, which was fed into the appropriate processing equipment.

### 2.3.2 Torque Rheometry

Torque rheometry data was collected on a Haake Rheomix 600 with a 69 ml net chamber capacity. Testing was performed on a 50 gram sample at a screw speed of 50 rpms for 10 minutes. Torque data was used to evaluate potential barrel zone temperatures for extrusion and potential compatible lubricants for TPER and nylon 12 WF composites.

### 2.3.3 Extrusion

Extrusion trials were performed on a conical counter-rotating twin-screw extruder (Cincinnati Milicron CM 35). The extruder has a downstream diameter of 35-mm, tapered from the feeding throat to the die, with a length to diameter ratio of 22. Test materials were extruded through a rectangular cross-sectioned slit die (3.7 X 0.95-cm) at a screw speed of 10 rpm (TPER/WF) and 20 rpm (nylon 12/WF), and spray-cooled with water upon exiting. Extrusion

temperatures were independently controlled in three barrel zones and two die zones (Table 2.2). Melt pressure was monitored immediately before the material entered the first die zone.

#### *2.3.4 Injection Molding*

Flexure samples (12 X 3 X 127 mm) were injection molded with a Sumitomo SE 50D machine. Temperature zones of the molding machine were independently controlled for TPER/WF formulations at 70°C, 180°C, 180°C, and 180°C, from feed zone to nozzle, respectively. For nylon 12/WF formulations, the molding temperature profile was increased to 170°C, 220°C, 220°C, and 220°C, from feed zone to nozzle. Mold temperature was maintained at 70°C with a cooling time of 40 seconds for TPER/WF, and reduced to 55°C and 30 seconds for nylon 12 formulations. The mold temperature and cooling time for TPER/WF formulations were increased to facilitate flow of the highly viscous composite melt in the mold cavity. Although not optimized, average cycle times of 90 and 60 seconds were recorded for all TPER/WF and nylon 12/WF samples respectively. Filling pressure was set at 1600-kgf/cm<sup>2</sup>, while the 1<sup>st</sup> and 2<sup>nd</sup> stage packing pressure was set at 500-kgf/cm<sup>2</sup> for TPER/WF formulations. In nylon 12/WF formulations, filling pressure was reduced to 1200-kgf/cm<sup>2</sup>, while the 1<sup>st</sup> and 2<sup>nd</sup> stage packing pressures were increased to 900-kgf/cm<sup>2</sup> and 750-kgf/cm<sup>2</sup>, respectively.

Prior to injection-molding the formulation, pellets were prepared using a co-rotating twin screw extruder (Leistritz ZSE-18) with a screw diameter of 17.8-mm and L/D ratio of 40. The 8 independently controlled barrel zones were set to 150°C, 160°C, 170°C, 180°C, 180°C, 180°C, 180°C, and 180°C from the feeding throat to the die adapter in TPER/WF formulations and set to 190°C, 205°C, 210°C, 210°C, 215°C, 215°C, 215°C, and 215°C in nylon 12/WF formulations. Screw speed was maintained at approximately 60 and 80 rpm for TPER/WF and nylon 12/WF blends, respectively, throughout the compounding of the composite material.

### *2.3.5 Mechanical Testing*

Both extruded and injection molded samples were tested in flexure according to ASTM D790 standards. Each sample was planed on the two wide faces to eliminate any irregularities in the surface of the material, and then conditioned for 48 hours prior to testing. Length, width, thickness, and mass were measured for each specimen after conditioning and used to compute density. Mechanical testing was performed on a screw driven Instron 4466 Standard with 10 kN electronic load cell. The support span for testing was 16 times the depth. A crosshead speed of 1.7 mm/min, for injection molded, and 3.8 mm/min, for extruded, were maintained throughout testing.

## **2.4 Results and Discussion**

### *2.4.1 Processing Temperature*

In developing the processing regime necessary for a WPC, proper barrel and die temperatures must be determined to facilitate good flow and melt strength of the extrudate. Extrusion temperatures below 200°C are typically used to minimize wood degradation and volatile formation (Saheb and Jog, 1999). Additional information regarding the thermal degradation of nylon 12 WPCs is available in Appendix A (Hatch, 2008). Prior to attempting extrusion, torque rheometry was utilized to observe the change in melt properties with temperatures varying between 180°C to 200°C for TPER/WF formulations. An initial temperature of 180°C was selected based on previous research where metering and die temperatures ranged between 180°C and 220°C (White et al., 2000). Due to the relatively high melt temperature ( $T_m = 178^\circ\text{C}$ ) for nylon 12, torque rheometry temperatures were selected between 190°C to 225°C. As shown in Figure 2.2, at all temperatures and formulations, the torque decreases rapidly and reaches a relatively stable value within one-minute. Nylon torque

curves never plateau at a constant torque, but continue to decrease well after one minute, indicating sensitivity to shear heating of the composite at these temperatures. For each composite, both the rate of change and the minimum torque decreased with increasing temperatures. However, based on experience with TPER/WF, all processing temperatures appear to be adequate for an extrusion process. Nylon 12/WF, on the other hand, appears to require a higher processing temperature to decrease the amount of torque required on the system, indicating better melt flow of the composite.

The time required to reach a stable minimum torque remains constant, with little variability for the various processing temperatures investigated. This value can be associated with the residence time required to achieve a uniform melt blend during extrusion. Based on our work, barrel residence times in WPC profile extrusion range from 3 to 8 minutes. Considering the minimum time of three minutes, a processing temperature of 180°C and 225°C is more than adequate to reach a uniform melt for TPER/WF and nylon 12/WF formulations, respectively. Therefore, barrel zone temperatures were then selected for extrusion with center barrel zones 2 and 3, both maintained at 180°C or 225°C based on polymer type. However, during nylon 12/WF extrusion, heating coil capacity in the 3<sup>rd</sup> and final barrel zone was limited to 205°C. Consequently, the first barrel zone was set at 225°C to ensure proper melt. Cooling of the extruded composite is very important in nylon 12 WPCs to mitigate the effects of prolonged exposure to these higher temperatures (Appendix B). For TPER/WF formulations, a maximum temperature of 150°C was controlled for the feed zone to ensure that premature melting of the material did not impede feeding of the dry blend.

Additional consideration must be given for the die temperatures to facilitate flow and achieve a well consolidated composite with good melt strength. Mechanical properties are listed

in Table 2.1 for TPER/WF and nylon 12/WF WPCs extruded with different die temperatures. Interpretation of this data for both polymer systems indicates that reducing the die temperature from 180°C to 120°C (TPER/WF) or 205°C to 190°C (nylon 12/WF) increased composite density (1.17 g/cm<sup>3</sup> to 1.25 g/cm<sup>3</sup> and 1.098 g/cm<sup>3</sup> to 1.154 g/cm<sup>3</sup>, respectively) (Figure 2.3). Likewise, the modulus of rupture (MOR) for TPER WPCs was lowest for a die temperature of 180°C and remained relatively constant below 160°C (Figure 2.3). The dramatic decrease in MOR at a high die temperature may be associated with the decreased density of the composite. Low die temperature was found to raise melt pressures at the extruder exit, which in turn affected density by promoting the penetration of the polymer matrix into the wood fiber voids. Melt pressure for TPER and nylon 12 WPCs are shown in Table 2.1 and indicate that at 180°C and 120°C the melt pressures for TPER WPCs are 287 and 938 psi, respectively. Analysis of nylon 12/WF composites yields a similar correlation between melt pressure, density, and MOR for die temperatures of 205°C to 190°C (Figure 2.3). Based on optimum mechanical properties, all further extrusion trials were conducted using the extrusion profiles detailed in Table 2.2, with die zone temperatures of 140°C and 190°C for TPER and nylon 12 WPCs, respectively.

#### *2.4.2 Effect of Lubricant*

It is important to select a proper lubricant for processing a wood fiber composite in order to lower the melt viscosity of the heavily filled WPC formulation and ensure a uniform flow through the die. However, in some cases, any added lubricant can impede the adhesion of the wood and polymer interface (Gupta et al, 2007). For both polymer systems, the oxidized polyethylene lubricant, OPE629A, showed excellent potential in preliminary torque rheometry tests by reducing the melt viscosity considerably (Figure 2.4). However, the WP2200 in TPER

WPCs and the Zinc Stearate/EBS wax blend in nylon 12 WPCs showed only moderate to low potential in lowering viscosity.

To further evaluate lubricant performance in extrusion, composites containing 3%, 2%, 1% OPE629A, 3% WP2200 (TPER), and 3%(2:1) zinc stearate/EBS wax (nylon 12) were produced (Table 2.1), and mechanical properties were characterized. TPER WPCs produced with both 3% WP2200 and 1% OPE629A exhibited poor external lubrication, which resulted in severe surface tearing of the composites (Figure 2.5). Melt pressures observed for both 1% OPE629A and 3% WP2200 were unstable and greater than 1000 psi, suggesting high flow resistance or poor melt strength in the die. Nylon 12 WPCs containing 3% zinc stearate/EBS wax and < 3 % OPE629A yielded similar tearing behavior and an increasing melt pressure trend. However, TPER composites produced with 2% or 3% OPE629A and nylon 12 composites produced with 3% OPE629A could be extruded without visible defects. Additionally, the homogenous cross sections in both composites suggested a uniform density and flow. The MOR of the TPER composite was 86.0 to 93.4 MPa at 3% and 2% OPE629A loading, respectively. MOE, density, and strain at failure all exhibited similar behavior, indicating that lubricant content significantly impedes TPER/WF interaction (Table 2.1). Therefore, based on the apparent influence of lubricant content on mechanical and physical properties of the composites, 2% OPE629A for TPER and 3% OPE629A for nylon 12 composites were selected as the lubricant loading for all remaining work.

#### *2.4.3 Influence of Wood Fiber Moisture Content*

Prior to extrusion, wood flour is typically dried to a moisture content (MC) of less than 2% to eliminate a majority of water vapor from the extrusion process. Excess water vapor can become trapped in the composite melt, leading to a reduction in density, bubbles that form stress

concentrations, and surface defects. In the third heating zone of the extruder, a vacuum was utilized to remove gases and vapor that form as byproducts during extrusion. To understand the effect of MC on the final composite, blends were extruded with MCs of 1.2-1.8% (dry), 3.0% (partially dried), and 9.3% as received (Table 2.3) following the extrusion profile in Table 2.2.

Mechanical testing of nylon 12 samples at 9.3% MC showed little statistical variation, while the MOR of TPER samples was reduced (Table 2.4). Of particular interest is that at MCs of less than 2% and 9.3 % respectively, densities obtained for nylon 12 (1.153 and 1.160 g/cm<sup>3</sup>) and TPER (1.228 and 1.237 g/cm<sup>3</sup>) did not differ significantly. This indicates that water vapor created during extrusion was either easily evacuated from both composites or does not act as a foaming mechanism.

#### *2.4.4 Mechanical Performance of Engineering Polymer Composites at Different Wood Loadings*

Both injection-molded and extruded samples of varying wood flour contents were evaluated to determine mechanical properties. Samples were formulated at wood contents from 40 to 70-wt% extruded (Table 2.4), and 0 to 60-wt% injection-molded (Table 2.5) for both nylon 12 and TPER WPCs. Injection molding of TPER WPCs beyond 50% was limited, due to the difficulty of maintaining optimum melt flow into the mold, which is consistent with other composites developed using injection molding techniques (Singh and Mohanty, 2007). Thermal properties for injection molded TPER and nylon 12 WPCs are presented in Appendices C and D (Hatch, 2008). As expected, MOE increases with wood content for both polymer systems (Figure 2.6), and strain to failure is reduced (Figure 2.7). Of significant interest is the impact of increasing wood fiber content on MOR (Figure 2.8). For injection molded TPER samples, MOR increases consistently from 82.4 MPa to 125.9 MPa (53 % increase in strength) at 50 % wood fiber (Table 2.5). A similar increase in MOR was observed for nylon 12 samples, resulting in a

96% (60% wood flour-injection) and 75% (50% wood flour- extruded) increase over injection molded pure nylon 12 (MOR = 48.43 MPa) (Table 2.4-5). The apparent increase in MOR of injection molded samples vs. extruded samples seems to be linked to the higher strains to failure sustained by injection molded samples (Figure 2.7). Representative stress strain curves for nylon 12, TPER, and HDPE (Gacitua, 2008) injection molded composites with 40% wood flour are presented in Figure 2.9.

Stiffness and density of TPER WPC's correlated very well between processing methods, indicating the stiffness of TPER WPC's is independent of the type of processing method employed (Figure 2.6, 2.10). Anderson (2007) found similar results, with little difference in stiffness of PE wood fiber composites using the methods discussed. The correlation between increased densities of injection-molded composites with increased wood loadings aligns with previous research using high wood loadings of 50-57% (Anderson, 2007; Stark, 2004).

## **2.5 Conclusions**

Mechanical performance of TPER/WF and nylon 12/WF composites is governed by many processing variables. A reverse extruder temperature profile was selected, which provided adequate melt pressures to facilitate the consolidation of both TPER and nylon 12 WPCs in the die and form a composite with high melt strength and density as it exited the die. Lubricant selection significantly affected processing of these composites, and OPE629A was ultimately selected for both systems. OPE629A was found to promote melt flow and not significantly inhibit adhesion of either TPER or nylon 12 to the wood fiber matrix. Wood fiber moisture content (MC) was found to have a negligible affect on nylon 12 composite mechanical performance, while TPER composites at 9.3% MC exhibited a reduction in strength.

A comparison of wood flour loadings using injection molded and extruded samples of TPER and nylon 12 WPCs demonstrated that increasing the wood content of the composite results in a corresponding increase in stiffness and a reduction in strain to failure. The modulus of rupture for TPER WPCs was increased by 53% in injected samples of 0 to 50% wood flour, while extruded material exhibited a peak wood flour loading of 40%. More promising results were observed for nylon 12 WPCs, in which MOR increased by 96% and 75% for injection molded and extruded specimens, respectively. Processing method, as expected, significantly influenced the mechanical properties of both WPCs.

## **2.6 Acknowledgements**

The authors gratefully acknowledge research funding and support by L & L Products Inc., EMS-Chemie (North America), and the Office of Naval Research, under the direction of Mr. Ignacio Perez, under Grant N00014-06-1-0847.

## **2.7 References**

- Anderson, S.P., "Wood Fiber Reinforced Bacterial Biocomposites: Effects Of Interfacial Modifiers and Processing on Mechanical and Physical Properties." Masters Thesis, Washington State Univ., Pullman, WA, December 2007.
- Chmielewski, C., Personal Communication. 06 March, 2008.
- Clemons, C., "Wood-Plastic Composites in the United States: The Interfacing of Two Industries." *Forest Products Journal*, Vol. 52, No. 6, pp. 10-18, 2002.
- Constantin, F., Fenouillot, F., Pascault, J., Williams, R. J., "Post-Crosslinkable Blends: Reactions Between a Linear Poly(hydroxyl-amino ether) and a Diepoxy." *Macromolecular Materials Engineering*, Vol. 289, pp. 1027-1032, 2004.
- Gacitua, W. G., "Influence of Wood Species on Properties of Wood /HDPE Composites." Doctoral Thesis, Washington State Univ., Pullman, WA, May 2008.

- Gupta, B.S., Reiniati, I., Laborie M.P., "Surface properties and adhesion of wood fiber reinforced thermoplastic composites." *Colloids and Surfaces A: Physicochemical Engineering Aspects*, Vol. 302, pp. 388-395, 2007.
- Hatch, M. C., "Processing, Mechanical, and Environmental Performance of Engineering Polymer Wood-Plastic Composites." Masters Thesis, Washington State Univ., Pullman, WA, August 2008.
- Klason, C., Kubat, J., Stromvall, H. E., "The Efficiency of Cellulosic Fillers in Common Thermoplastics. Part 1. Filling without Processing Aids or Coupling Agents." *International Journal of Polymeric Materials*, Vol. 10, Issue 3, pp. 159-187, 1984.
- Lu, J.Z., Doyle, T.W., Li, K., "Preparation and Characterization of Wood-(Nylon 12) Composites." *Journal of Applied Polymer Science*, Vol. 103, 270-276, 2007.
- Saheb, D. N., Jog, J. P., "Natural Fiber Polymer Composites: A Review". *Advanced Polymer Technology*, Vol. 18, Issue 4, pp. 351-363, 1999.
- Sears, K.D, Jacobson, R., Caulfield, D.F., Underwood, J., "Reinforcement of Engineering Thermoplastics with High Purity Wood Cellulose Fibers." Forest Products Society, Sixth International Conference on Woodfiber-Plastic Composites., Madison, WI. 15 May, 2001.
- Singh, S., Mohanty, A.K., "Wood Fiber Reinforced Bacterial Bioplastic Composites: Fabrication and Performance Evaluation." *Composites Science and Technology*, Vol. 67, pp. 1753-1763, 2007.
- Smith, P.M., Wolcott, M.P., "Opportunities for Wood/Natural Fiber-Plastic Composites in Residential and Industrial Applications." *Forest Products Journal*, Vol. 56, Issue 3, pp. 4-11, March 2006.
- Stark, N.M., Matuana, L.M., Clemons, C.M., "Effect of Processing Method on Surface and Weathering Characteristics of Wood-Flour/ HDPE Composites." *Journal of Applied Polymer Science*, Vol. 93, pp. 1021-1030, 2004.
- White, J. E., Silvis, H. C., Winkler, M.S., Glass, T. W., Kirkpatrick, D. E., "Poly(hydroxyaminoethers): A New Family of Epoxy-Based Thermoplastics". *Journal of Advanced Materials*, Vol.12, No. 23, pp. 1791-1800, 2000.

## 2.8 Tables

**Table 2.1.** Mechanical properties, density, and processing melt pressures of extruded TPER/WF and nylon 12/WF composite formulations at various die temperatures and lubricant contents.

% Wood	% TPER	% OPE	Die Temp. [°C]	Modulus of Rupture [MPa]	Modulus of Elasticity [GPa]	Strain @ Failure [%]	Density [g/cm <sup>3</sup> ]	Melt Pressure [psi]
60	37	3	120	81.43 (6.71)	6.040 (0.109)	1.21 (0.12)	1.246 (0.016)	938
60	37	3	140	86.03 (8.45)	6.130 (0.172)	1.26 (0.10)	1.245 (0.011)	530
60	37	3	160	85.33 (5.32)	6.079 (0.143)	1.26 (0.09)	1.217 (0.013)	375
60	37	3	180	70.14 (8.00)	5.421 (0.422)	1.16 (0.15)	1.168 (0.026)	287
60	38	2	140	93.42 (8.99)	6.416 (0.224)	1.33 (0.10)	1.233 (0.019)	847
	<b>NYLON 12</b>							
60	37	3	190	76.05 (7.42)	4.207 (0.228)	1.81 (0.21)	1.154 (0.008)	200
60	37	3	200	55.23 (7.33)	3.750 (0.122)	1.49 (0.24)	1.089 (0.013)	150

**Table 2.2.** Extrusion temperature profile for TPER/WF and nylon 12/WF composites.

	TPER [°C]	Nylon 12 [°C]
<b>Barrel Zone 1 (Feed)</b>	150	225
<b>Barrel Zone 2</b>	180	225
<b>Barrel Zone 3</b>	180	205
<b>Die Zone 1 &amp; 2</b>	140	190
<b>Screw</b>	155	199

**Table 2.3.** Mechanical properties, density, and processing melt pressures of TPER/WF and nylon 12/WF composites at various initial wood fiber moisture contents (MC).

% Wood	% TPER	% OPE	Wood Fiber MC [%]	Modulus of Rupture [MPa]	Modulus of Elasticity [GPa]	Strain @ Failure [%]	Density [g/cm <sup>3</sup> ]	Melt Pressure [psi]
60	37	3	1.8	91.96 (7.04)	6.37 (0.120)	1.31 (0.13)	1.228 (0.010)	530
60	37	3	3.0	93.40 (5.44)	7.183 (0.189)	1.15 (0.07)	1.264 (0.011)	793
60	37	3	9.3	84.55 (5.49)	6.815 (0.247)	1.09 (0.11)	1.237 (0.013)	625
	<b>NYLON 12</b>							
60	37	3	1.2	78.92 (8.98)	4.649 (0.162)	1.77 (0.34)	1.153 (0.014)	150
60	37	3	3.0	77.63 (5.70)	4.434 (0.229)	1.81 (0.24)	1.141 (0.019)	180
60	37	3	9.3	78.89 (5.68)	4.312 (0.178)	1.94 (0.30)	1.160 (0.016)	220

**Table 2.4.** Mechanical properties, density, and processing melt pressures of extruded TPER/WF and nylon 12/WF composites at various wood fiber loadings.

% Wood	% TPER	% OPE	Modulus of Rupture [MPa]	Modulus of Elasticity [GPa]	Strain @ Failure [%]	Density [g/cm <sup>3</sup> ]	Melt Pressure [psi]
40	58	2	103.32 (3.81)	5.78 (0.131)	1.72 (0.12)	1.243 (0.005)	287
50	48	2	97.93 (6.70)	6.28 (0.115)	1.43 (0.12)	1.243 (0.005)	375
60	38	2	91.96 (7.04)	6.37 (0.120)	1.31 (0.13)	1.228 (0.010)	530
70	28	2	77.58 (7.42)	6.97 (0.143)	0.95 (0.11)	1.241 (0.011)	938
	<b>NYLON 12</b>						
40	57	3	43.61 (4.63)	1.728 (0.098)	3.69 (0.61)	0.927 (0.011)	130
50	47	3	84.90 (3.66)	3.973 (0.082)	2.47 (0.23)	1.144 (0.008)	150
60	37	3	77.80 (5.53)	4.258 (0.112)	1.89 (0.23)	1.160 (0.10)	200
70	27	3	47.18 (10.05)]	3.870 (0.323)	1.18 (0.21)	1.128 (0.029)	400

**Table 2.5.** Mechanical properties and density of injection-molded TPER/WF and nylon 12/WF composites at various wood fiber loadings.

% Wood	% TPER	% OPE	Modulus of Rupture [MPa]	Modulus of Elasticity [GPa]	Strain @ Failure [%]	Density [g/cm <sup>3</sup> ]
0	100	0	84.43 (0.61)	2.762 (0.007)	4.16 (0.06)	1.173 (0.003)
0	97	2	82.81 (1.22)	2.639 (0.040)	3.60 (0.15)	1.160 (0.006)
20	78	2	105.22 (1.13)	4.204 (0.065)	3.29 (0.06)	1.202 (0.007)
30	68	2	115.59 (1.96)	5.091 (0.138)	2.64 (0.10)	1.226 (0.007)
40	58	2	122.17 (0.68)	5.702 (0.077)	2.37 (0.04)	1.253 (0.002)
50	48	2	125.94 (2.06)	6.386 (0.179)	1.90 (0.12)	1.270 (0.004)
	<b>NYLON 12</b>					
0	100	0	48.43 (0.71)	1.182 (0.013)	4.86 (0.12)	0.994 (0.001)
0	97	3	43.89 (0.29)	1.056 (0.022)	4.80 (0.07)	0.976 (0.002)
20	77	3	63.50 (0.90)	1.888 (0.034)	4.57 (0.07)	1.027 (0.004)
30	67	3	74.74 (0.51)	2.411 (0.030)	4.30 (0.08)	1.066 (0.003)
40	57	3	84.16 (0.66)	2.871 (0.054)	4.13 (0.14)	1.093 (0.003)
50	47	3	91.11 (0.60)	3.589 (0.043)	3.09 (0.09)	1.133 (0.003)
60	37	3	94.96 (1.07)	4.480 (0.131)	2.36 (0.08)	1.178 (0.006)

## 2.9 Figures

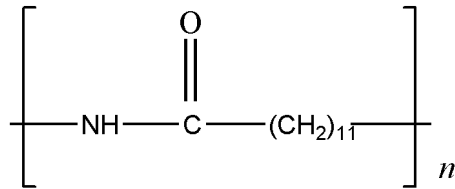
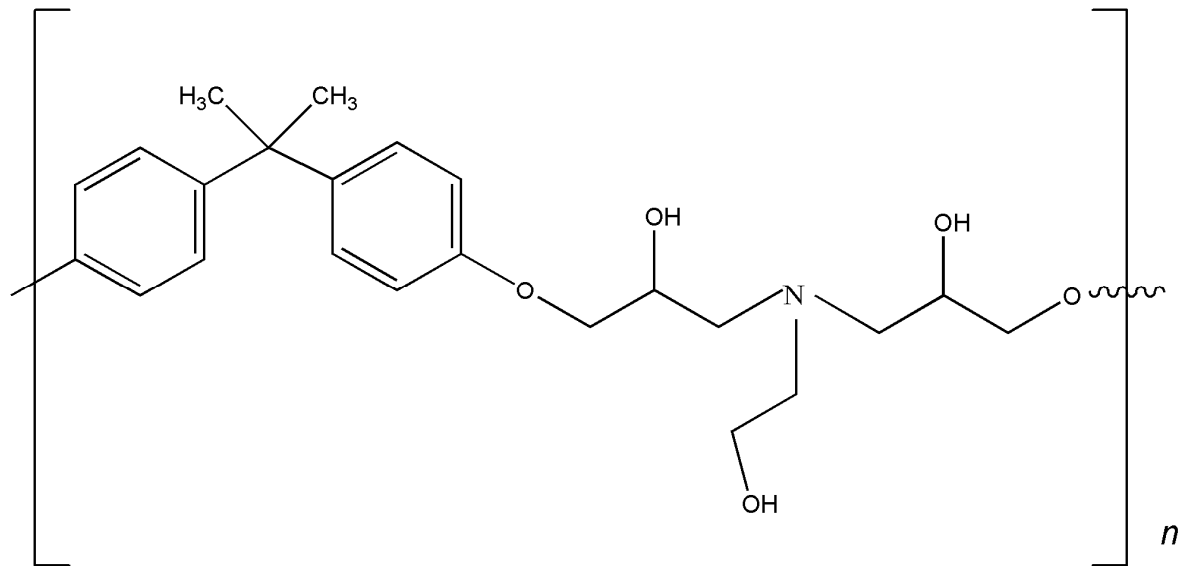


**Figure 2.1.** Primary chemical structure of TPER (Top) and nylon 12 (Bottom) polymers (TPER adapted from Constantin et al., 2004).

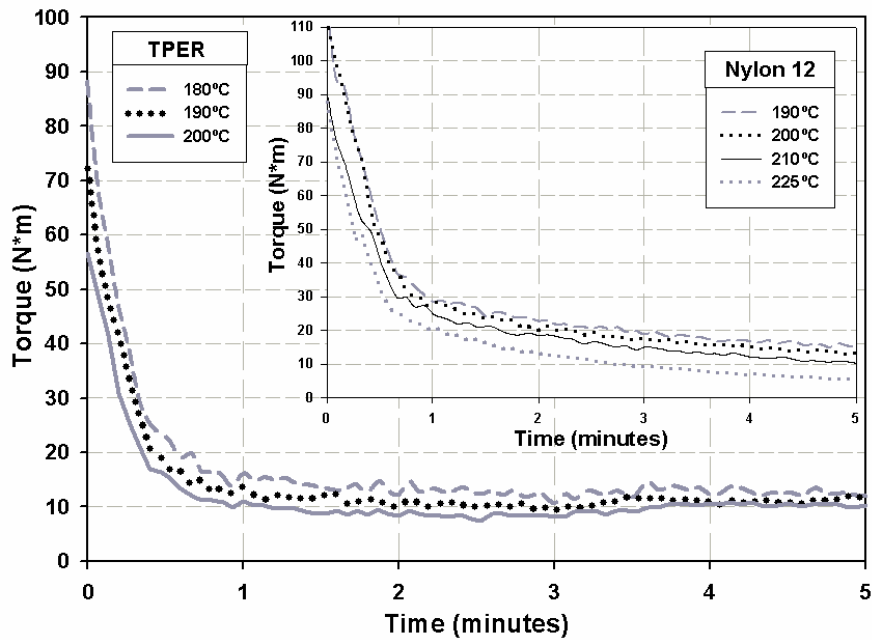


**Figure 2.2.** Variation of torque with respect to time of 40% TPER/ 60% WF and 40% nylon 12/ 60% WF composites (no lube) at various chamber temperatures.

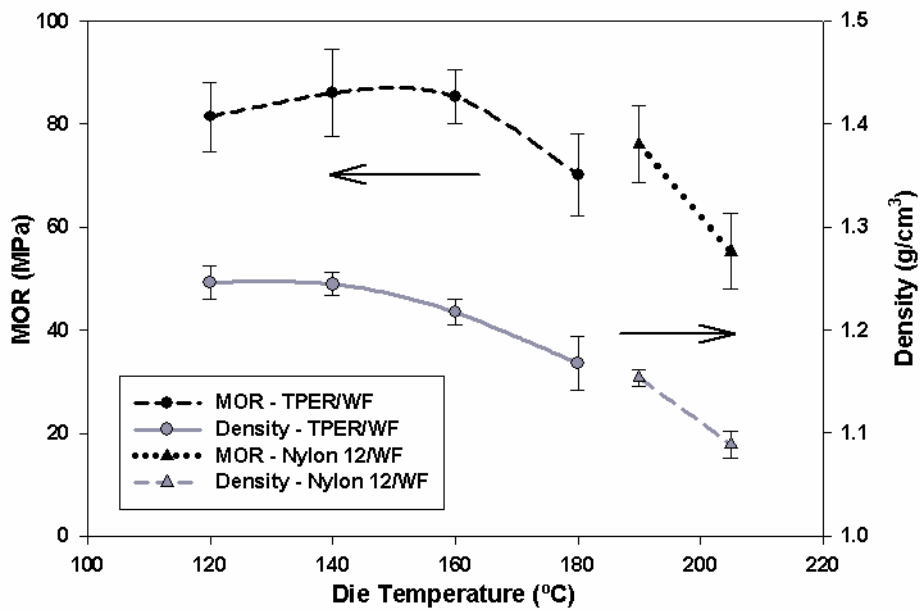


**Figure 2.3.** MOR and density of TPER/WF and nylon 12/WF composites at various extrusion die temperatures.

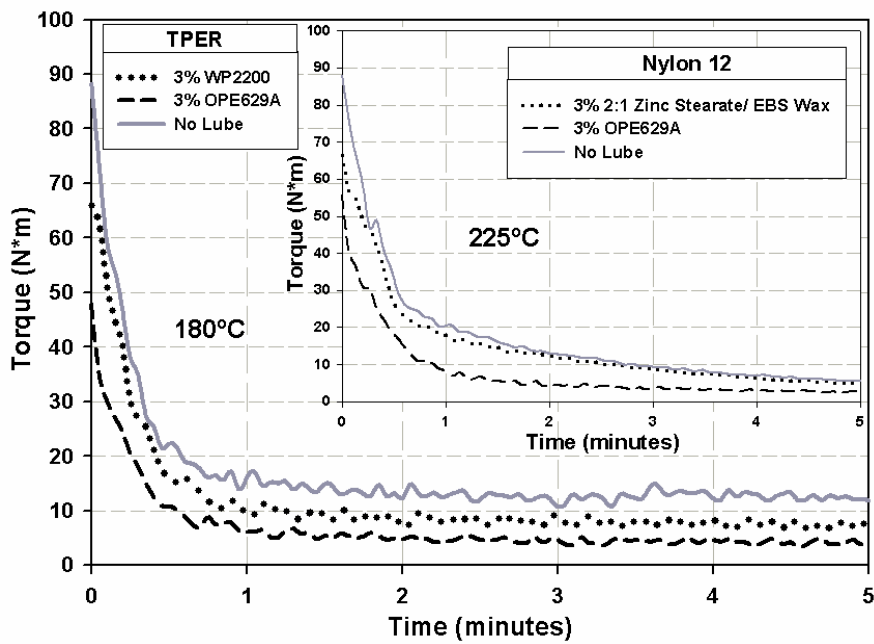


**Figure 2.4.** Variation of torque with respect to time of various formulations of 37-40% TPER/60% WF and 37-40% nylon 12/60% WF.



**Figure 2.5.** Extruded TPER/WF composites containing 2% OPE629A, 1% OPE629A, and 3% WP2200 from left to right, respectively.

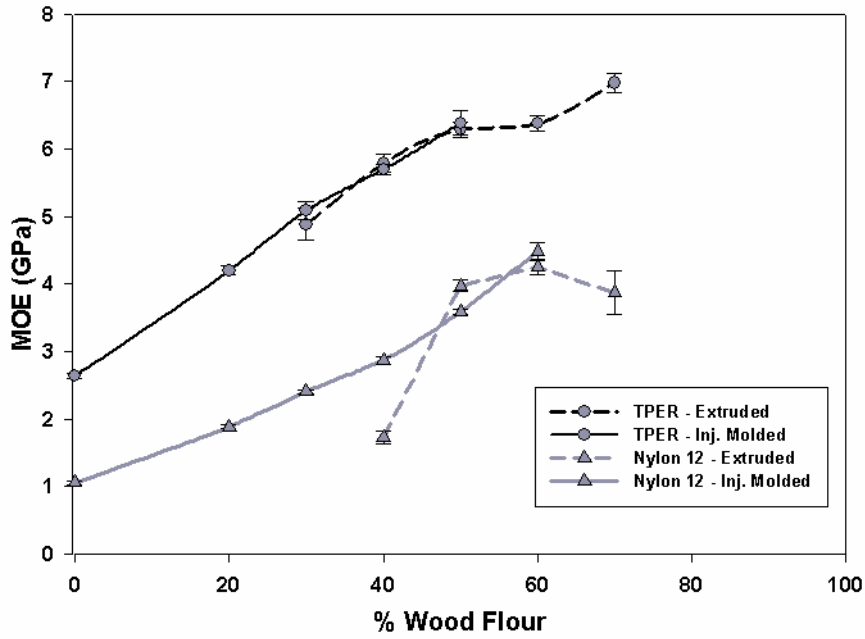


**Figure 2.6.** Flexural modulus of elasticity (MOE) of TPER/WF and nylon 12/WF composites with various wood flour contents.

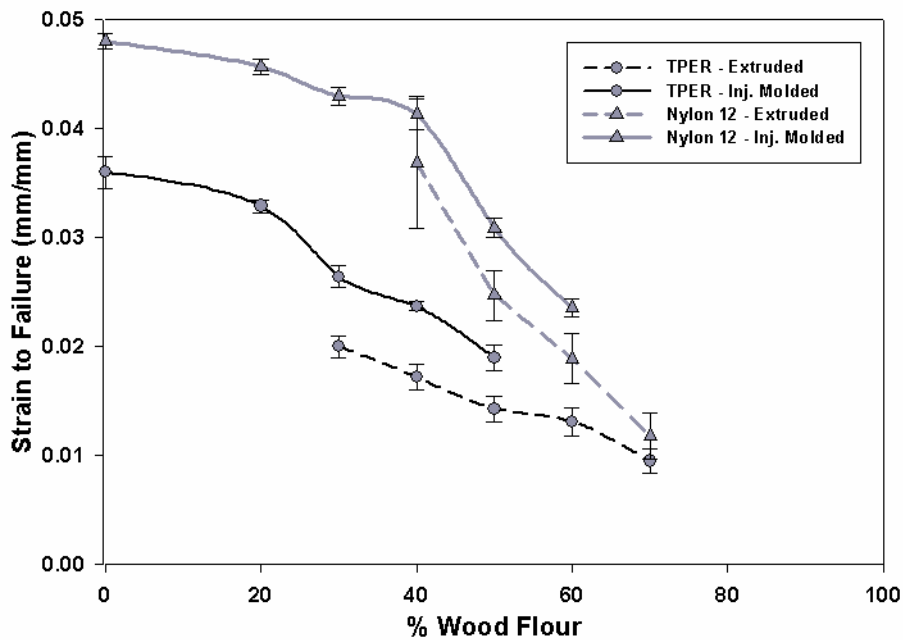


**Figure 2.7.** Strain to failure of TPER/WF of TPER/WF and nylon 12/WF composites with various wood flour contents.

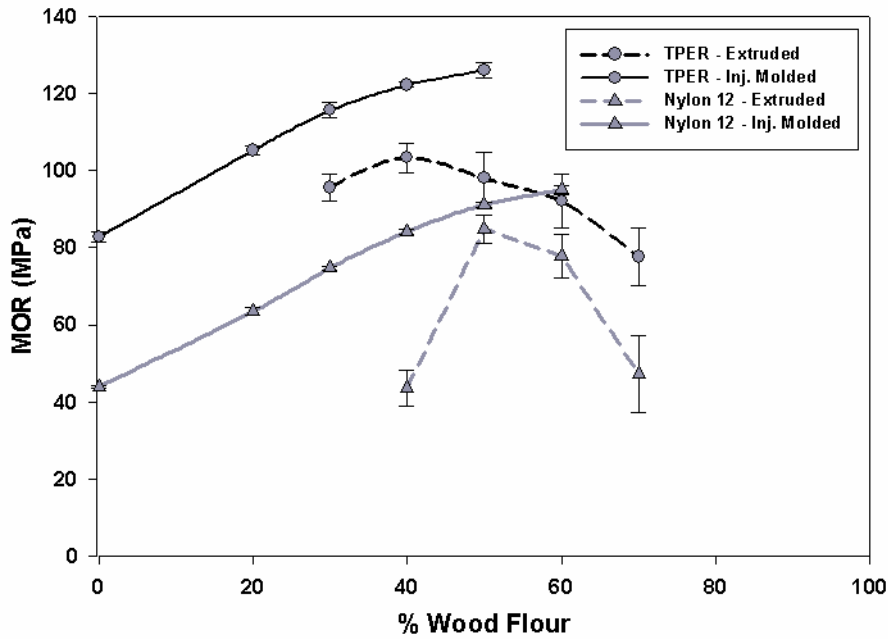


**Figure 2.8.** Flexural modulus of rupture (MOR) of TPER/WF and nylon 12/WF composites with various wood flour contents.

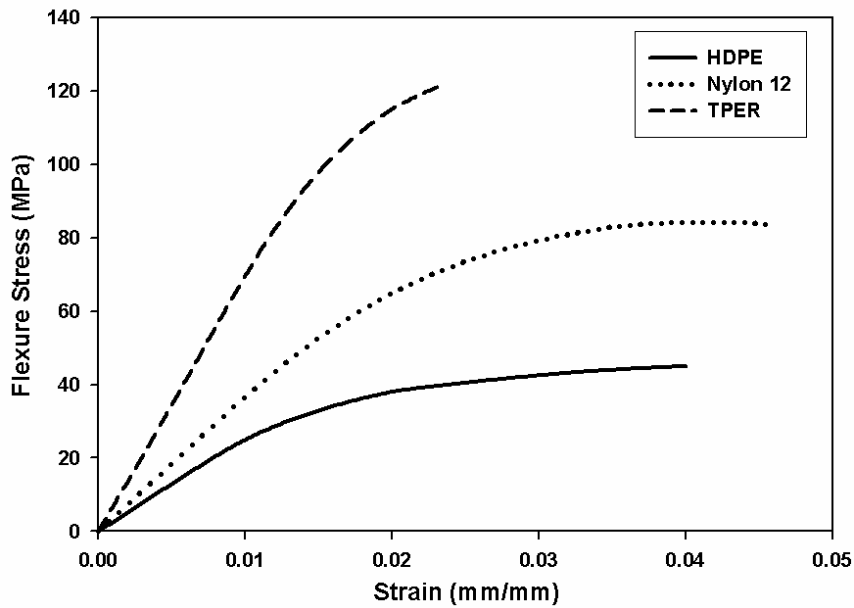


**Figure 2.9.** Stress-strain curves for injection molded TPER, nylon 12, and HDPE WF composites with 40% wood fiber. (HDPE curve adapted from Gacitua, 2008)

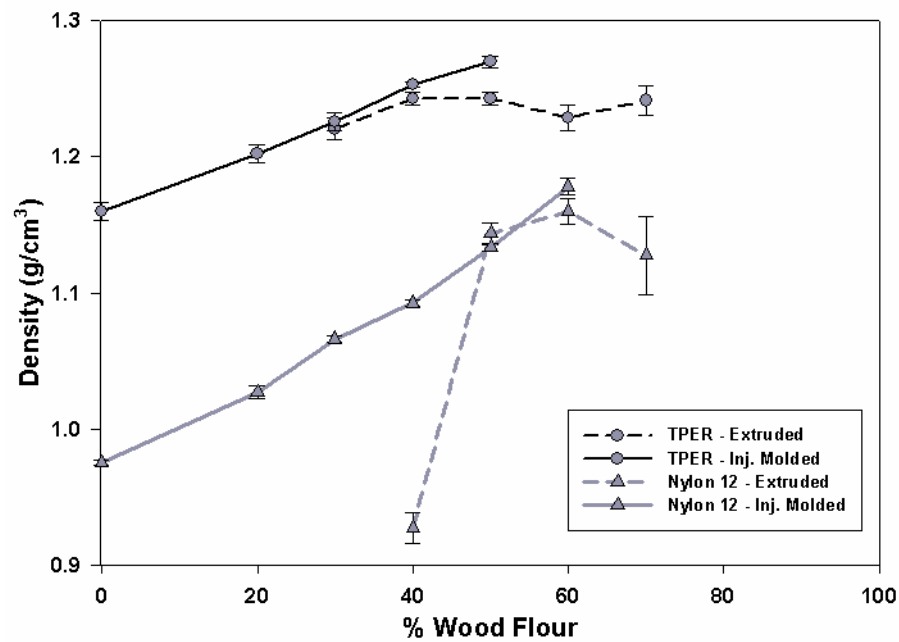


**Figure 2.10.** Density of TPER/WF and nylon 12/WF composites with various wood flour contents.

## **CHAPTER 3 - MOISTURE AND TEMPERATURE INFLUENCE ON TPER AND NYLON 12 WOOD-PLASTIC COMPOSITES**

### **3.1 Abstract**

Building materials are often subjected to many different climates and environments. Current WPCs have been proven to be mechanically sensitive to changes in temperature and moisture content. Although the incorporation of nylon 12 and thermoplastic epoxy resin (TPER) into WPCs instead of traditional high density polyethylene (HDPE) has shown promise, there was no data on environmental influences prior to this study. Four extruded wood flour composites were produced (one each using TPER and HDPE, and two using nylon 12). Flexure tests were performed at temperatures of -30, 0, 21.1, 40, 65.6°C and samples soaked in a water bath from 0 to 121 days. TPER exhibited the least mechanical sensitivity to temperature changes, followed by nylon 12 and HDPE WPCs. Rates of moisture absorption for nylon 12 and TPER WPCs indicate that they can sustain longer periods of saturation than HDPE WPCs. For nylon 12 and TPER composites at 15% moisture content, stiffness and strength were reduced by 60%.

### **3.2 Introduction**

The use of thermoplastic polymers in natural fiber composites have recently grown in popularity, primarily as a means to promote recyclability and native resistance to decay. Previous research has shown that wood-plastic composites (WPCs) based on thermoplastic epoxy resin (TPER) and nylon 12 exhibit superior mechanical strength properties to current WPCs (Hatch, 2008). However, when used in engineered applications, influences of temperature and moisture must be considered in the structural design capacities (Marcovich et al., 1997; Huang et al., 2006; Stark, 2001; Schildmeyer, 2006; Anderson, 2007). Current commercial

WPCs principally contain polyolefins, which are hydrophobic in nature. However, TPER contains similar affinity to water and hydroxyl functionality to hydrophilic wood polymers (White et al., 2000). Nylon 12 absorbs water less easily than the more commercially prevalent moisture sensitive nylon 6, but both nylons absorb more moisture than polyolefins.

The mechanical properties of WPCs based on HDPE and polypropylenes (PP) are strongly correlated to application temperature (Schildmeyer, 2006). In addition, the thermally stable wood component in WPCs can reduce the sensitivity of mechanical properties to these temperature changes. With PP, an increase from room temperature to 65°C resulted in 30% and 50% reductions in tensile strength and modulus, respectively. Evaluation of moisture and temperature dependence of TPER and nylon 12 composites is necessary for their development of as viable structural composites.

Assessing temperature and moisture influences on performance of TPER WPCs and nylon 12 WPCs was the overall goal of this research. Specific objectives of the study were to:

1. Evaluate the sensitivity of flexural properties to various application temperatures,
2. Determine the influence of moisture content on flexural and physical properties and compare moisture absorption rates, and
3. Develop factors to adjust composite flexural capacities for temperatures and moisture effects.

### **3.3 Materials and Methods**

#### *3.3.1 Material*

Four WPC formulations were examined utilizing three commercial polymers: TPER (L-TE05-10, MFI: 10, Tg: 81°C), provided by L&L Products (Romeo, MI), nylon 12 (Grilamid® L

20 G,  $T_m$ : 178°C, MFI: 20, density: 1.01 g/cm<sup>3</sup>), provided by EMS-Chemie (Sumter, SC), and HDPE (LB010000, MFI: 0.5, density: 0.953 g/cm<sup>3</sup>) from Equistar (Houston, TX). A 60 mesh pine (*Pinus spp*) flour with a moisture content of 9-10% was acquired from American Wood Fibers (Schofield, WI). An oxidized polyethylene homopolymer (OPE629A, Honeywell, Morristown, NJ) was used as a lubricant for both TPER and nylon 12 formulations, and Glycolube® WP2200 (Lonza Inc., Allendale, NJ) was employed for HDPE blends. Specific formulations for each composite are outlined in Table 3.1.

A steam tube dryer was utilized to reduce the flour moisture content to < 2% by total mass (oven dry weight). Prior to extrusion, each composite formulation, consisting of wood flour, polymer, and lubricants, was dry-blended in a low intensity blender for 5 – 10 minutes.

### 3.3.2 Extrusion

The various WPCs were extruded into a rectangular section using a slit die (3.7 X 0.95-cm) and then spray cooled with water. Extrusion was performed on a conical counter-rotating twin-screw extruder (Milicron CM 35) with a downstream diameter of 35-mm and L/D ratio of 22. Extruder temperatures were independently controlled in 3 barrel zones, and 2 die zones with the temperature schedules presented in Table 3.2. An additional thermal conditioning heat treatment was applied to some of the wood flour pre-extruding it at the barrel and die schedule for nylon 12 (Table 4.1) at a screw speed of 30 rpms. The nylon 12 WPCs containing this “pre-extruded wood flour” (PWF) were produced using the same extrusion profile and formulation as nylon 12 WPCs.

### *3.3.3 Environmental Conditioning of Test Specimen*

Initial conditioning for both temperature and moisture samples was performed for 48 hours according to ASTM D790. Before the flexural testing at elevated temperature was performed, each sample was placed in an environmental chamber at 65.6°C for 12 hours to facilitate relaxation of residual stresses from processing (Anderson, 2007). Subsequently, each sample was conditioned at the respective testing temperature for 12 hours followed by the final mechanical testing at the assigned temperatures of -30, 0, 21.1, 40, 65.6°C ( $\pm 2^\circ\text{C}$ ) in an environmental chamber. Water absorption was evaluated following submersion in de-ionized water from 0 to 121 days. At prescribed time intervals, specimens were removed and evaluated for physical dimensions (length, width, thickness) and mass. These measurements were subsequently used to compute percent moisture content, density, and volumetric strain. After physical measurements were complete, the samples were tested in flexure according the protocol given below.

### *3.3.4 Mechanical Testing*

All flexure testing was performed according to ASTM D790 standards with the exception of specimen treatments used to produce the desired temperature and moisture conditions. Mechanical testing of moisture samples was performed on a screw driven Instron 4466 Standard with 10 kN electronic load cell. The universal test machine used for evaluating temperature samples consisted of 222-kN servo-hydraulic test frame (MTS Corp.) with an inline 2.2 kN load cell and environmental chamber. The support span for all testing was 16 times the nominal depth (12.7 cm) with a constant crosshead speed maintained at 3.8 mm/min. Strain to failure for each sample was defined as the resultant strain coincident with the maximum load.

### 3.4 Results and Discussion

#### 3.4.1 Temperature Influences

All of the WPC formulations exhibited a decreasing trend of MOE and MOR with increasing temperatures from -30°C to 65.6°C (Figure 3.1). As with previous research (Schildmeyer, 2006), the strain to failure of the nylon 12 and HDPE WPCs increased over the same temperature range (Figure 3.2). However, a constant strain to failure was noted for the TPER composites with no significant deviation from 0.0125 mm/mm (1.25 %) over the temperature range examined. Although speculative, the constant failure strain of TPER WPCs may be associated with strong fiber-matrix interaction afforded by the hydroxyl-functionality of the TPER polymer.

To evaluate the overall affect of temperature among the different WPC polymer systems, relationships were produced to determine the temperature corrected composite strength ( $\Gamma_{t,R}$ ) and modulus ( $\Gamma_{t,E}$ ) given by:

$$\Gamma_{t(E,R)} = C_{t(E,R)} \cdot \Gamma_{i(E,R)} \quad \text{Eq. 3.1}$$

where:

$$C_{t(E,R)} = 1 - \lambda_{(E,R)} \cdot (\Delta T) \quad \text{Eq. 3.2}$$

where  $\Gamma_i$  is the composite strength or modulus at ambient temperature (21.1°C),  $C_t$  is the temperature modification factor,  $\Delta T$  is the change in composite temperature from ambient,  $\lambda$  is the slope of the normalized linear curve, and E and R denote the modulus of elasticity and rupture stress, respectively. These values were derived after normalizing the composite mechanical properties to 21.1°C ( $\Delta T = 0$ ). A similar correction for temperature affects was

proposed by Schildmeyer (2006) for the design of PP composites, which utilized a linear correction for MOR and a second order relationship for MOE. Contrary to his research, the composites studied here appear to follow a linear correction for both MOE and MOR (Figure 3.3). The relationships developed for MOR and MOE highlight how sensitive the current HDPE composites can be to temperature deviations. The TPER composites were affected less by temperature changes than any of the other composites evaluated. The nylon 12 materials display an intermediate behavior, positioned between TPER and HDPE.

#### *3.4.2 Moisture Absorption*

Moisture absorption and the resulting volumetric strain were observed following submersion in liquid water for times between 0 and 121 days. Water absorption of WPCs has been reported to be characterized by Fickian, non-steady state diffusion (Anderson, 2007, Chowdhury and Wolcott, 2007). To accurately analyze the Fickian diffusion coefficient, moisture content (MC) is plotted vs. the square root of time producing a linear region followed by a non-linear approach to the saturated moisture content,  $M_{\text{sat}}$ . The HDPE formulations exhibited this behavior, reaching saturation within 60-days (Figure 3.4). Although the TPER and nylon composites displayed similar behavior, they did not reach saturation within the test period, negating the ability to quantify the diffusion coefficient. The moisture absorption rate of TPER and nylon 12 composites was significantly less compared to the HDPE composite. Possible explanations for this behavior include the adhesion of wood to the polymer matrix, which could reduce water transport via intermolecular hydrogen bonding, the reduction in void space, which could eliminate direct flow pathways within the composite, and the hydroscopicity of the polymers, which could discourage water absorption. The latter is clearly not the case, since both nylon 12 and TPER polymers are hydrophilic, while HDPE is hydrophobic. For each composite

evaluated except TPER, increased MC resulted in an equivalent increase in volumetric strain (Figure 3.5). Over-swelling of TPER composites is potentially systematic of the highly hydrophilic nature of this polymer system.

Comparison of both nylon 12 composites clearly shows the effect that heat treatment of wood fibers has on reducing water absorption. High temperature processing of wood increases stiffness and decreases hygroscopicity due to the reduction in hemicellulose content of the wood along with functional hydroxyl groups (Hillis, 1984; Saheb and Jog, 1999). Cross-linking of lignin networks and an increased proportion of crystalline cellulose may significantly influence heat treated wood properties (Boonstra and Tjeerdsma, 2006).

### 3.4.3 Moisture Content and Mechanical Properties

Similar relations to those derived for temperature sensitivity were developed for the influence of composite moisture content on mechanical properties. It was determined that MOR data correlated best to a linear function normalized to 0% MC, while MOE data followed a logarithmic function. MOE was normalized to 1% MC due to the tendency of a log function to approach infinity,  $MOE \rightarrow \infty$ , as MC approaches 0%. MOR was observed to follow a decreasing linear trend with increasing moisture content for each composite. Further adjustment of Eq. 3.2 provides the moisture content strength reduction factor ( $C_{m,R}$ ) given as:

$$C_{m(R)} = 1 - \delta_{(R)} \cdot (MC) \quad \text{Eq. 3.3}$$

where  $\delta$  is the slope of the normalized linear curve. Consequently, regression of stiffness modulus data resulted in a logarithmic function of MC ( $\log MC$ ) which provided the best correlation. Data was then normalized to 1% MC, ( $\log(0) \rightarrow -\infty$ ). Thus, the relation for the modulus reduction factor ( $C_{m,E}$ ) can be expressed as:

$$C_{m_E} = 1 - \omega_E \cdot \log(MC) \quad \text{Eq. 3.4}$$

where  $\omega$  is a constant. The moisture corrected modulus ( $\Gamma_{m,E}$ ) and strength ( $\Gamma_{m,R}$ ) are then obtained from substitution of Eq. 3.3 and 3.4 into the following:

$$\Gamma_{m(R,E)} = C_{m(R,E)} \cdot \Gamma_{o(R,E)} \quad \text{Eq. 3.5}$$

where  $\Gamma_o$  is the strength and modulus at 0% and 1%, respectively. Reduction factors,  $C_m$ , for both stiffness and strength for each composite is shown in Figure 3.6. For nylon 12/PWF the reduction factor curve is only valid up to 8% MC, since moisture absorption of this composite was significantly inhibited. The average strength projected for 0 % MC for TPER, nylon 12, nylon 12/PWF, and HDPE was 98.9, 66.0, 71.5, and 21.4 MPa, respectively. At 1% MC the average stiffness modulus for TPER, nylon 12, nylon 12/PWF, and HDPE was 6.77, 3.90, 3.81, and 2.89 GPa, respectively.

Closer analysis of the curves shows moisture's influence on the strength and stiffness of engineering polymer WPCs, especially strength. The strength of the HDPE composite under investigation exhibited only a decrease of 40% at 20% MC where both nylon 12 and TPER composites showed a dramatic decrease of approximately 70% and 80%, respectively, at 18 % MC. However, the strength of nylon 12 and TPER composites at 0 % is roughly 300% to 460% higher than HDPE, which even with the strength loss projected for these composites at 70 and 80% still exceed the strength of dry HDPE.

Only minor variations in stiffness reduction factors ( $C_m$ ) between composites were observed (Figure 3.5). Both nylon 12/WF and TPER composites followed the same trend for stiffness, while HDPE showed slightly less impact from moisture content. Improved stiffness

performance of nylon 12 WPCs was observed with pre-extruded wood flour at 8% MC in which  $C_{m,E}$  was reduced by approximately 12%.

### **3.5 Conclusions**

WPCs are promoted for their resistance to environmental factors affecting traditional wood member performance and life cycle expectancy, but are susceptible to moisture due to their high wood content. Environmental sensitivity of thermoplastic polymers can significantly affect the moisture and temperature response of the composite. Results produced using nylon 12 and TPER WPCs were similar to those using traditional HDPE WPCs.

Testing for TPER and nylon 12 WPCs at various temperatures from -30°C to 65.6°C indicated that both MOR and MOE are sensitive to temperature changes. When MOR ( $C_{t,R}$ ) and MOE ( $C_{t,E}$ ) were normalized to ambient temperature (21.1°C), clear comparisons could be made. TPER was the least sensitive to temperature, followed by nylon 12 and then HDPE. However, the overall strength of TPER and nylon 12 composites remained significantly higher than HDPE.

TPER composites more readily absorbed water than nylon 12 composites, while HDPE composites had a higher comparative absorption rate. Heat treatment of wood flour prior to extrusion with nylon 12 reduced moisture absorption and increased composite stiffness. For nylon 12 and TPER composites, reductions in both MOE and MOR were approximately 60% at 15% MC. Overall, the mechanical properties of both TPER and nylon 12 composites were more sensitive to moisture than traditional HDPE composites.

### 3.6 Acknowledgements

The authors gratefully acknowledge research funding and support by L & L Products Inc., EMS-Chemie (North America), and the Office of Naval Research, under the direction of Mr. Ignacio Perez, under Grant N00014-06-1-0847.

### 3.7 References

- Anderson, S., "Wood Fiber Reinforced Bacterial Biocomposites: Effects of Interfacial Modifiers and Processing on Mechanical and Physical Properties." Master's Thesis, Washington State Univ., Pullman, WA, Dec. 2007.
- Boonstra, M.J., Tjeerdsma, B., "Chemical Analysis of Heat Treated Softwoods." *Holz als Roh- und Werkstoff*, Vol. 64, pp. 204-211, 2006.
- Chowdhury, M.J.A., Wolcott, M.P., "Compatibilizer Selection to Improve Mechanical And Moisture Properties of Extruded Wood-HDPE Composites." *Forest Products Journal*, Vol. 57, No. 9, 2007.
- Hatch, M., "Processing of Engineering Polymer Wood Plastic Composite: Thermoplastic Epoxy Resin (TPER) and Nylon 12." Master's Thesis, Washington State Univ., Pullman, WA, Chpt. 2, April 2008.
- Hillis, W.E., "High temperature and chemical effects on wood stability." *Wood Science Technol.*, Vol. 18, pp. 281-193, 1984.
- Huang, S.H., Cortes, P., Cantwell, W.J., "The influence of moisture on the mechanical properties of wood polymer composites." *Journal of Material Science*, Vol. 41, pp. 5386-5390, 2006.
- Marcovich, N. E., Reboredo, M. M., Aranguren, M. I., "Dependence of the Mechanical Properties of Woodflour-Polymer Composites on the Moisture Content." *Journal of Applied Polymer Science*, Vol. 68, pp. 2069-2076, 1998.
- Saheb, D. N., Jog, J. P., "Natural Fiber Polymer Composites: A Review". *Advanced Polymer Technology*, Vol. 18, Issue 4, pp. 351-363, 1999.
- Schildmeyer, A.J., "Temperature and Time Dependent Behaviors of a Wood-Polypropylene Composite. Master's Thesis, Washington State Univ., Pullman, WA, 2006.
- Smith, P.M., Wolcott, M.P., "Opportunities for Wood/Natural Fiber-Plastic Composites in Residential and Industrial Applications." *Forest Products Journal*, Vol. 56, Issue 3, pp. 4-11, March 2006.

Stark, N., "Influence of Moisture Absorption on Mechanical Properties of Wood Flour-Polypropylene Composites." *Journal of Thermoplastic Composite Materials*, Vol. 14, 2001.

White, J. E., Silvis, H. C., Winkler, M.S., Glass, T. W., Kirkpatrick, D. E., "Poly(hydroxyaminoethers): A New Family of Epoxy-Based Thermoplastics". *Journal of Advanced Materials*, Vol. 12, No. 23, 2000.

### 3.8 Tables

**Table 3.1.** Formulation for each WPC polymer system.

	<b>TPER</b>	<b>Nylon 12</b>	<b>HDPE</b>
<b>Wood Flour :</b>	60 %	60 %	60 %
<b>Polymer :</b>	38 %	37 %	38 %
<b>Lubricant :</b>	2 %	3 %	2 %
<b>Lubricant Type :</b>	OPE629A	OPE629A	WP2200

**Table 3.2.** Extrusion profile for each WPC polymer system.

	<b>TPER</b>	<b>Nylon 12</b>	<b>HDPE</b>
<b>Barrel Zone 1 (Feed) [°C]</b>	150	225	165
<b>Barrel Zone 2 [°C]</b>	180	225	165
<b>Barrel Zone 3 [°C]</b>	180	205	165
<b>Die Zone 1 [°C]</b>	140	190	170
<b>Die Zone 2 (Exit) [°C]</b>	140	190	170
<b>Screw [°C]</b>	155	199	165
<b>Screw Speed [rpm]</b>	10	20	10

### 3.9 Figures

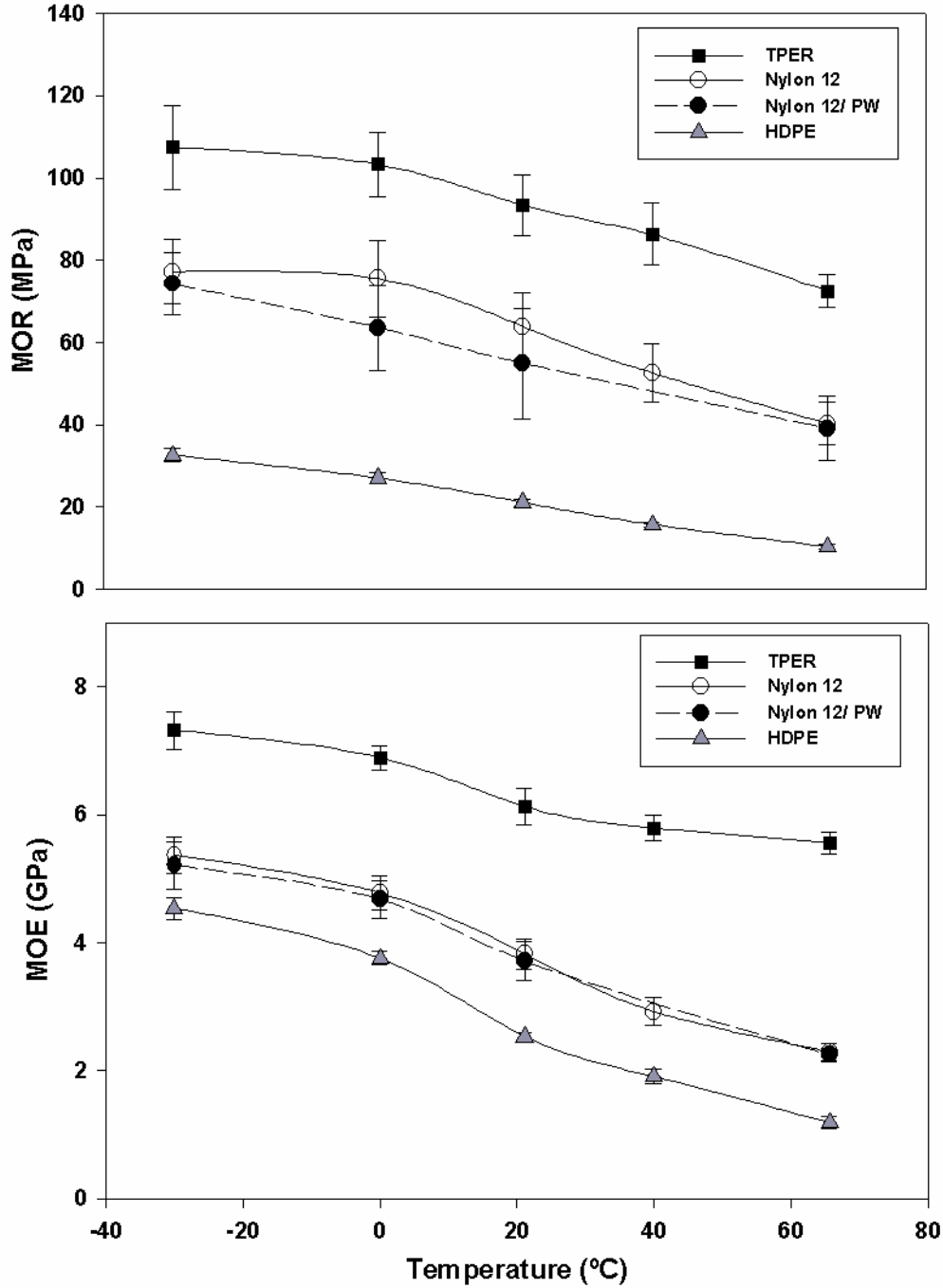


**Figure 3.1.** Modulus of rupture (MOR) and modulus of elasticity (MOE) of WPCs at various temperatures.

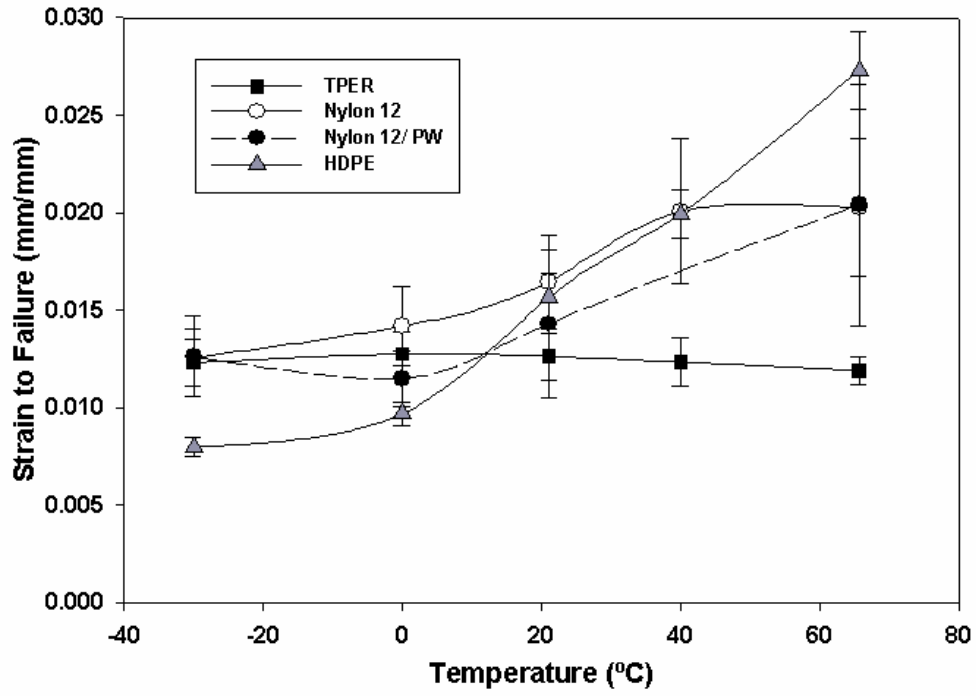
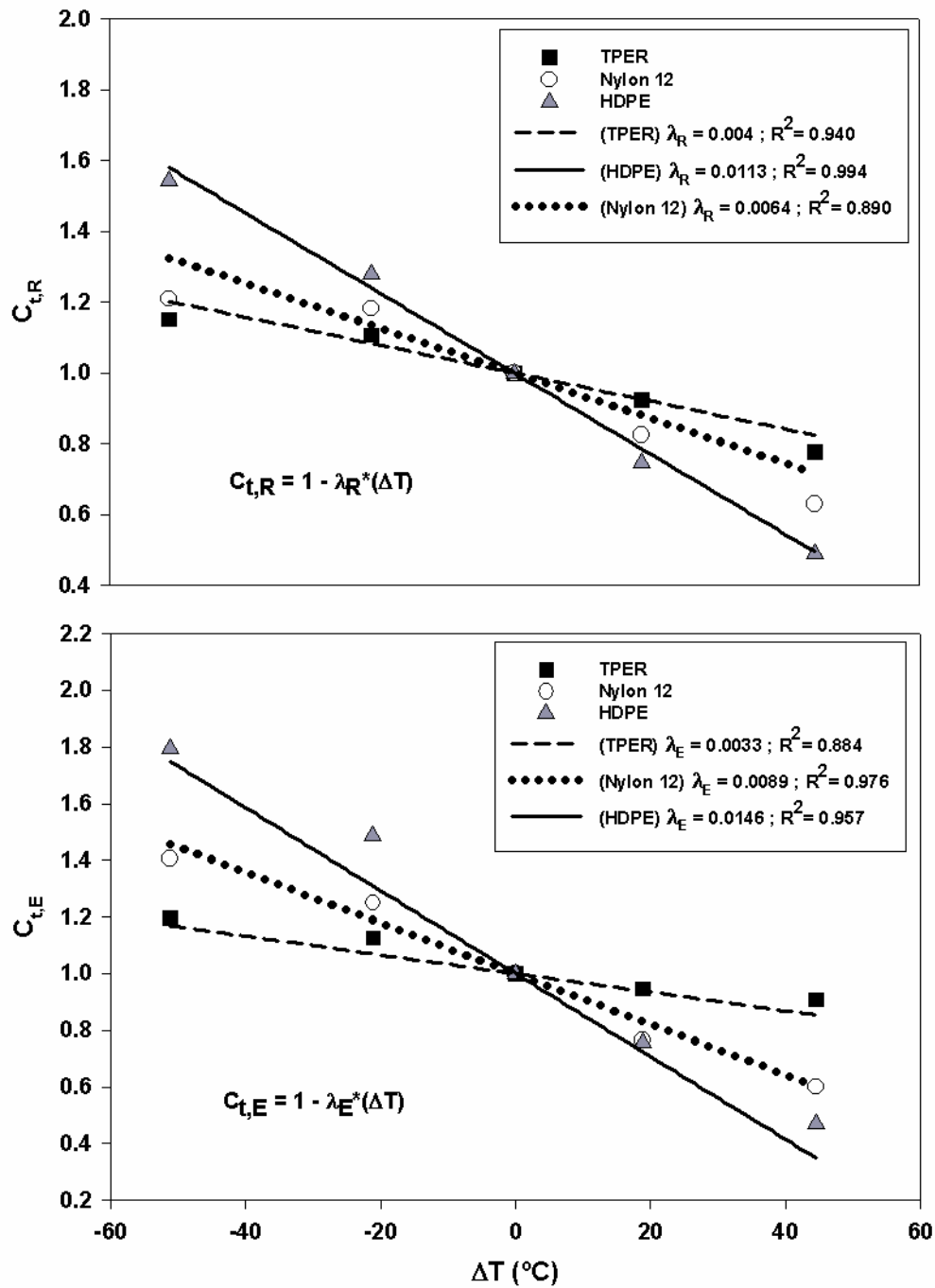


Figure 3.2. Strain to failure of WPCs at various temperatures.



**Figure 3.3.** Temperature modification factor,  $C_t$ , from ambient (21.1°C) for MOR ( $C_{t,R}$ ) and MOE ( $C_{t,E}$ ) of WPCs.

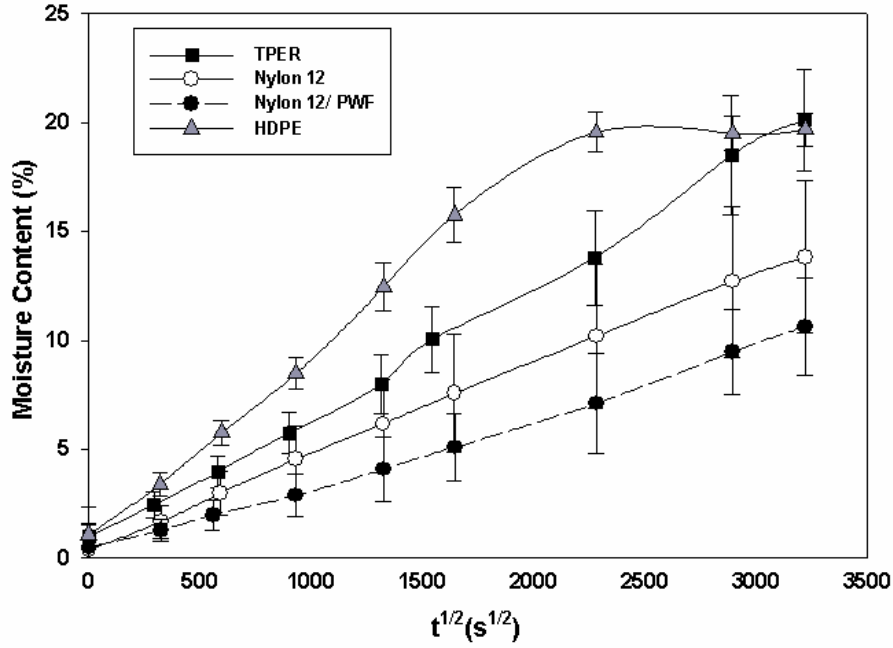


Figure 3.4. Moisture absorption of WPCs from 0 to 121 days of water soaking.

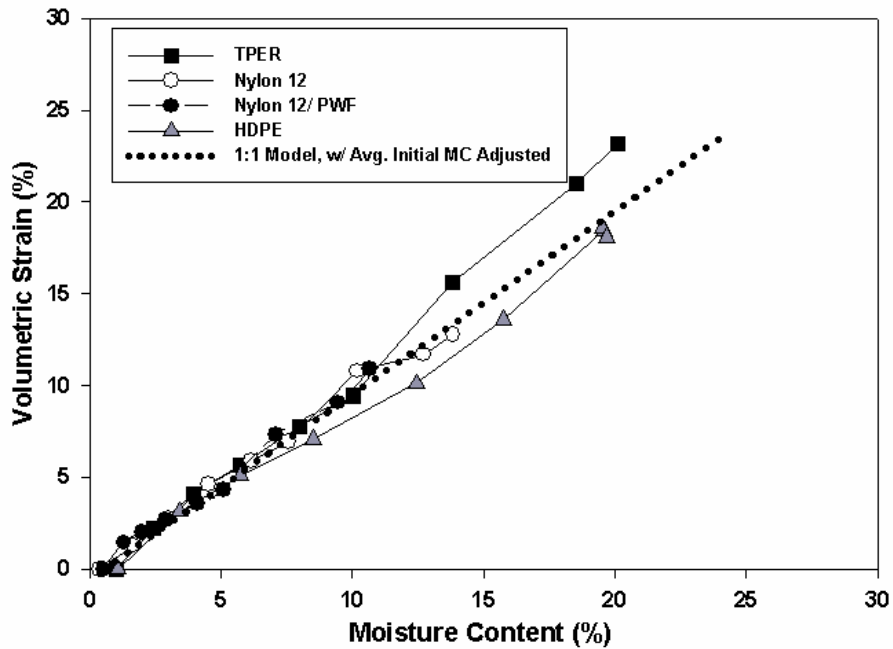
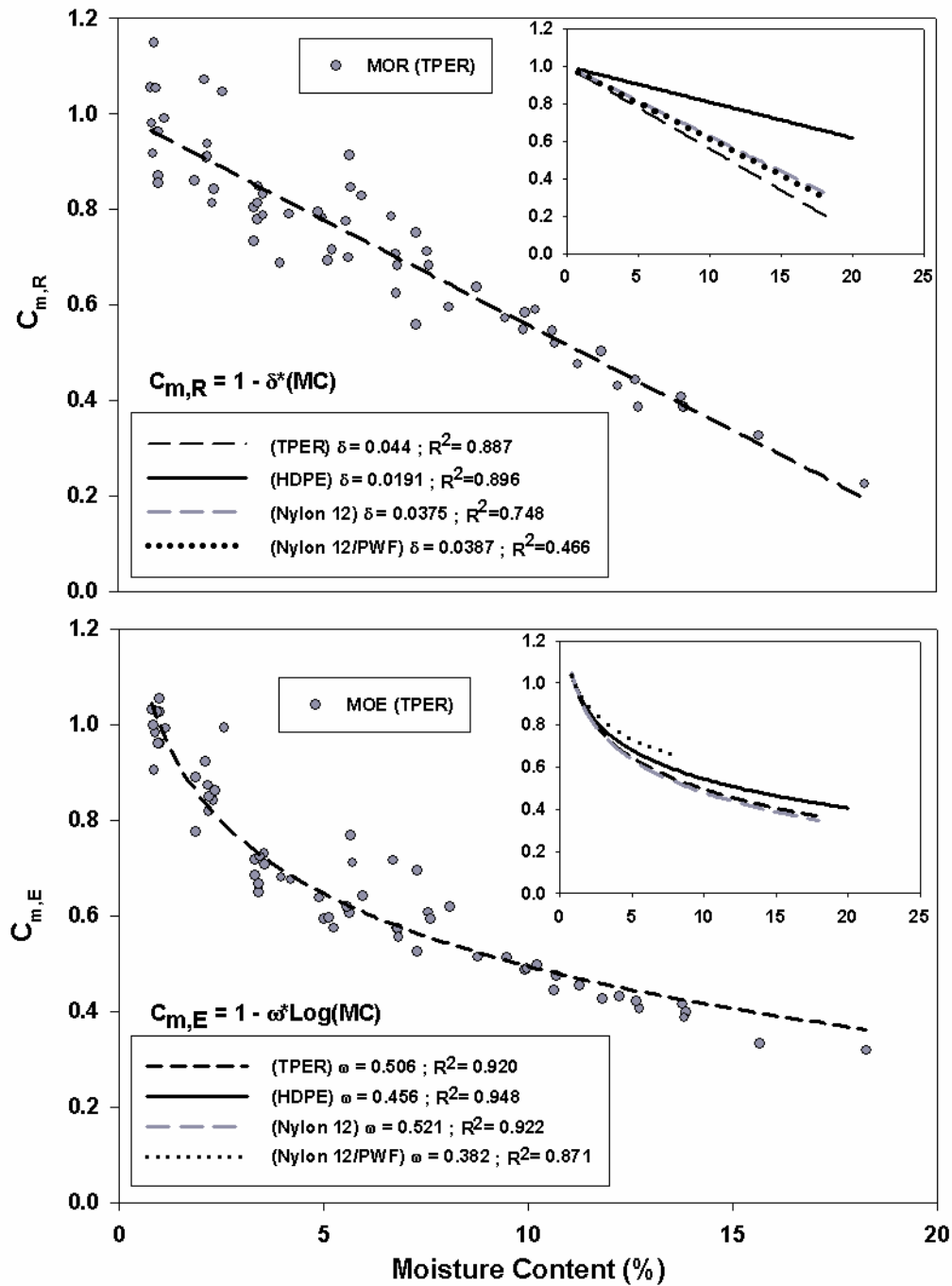


Figure 3.5. Moisture content vs. volumetric strain of WPCs.



**Figure 3.6.** Moisture Content modification factor,  $C_m$ , for MOR ( $C_{m,R}$ ) and MOE ( $C_{m,E}$ ) of WPCs.

## **CHAPTER 4 – APPLICATION OF ELASTICITY SHEAR-LAG MODELS TO WOOD-PLASTIC COMPOSITES**

### **4.1 Abstract**

Many mechanically based shear-lag models cannot accurately predict the modulus of short-fiber WPC composites. While traditional shear-lag theory is effective for natural fiber composite applications, it does not apply to hollow WPC fibers, which are filled and encased by a polymer matrix. The double shear-lag (DSL) model is more effective with WPCs, since their structure induces shear flow on the inner fiber surface. To validate the DSL model, this study explored the elasticity modulus for WPC samples of nylon 12, thermoplastic epoxy resin, and high density polyethylene with a natural fiber wood filler. Variation between DSL and modulus values resulted in an error between 0.2 to 21.8%, which is a significant improvement over shear-lag models proposed by Nardone and Prewo (1986), and Facca (2006). Use of the DSL model therefore provided a more consistent and accurate predictive method for WPCs modulus.

### **4.2 Introduction**

The development of wood-plastic composites (WPCs) is continually influenced by the introduction of new and improved thermoplastics, as well as the numerous wood species available. Currently, most WPCs are experimentally designed, and little research focuses on the computational prediction of mechanical properties. One of the most commonly used models for predicting the elasticity and strength of discontinuous fiber composites was derived by Cox et al. (1952), which later became known as shear-lag theory. To utilize Cox's shear lag model (CSLM), several simplifying assumptions regarding the composite system are required: 1) discontinuous fibers are uniformly aligned and packed within the matrix, 2) stresses are transferred via shear between the matrix and embedded fiber interface, 3) both matrix and fiber

are perfectly elastic, isotropic materials, and 4) yielding and slip between fiber and matrix can be ignored.

Researchers have modified this model for specific composite applications such as paper, structural geology, mica reinforced plastics, WPCs, and carbon fiber reinforced composites (Zhao, 1997; Lusi et al., 1973; Facca et al., 2006; Nardone and Prewo, 1986). Nairn (1997) developed improved relations for modeling axisymmetric composites through a continuum mechanics approach to the stress transfer process. Facca et al. (2006) applied Nairn's model to WPCs, adding methodologies to address fiber geometry and modulus corrections for hollow wood fibers. However, their application of this model to WPCs resulted in a substantial over-prediction of modulus, while traditional CSLM resulted in a significant under-prediction of properties (Facca, 2006). Therefore, the application of shear lag models to predict WPC properties still requires development.

Our research focused on the refinement of the CSLM as derived by Cox (1952) and later modified by Facca (2006) for application to WPCs. We proposed a refined shear lag model to incorporate the effects of polymer matrix penetration within the hollow wood fibre cavity and the variation in fiber alignment from melt flow processes. Finally, we validated the model for a variety of WPCs while also investigating the model sensitivity to specific variables.

## **4.3 Analytical Models**

### *4.3.1 Cox Shear Lag Model (CSLM)*

In deriving the CSLM, Cox assumed that the composite was tension-loaded and composed of an isotropic elastic matrix embedded with elastic cylindrical fibers that are discontinuous and oriented parallel to the applied stress (Figure 4.1a). The model ignored transverse stresses and strain discontinuities (i.e. slip) at the matrix-fiber interface. Cox did not

consider traction at the fiber ends, even those these forces can significantly influence composite properties (Zhao and Ji, 1997; Nardone and Prewo, 1986).

Cox's shear lag equation is based on a modified rule of mixtures, where the effectiveness of the fiber stiffness is adjusted by the factor  $\alpha$ :

$$E_c = \frac{\sigma_c}{\varepsilon_c} = \alpha \cdot E_f V_f + E_m V_m \quad \text{Eq. 4.1}$$

and  $\sigma$  is stress,  $\varepsilon$  is strain,  $E$  is the elastic modulus,  $V$  represents the volume fraction, subscripts c, m, and f denote the composite, matrix, and fiber components, respectively. Using the classical assumptions for Cox's shear lag theory, normal stress in the fiber is assumed to develop from zero at the fiber end to a maximum at half the fiber length ( $L/2$ ). By invoking global stress equilibrium for the free body diagram represented in Figure 4.1a the factor  $\alpha$  can be represented as:

$$\alpha = 1 - \frac{\tanh\left(\frac{\beta \cdot L}{2}\right)}{\left(\frac{\beta \cdot L}{2}\right)} \quad \text{Eq. 4.2}$$

where  $\beta$  is a variable that accounts for shear stress transfer. In representing  $\beta$ , Cox considered the Young's modulus of the fiber ( $E_f$ ) and the shear modulus of the matrix, which is represented here via the commonly used isotropic relation  $G_m = E_m/2(1+\mu_m)$  where  $\mu_m$  gives the Poisson's ratio. Cox derives the following relation for  $\beta$ :

$$\beta = \frac{1}{R_o} \cdot \left[ \frac{E_m}{E_f(1 + \mu_m) \cdot \ln\left(\frac{R}{R_o}\right)} \right]^{\frac{1}{2}} \quad \text{Eq. 4.3}$$

Here, Cox accounts for geometry using the equivalent fiber radius ( $R_o$ ), and fiber to fiber separation ( $R$ ), in which  $\ln(R/R_o)$  accounts for the fiber packing within the composite matrix (Figure 4.1a). This topic was addressed in shear lag analysis by Facca (2006) replacing  $\ln(R/R_o)$  with the more commonly used  $0.5 \cdot \ln(P_F/V_F)$ , where inter-fiber interactions are considered by the fiber volume fraction ( $V_F$ ), and packing factor ( $P_F$ ) defined as either hexagonal,  $P_F = 2\pi / \sqrt{3}$ , or square,  $P_F = \pi$ , packing configuration. Variations on Cox's derivation of the  $\alpha$  parameter have also been used by researchers to account for different phenomena not considered in the original model (Luisi et al., 1973; Zhao and Ji, 1997; Nairn, 1997; Nardone and Prewo, 1986).

#### 4.3.2 Previous Refinements for Applying CSLM to WPCs

Facca et al. (2006) applied the CSLM to predict elastic properties of wood-plastic composites. Several modifications were necessary, because basic assumptions were not consistent with material morphology. First, the individual elements comprising wood flour are typically bundles of several hollow wood fibers. Since these prismatic reinforcing elements are neither cylindrical nor of constant cross-section, Facca et al. estimated an equivalent outer radius,  $R_o$ , assuming negligible collapse of wood fibers during processing:

$$R_o = \frac{W + T}{\pi} \quad \text{Eq. 4.4}$$

where  $W$  is the fibre width, and  $T$  is the fiber thickness.

Secondly, Facca et al. adjusted the fiber modulus for both density and moisture content. These corrections are necessary because published values for  $E$  of different wood species assume (1) a moisture content higher than exists in the wood composite and (2) voids in hollow cells influence wood in its native form. In contrast, when wood functions as a reinforcing element in

the composite matrix, its moisture content is near zero due to thermal processing, and voids are often eliminated due to cell collapse or polymer filling. The moisture corrected fiber density,  $\rho_{mc}$ , is determined based on the tested moisture content of the fibre, MC, utilizing the following:

$$\rho_{mc} = \frac{G_B}{1 - \left[ 0.265 \left( \frac{30 - MC}{30} \right) \cdot G_B \right]} \quad \text{Eq. 4.5}$$

where  $G_B$  is the specific gravity of green wood. Then, the fiber modulus can be adjusted for MC using the following equation:

$$E_{MC} = \frac{E_{12}}{\left( \frac{E_{12}}{E_G} \right) \cdot \left[ \frac{(12 - MC)}{25 - 12} \right]} \quad \text{Eq. 4.6}$$

where  $E_{MC}$  is the fiber modulus corrected for moisture content, and  $E_{12}$  and  $E_G$  are the fiber modulus at 12% moisture content and green, respectively. Once corrections for MC have been performed, the final correction is made to account for density:

$$E_f = E_{MC} \cdot \left( \frac{\rho_{cw}}{\rho_{mc}} \right) \quad \text{Eq. 4.7}$$

where  $E_f$  is the fiber modulus corrected for moisture content and density, and  $\rho_{cw}$  is the fiber cell wall density. After this final adjustment,  $E_f$  represents an estimated Young's modulus for the fiber cell wall. This value will be much higher than that of the native wood because the void structure is effectively removed and is valid if the fibers are collapsed or filled during processing.

#### 4.3.3 Double Shear Lag (DSL) Model

A conceptual limitation to the Cox shear lag equation as applied by Facca (2006) is that it assumes only a single shear plane on the outer surface of the fiber. Although this scenario may

occur when wood fibers collapse during processing, the high pressures and temperatures used to process WPCs typically promote penetration of the molten polymer matrix into the fiber cavity (Figure 4.2). This creates two independent shear planes on the inner and outer surfaces of the polymer filled wood fibers.

The double shear lag (DSL) model proposed in this paper evaluates a composite with two shear surfaces which increase the overall stiffness of the final composite (Figure 4.1b). The new model considers an additional inner surface in which shear stresses are transferred between a polymer matrix and polymer-filled wood fiber along the inner and outer cell wall radius,  $R_i$  and  $R_o$ . Estimation of the inner radius can be derived by assuming cell wall mass is equivalent to the bulk fiber mass as given by:

$$\pi \left[ (R_o)^2 - (R_i)^2 \right] \cdot L \cdot \rho_{cw} = \pi (R_i)^2 \cdot L \cdot \rho_{mc} \quad \text{Eq. 4.8}$$

and then reduces to:

$$R_i = \left[ (R_o)^2 \cdot \left( 1 - \frac{\rho_{mc}}{\rho_{cw}} \right) \right]^{1/2} \quad \text{Eq. 4.9}$$

Having estimated the inner radius ( $R_i$ ) of the wood fiber, the CSLM must consider the shear stresses induced on both surfaces. The following is a general overview of modifications to the CSLM. A full derivation of the DSL model following a similar process used by Facca (2006) can be found in (Hatch, 2008b). Consider the equilibrium relation for the free body diagram represented in Figure 4.1b where the normal tensile stresses ( $\sigma_F$ ) are balanced by shear stresses ( $\tau$ ) at any given location ( $x$ ) along the fiber:

$$\frac{d}{dx} \sigma_f = \frac{-2 \cdot \tau_i}{R_i} + \frac{-2 \cdot \tau_o}{R_o} \quad \text{Eq. 4.10}$$

here subscripts (i) and (o) denote the inner and outer radius of the wood fiber. The normal tensile stresses in the composite are assumed to be a summation of shear stresses induced on each surface. From Eq. 4.10, using Hooke's law, isotropic relations, and  $R_i\tau_i = R_o\tau_o$ , the following second order partial differential equation is obtained:

$$\frac{d\sigma_f^2}{d^2x} = \left( \frac{1}{R_i^2} + \frac{1}{R_o^2} \right) \cdot \frac{-2 \cdot \left( \frac{-\varepsilon_c \cdot E_f + \sigma_f}{E_f} \right) \cdot E_m}{\ln\left(\frac{P_F}{V_f}\right) (1 + \mu_m)} \quad \text{Eq. 4.11}$$

which is simply a series form of that developed originally by Cox (1952). We then follow the initial solution but now consider the DSL to derive a definition for  $\beta_{i+o}$  :

$$\sigma_f = E_f \varepsilon_c + R \cdot \sinh(\beta_{i+o} \cdot x) + S \cdot \cosh(\beta_{i+o} \cdot x) \quad \text{Eq. 4.12}$$

where:

$$\beta_{i+o} = \left[ \left( \frac{1}{R_i^2} + \frac{1}{R_o^2} \right) \cdot \frac{2 \cdot E_m}{E_f (1 + \mu_m) \cdot \ln\left(\frac{P_F}{V_f}\right)} \right]^{\frac{1}{2}} \quad \text{Eq. 4.13}$$

To solve Eq. 4.12, boundary conditions must be considered. In the original CSLM, tractions at the fiber ends were ignored ( $\sigma_f(\pm L/2) = 0$ ), but this could cause significant under-prediction of the modulus when analyzing composites with small aspect ratio fibers (Zhao and Ji, 1997). Overcoming this obstacle, Nardone and Prewo (1986) assumed that the ends of the fibers were perfectly bonded to the composite matrix,

leading to the end condition that  $\sigma_f(\pm L/2) = \sigma_c$ . Using this boundary condition, we may integrate Eq. 4.12 from  $x = 0$  to  $L/2$  yielding the average fiber stress ( $\sigma_{f,avg}$ ) expression:

$$\sigma_{f,avg} = E_f \varepsilon_c \left[ 1 + \left( \frac{E_m}{E_f} - 1 \right) \cdot \frac{\tanh\left[\left(\beta_{i+o}\right) \cdot \frac{L}{2}\right]}{\frac{(\beta_{i+o}) \cdot L}{2}} \right] \quad \text{Eq. 4.14}$$

The final form of the DSL model then becomes:

$$E_c = E_f \left[ 1 + \left( \frac{E_m}{E_f} - 1 \right) \cdot \frac{\tanh\left[\left(\beta_{i+o}\right) \cdot \frac{L}{2}\right]}{\frac{(\beta_{i+o}) \cdot L}{2}} \right] \cdot V_f + E_m \cdot V_m \quad \text{Eq. 4.15}$$

This form of the shear lag equation (Eq. 4.14) is similar to that reported by Zhao and Ji (1997) based on the same boundary conditions proposed by Nardone and Prewo (1986). However,  $\beta_{i+o}$  is not equal to the  $\beta$  derived by Zhao and Ji (1997), as  $\beta$  is equivalent to the original  $\beta$  developed by Cox (1952).

#### 4.3.4 Modulus Fiber Orientation Modification

The shear lag models from both Cox and Facca (2006) assume the ideal condition that fibers are aligned parallel to the applied stress. However, this is not the case for WPCs where fibers are frequently oriented with some degree of rotation due to extensional flow characteristics during processing (Gacitua, 2008; Kim, 2001). Therefore, a modified fibre modulus,  $E_{F,mod}$ , must be incorporated for fiber misorientation. The orientation effect can be easily approximated by the following transformation equation (Agarwal and Broutman, 1990):

$$E_{F, \text{mod}} = \frac{E_F}{\cos^4 \theta + \left( \frac{E_1}{G_{12}} - 2 \cdot \mu_{12} \right) \sin^2 \theta \cdot \cos^2 \theta + \frac{E_1}{E_2} \cdot \sin^4 \theta} \quad \text{Eq. 4.16}$$

where  $\theta$  is the mean fiber orientation angle in radians with respect to the loading direction. The anisotropic elastic constants for the fiber are defined as:  $E_1$  is the longitudinal modulus,  $E_2$  is the transverse modulus,  $G_{12}$  is the modulus of rigidity, and  $\mu_{12}$  is the Poisson's ratio (Wood Handbook, 1999). Replacing  $E_F$  with  $E_{F, \text{mod}}$  in Eq. 4.13 and 4.15 will therefore account for fiber orientation caused by molding of WPCs given a known mean fiber orientation angle,  $\theta$ .

## 4.4 Experimental Materials and Methods

### 4.4.1 Experimental Materials

Four WPCs composed primarily of wood flour and thermoplastics were selected from previous research for model validation (Hatch, 2008a; Facca, 2006; Facca et al., 2006). Thermoplastics used for the nylon 12 and thermoplastic epoxy resin (TPER) WPCs consisted of either nylon 12 (Grilamid L 20 G, MFI: 20, density: 1.01g/cm<sup>3</sup>), supplied by EMS-Chemie (Sumter, SC) or TPER (L-TE05-10, MFI: 10), provided by L&L Products (Romeo, MI). These composites were produced with between 0 to 60-wt % (50% for TPER) 60-mesh pine (*Pinus spp*) flour (American Wood Fibers, Schofield, WI). To facilitate molding, OPE629A, a lubricant of oxidized polyethylene homopolymers (Honeywell, Morristown, NJ) was incorporated at 2% and 3% for TPER and nylon 12 WPCs, respectively, in all formulations. WPCs were processed using extrusion compounding followed by injection molding to form flexure specimens (3 x 12 x 127 mm), which were tested according to ASTM D790 (Hatch, 2008a).

Data presented by Facca (2006b) for WPCs produced with high-density polyethylene (HDPE) (Formolene HB5502B, MI: 0.35, density:  $0.955 \text{ g/cm}^3$ , produced by CCC Plastics) was also used for model validation. These composites were produced with between 10 to 60-wt% 20-mesh and 40-mesh oak wood flour provided by American Wood Fibers (Schofield, WI) and did not include lubricant. . Facca (2006b) first compounded the composite material, molded it into puck shaped coupons, reheated the material to  $160^\circ\text{C}$  and compression molded it into tension specimens ( $3.18 \times 12.7 \times 356 \text{ mm}$ ). The compression mold was designed for one-dimensional extensional flow. Each specimen was tested in tension according to ASTM 638.

#### 4.4.2 Methods

Modeling of the composite modulus required several material properties, which are listed in Table 4.1. The wood fiber moisture content (MC) was obtained by oven drying the fibers at 100 to  $110^\circ\text{C}$  for 6 – 12 hours (Hatch, 2008; Facca, 2006b). Variability apparent in Table 4.1 between oak and pine MC can be linked to additional drying of the pine wood flour in a steam tube dryer prior to processing. The cell wall density,  $\rho_{\text{cw}}$ , was assumed to be  $1.50 \text{ g/cm}^3$ , respectively (Wood Handbook, 1999; Facca, 2006b). Mean fiber dimensions L, T, and W (where  $T \approx W$  for 60-mesh pine) were estimated ( $n \geq 200$ ) with an optical microscope (Table 4.1). Fiber packing,  $P_F$ , was assumed to be square ( $P_F = \pi$ ) following WPC modeling by Facca (2006b).

Additional fiber properties were determined using the Wood Handbook (1999), assuming eastern white pine (*Pinus strobus*), which included: specific gravity of green wood ( $G_B = 0.34$ ), flexural modulus of elasticity at 12% MC and green ( $E_{12} = 9.35 \text{ GPa}$ ,  $E_G = 7.48 \text{ GPa}$ ), and Poisson's ratio ( $\mu_{12} \cong 0.35$ ). General fiber properties for oak hardwood were reported by Facca (2006a) and originated from the Wood Handbook (1999) (Table 4.1). The Poisson's ratio for the

matrix polymers was assumed in all cases to be equal to 0.35, variation of this parameter had no significant affect on the model predictions of modulus.

The final assumption corrects fiber misorientation in the composite. Gacitua (2008) measured mean particle orientation on HDPE samples produced with the same mold as the TPER and nylon samples in this study. His results estimated the mean angle,  $\theta$ , as 12.5°. The same orientation angle was utilized for Facca's compression molded samples, since it was reported that molding flow properties (one-dimensional extensional flow) and specimen size were similar to injection molded samples by Gacitua (2008). Using elastic ratio values reported in the Wood Handbook (1999),  $E_2/E_1$  and  $E_1/G_{12}$  were averaged for each species grouping.

#### **4.5 Results and Discussion**

Three shear lag models were evaluated and compared to WPC experimental data reported by Hatch (2008) and Facca (2006a). These modes were: (1) the CSLM as evaluated by both Cox (1952) and Facca et al. (2006), (2) Nardone and Prewo (1986) as derived by Zhao and Ji (1997), and (3) the double shear-lag (DSL) model proposed in this paper. In TPER and nylon 12 WPCs, the effect of 2-3% lubricant was compensated for in modeling by determining the polymer matrix modulus,  $E_m$ , for pure polymer specimen containing the respective lubricant percentage.

Application of the DSL model to each of the four WPCs correlated very well to existing experimental data (Figure 4.3-4). With increasing fiber volume fraction ( $V_f$ ), in the composites the model adequately simulates the trend of increasing MOE exhibited for each WPC. Excellent results were obtained for 40 mesh oak /HDPE composites, in which the DSL model ( $\theta = 12.5^\circ$ ) provides nearly an exact prediction, deviating between only 0.3 – 3.8% error (Table 4.2).

Results for nylon 12, TPER, and 20 mesh oak/HDPE were reasonable, but not as persuasive, with maximum errors reaching up to 16.9, 11.8, and 21.0%, respectively. However, focusing on

the nylon 12 and 20 mesh Oak/HDPE at  $V_f < 35\%$  reduces the maximum calculated error to 12.4 and 13.1%, respectively. As shown in Table 4.2 and Figures 4.3-4, the DSL model tends to under-predict by 5 to 15 % in most cases.

Although still in need of improvement, the DSL model provides much more accurate predictions of composite modulus than the other models. Both the CSLM and Nardone and Prewo (1986) models tend to under-predict the modulus of WPC's (Figure 4.3-4). Facca (2006a) presented similar results and observations for the CSLM model. Although the DSL, CSLM and Nardone and Prewo (1986) models each under-predict modulus, observations noted in Figure 4.3 and 4.4 clearly show that the DSL model provides a much more accurate and consistent assessment of modulus. The DSL model provides more accurate assessments by conceptually incorporating two matrix-fiber shear surfaces that were lacking in the original CSLM model. The DSL model was further enhanced by considering tractions at fiber ends, suggested by Nardone and Prewo (1986). As stated previously, ignoring tractions in fibers with small aspect ratios further reduces the accuracy of the model prediction.

Fiber aspect ratio, not particle size, significantly influences WPC mechanical properties, including modulus (Stark and Rowlands, 2003). To assess the influence of fiber aspect ratio on the DSL model prediction,  $L/R_o$  for the fiber was varied from 6 to  $\infty$  (Figure 4.5). It follows from  $L/R_o \rightarrow \infty$  that Eq. 4.15 approaches the ROM equation as expected. Fiber aspect ratios for the outer ( $L/R_o$ ) and inner ( $L/R_i$ ) fiber surface are reported in Table 4.1 for each WPC. The inner fiber aspect ratio is much larger than the outer, assuming that the fiber length ( $L$ ) is applicable to both surfaces. This means that the inner fiber surface has a greater influence on the modulus than the outer surface, and both are considered in the term,  $\beta_{i+o}$ . Comparison of 40 mesh and 20 mesh oak reveals that the fiber aspect ratio ( $L/R_o$ ) varies significantly between the two, although

experimental modulus data for both composites is similar. Therefore, the excellent fit of the DSL model to the 40 mesh Oak/HDPE composite follows from analysis of the higher aspect ratio fiber.

Another wood fiber property important when comparing a wide range of wood species is the bulk specific gravity of green wood,  $G_B$ , which directly affects fiber modulus,  $E_f$ , when Eq. 4.5 is applied to Eq. 4.6. The significance of  $G_B$  is further evident in comparisons made in Figure 4.6 for both nylon 12 and TPER WPCs. Increasing  $G_B$  from 0.3 to 0.7 reduces the modulus prediction more significantly for TPER WPCs, due to the relatively high initial matrix modulus,  $E_m$ . Overall, the DSL model and experimental data show consistent correlation when considering the wood species oak ( $G_B = 0.60$ ) in Figure 4.4 and pine ( $G_B = 0.34$ ) in Figures 4.3. The flexural modulus of both wood fiber ( $E_f$ ) and matrix ( $E_m$ ) are specific to wood species and polymer type, respectively. Increasing either  $E_f$  or  $E_m$  will result in a higher predicted composite modulus as evident in Figure 4.7. These figures indicate that changes in the matrix modulus, although much smaller than the fiber modulus, have a larger affect on overall composite stiffness.

Several reasons for variability between each WPC, may be due to processing influences specific to each formulation. For each WPC, it was assumed that  $\theta$  is constant for all  $V_f$ . According to Kim (2001), orientation of fibers varies at high wood contents in injection molded WPCs due to the influence of fiber interaction. In TPER WPCs the rate of modulus increase at  $V_f > 20\%$  appears to slow, which did not occur for the other WPCs evaluated. Hatch (2008) found that at higher  $V_f$ , molding of TPER WPCs became more difficult, possibly contributing to increased mis-alignment of fibers. The influence of mean fiber orientation,  $\theta$ , on the DSL model for TPER and nylon 12 WPCs is presented in Figure 4.8.

Additional DSL model validation is recommended if the model is applied to other wood fiber species or polymer systems, as problems can arise where specific conditions are not considered by the model such as: processing method, ineffective polymer penetration, and fiber collapse.

#### **4.6 Conclusions**

Shear lag models proposed by Facca (2006b) and Nardone and Prewo (1986) were applied to four WPCs. Both models were found to be inadequate at accurately predicting the composite modulus. Derivation of the basic shear-lag theory (Cox et al., 1952) for both models clearly showed the shortcomings of these two models. First, shear-lag theory assumes a solid cylinder embedded in a polymer matrix, although wood fiber consists of hollow tubes ideally filled and encased by the polymer matrix. To include the inner fiber/matrix surface, we added an additional shear term to the DSL model. Tractions at fiber ends were also ignored by Cox and Facca, which reduced the predicted modulus for composites with small fiber aspect ratios. Nardone and Prewo modified their model to incorporate such stresses, and the final DSL model considers this. One additional variation was made to correct for fiber mis-alignment by modifying the fiber modulus according to a mean fiber orientation.

Application of the DSL model to experimental data for several WPCs clearly displayed improvement over previous shear-lag models. Further, sensitivity to orientation, wood fiber specific gravity,  $G_B$ ,  $E_f$ ,  $E_m$ , and fiber aspect ratio clearly indicate the robustness of this model. The application of the DSL model should be reassessed for each WPC, as several critical assumptions can be violated by poor polymer penetration, fiber collapse, and influences associated with processing.

## 4.7 References

- Agarwal, B.D., Broutman, L.J., Analysis and Performance of fiber composites. John Wiley & Sons Inc., p.59, 1990.
- Chin, W., Liu, H., Lee, Y., "Effects of Fiber Length and Orientation Distribution on the Elastic Modulus of Short Fiber Reinforced Thermoplastics." *Polymer Composites*, Vol. 9, No. 1, pp.27-35, 1988.
- Cox, H.L., "The elasticity and strength of paper and other fibrous materials." *British Journal of Applied Physics*, Vol. 3, pp. 72-79, 1952.
- Facca, A.G., "Predicting Tensile Strength and Modulus of Single and Hybrid Natural Fibre Reinforced Thermoplastic Composites." Doctoral Thesis, University of Toronto, Toronto, Canada, 2006.
- Facca, A.G., Kortschot, M.T., Yan, N. "Predicting the Elastic Modulus of Natural Fibre Reinforced Thermoplastics." *Composites Part A*, Vol. 37, pp. 1660-1671, 2006.
- Gacitua, W. G., "Influence of Wood Species on Properties of Wood /HDPE Composites." Doctoral Thesis, Washington State Univ., Pullman, WA, May 2008.
- Hatch, M., "Processing, Mechanical, and Environmental Performance of Engineering Polymer Wood-Plastic Composites." Master's Thesis, Washington State Univ., Pullman, WA, Chpt. 2, April 2008a.
- Hatch, M., "Processing, Mechanical, and Environmental Performance of Engineering Polymer Wood-Plastic Composites." Master's Thesis, Washington State Univ., Pullman, WA, Appendix E, April 2008b.
- Kim, E.G., Park, J.K., Jo, S.H., "A study on fiber orientation during the injection molding of fiber-reinforced polymeric composites (Comparison between image processing results and numerical simulation)." *Journal of Materials Processing Technology*, Vol.111, pp. 225-232, 2001.
- Lusis, J., Woodhams, R. T., Xanthos, M., "The Effect of Flake Aspect Ratio on the Flexural Properties of Mica Reinforced Plastics." *Polymer Engineering and Science*, Vol. 13, No. 2, pp. 139-145, 1973.
- Nairn, J.A., "On the use of shear-lag methods for analysis of stress transfer in unidirectional composites." *Mechanics of Materials*, Vol. 26, pp.63-80, 1997.
- Nardone, V.C., Prewo, K.M., "The Strength of Discontinuous Silicon Carbide Reinforced Aluminum Composites." *Scripta Metallurgica*, Vol. 20, pp. 43-48, 1986.

Stark, N.M., Rowlands, R.E., "Effects of Wood Fiber Characteristics on Mechanical Properties of Wood/Polypropylene Composites." *Wood and Fiber Science*, Vol. 35, No. 2, pp. 167-174, 2003.

"Wood Handbook - Wood as an Engineering Material." Madison, WI: U.S. Department of Agriculture, Forest Service, Forest Products Laboratory, Gen. Tech. Rep. FPL-GTR-113, 1999.

Zhao, P., Ji, S., "Refinements of shear-lag model and its applications." *Tectonophysics*, Vol. 279, pp 37-53, 1997.

## 4.8 Tables

**Table 4.1.** Data input for shear-lag models.

	<b>Properties</b>	<b>TPER 60-mesh Pine</b>	<b>Nylon 12 60-mesh Pine</b>	<b>HDPE* 20-mesh Oak</b>	<b>HDPE* 40-mesh Oak</b>	
Composite	Moisture Content (MC%): $\theta$ :	2.0		5.47	7.92	
		12.5° (0.218 rad.)				
Matrix	$E_m$ (GPa): $\mu_m$ :	2.64	1.06	1.07		
		0.35				
Flour (measured)	Fiber Length, L( $\mu\text{m}$ ): Fiber Width, W( $\mu\text{m}$ ): Fiber Thickness, T( $\mu\text{m}$ ):	329 66 66		1640 500 172	1220 343 45	
Solid Wood**	Species:	Eastern White Pine		Oak*		
	$G_B$ :	0.34		0.60		
	$E_1$ (GPa)   MC = 12%	Green	9.35		12.0	
			7.48		9.2	
	$\mu_{12}$ :	0.35		0.35		
	$E_1/E_2$ :	13.3		11.8		
	$E_1/G_{12}$ :	13.3		10.0		
Computed or Assumed Wood	$R_o$ ( $\mu\text{m}$ ): $R_i$ ( $\mu\text{m}$ ): $\rho_{cw}$ ( $\text{g}/\text{cm}^3$ ):	42 36		124 87	214 150	
		1.5				

\* Data adapted from Facca et al. (2006)  
\*\* Estimated average from Wood Handbook (1999)

**Table 4.2.** DSL model ( $\theta = 12.5^\circ$ ) error for TPER, Nylon 12, and HDPE WPCs.

<b>Fiber Volume Fraction</b>	<b>% Error</b>		<b>Fiber Volume Fraction</b>	<b>% Error</b>	<b>Fiber Volume Fraction</b>	<b>% Error</b>
	<b>TPER / 60 mesh Pine</b>	<b>Nylon 12 / 60 mesh Pine</b>		<b>HDPE / 20 mesh Oak</b>		<b>HDPE / 40 mesh Oak</b>
0.138	10.2	11.5	0.057	9.8	0.058	1.4
0.207	11.8	13.5	0.115	6.7	0.122	4.2
0.276	7.5	11.2	0.180	12.8	0.191	-0.2
0.345	4.2	14.7	0.254	12.6	0.262	1.1
0.414	-	19.2	0.323	13.9	0.347	-2.9
-	-	-	0.403	21.8	0.426	-0.7

### 4.9 Figures

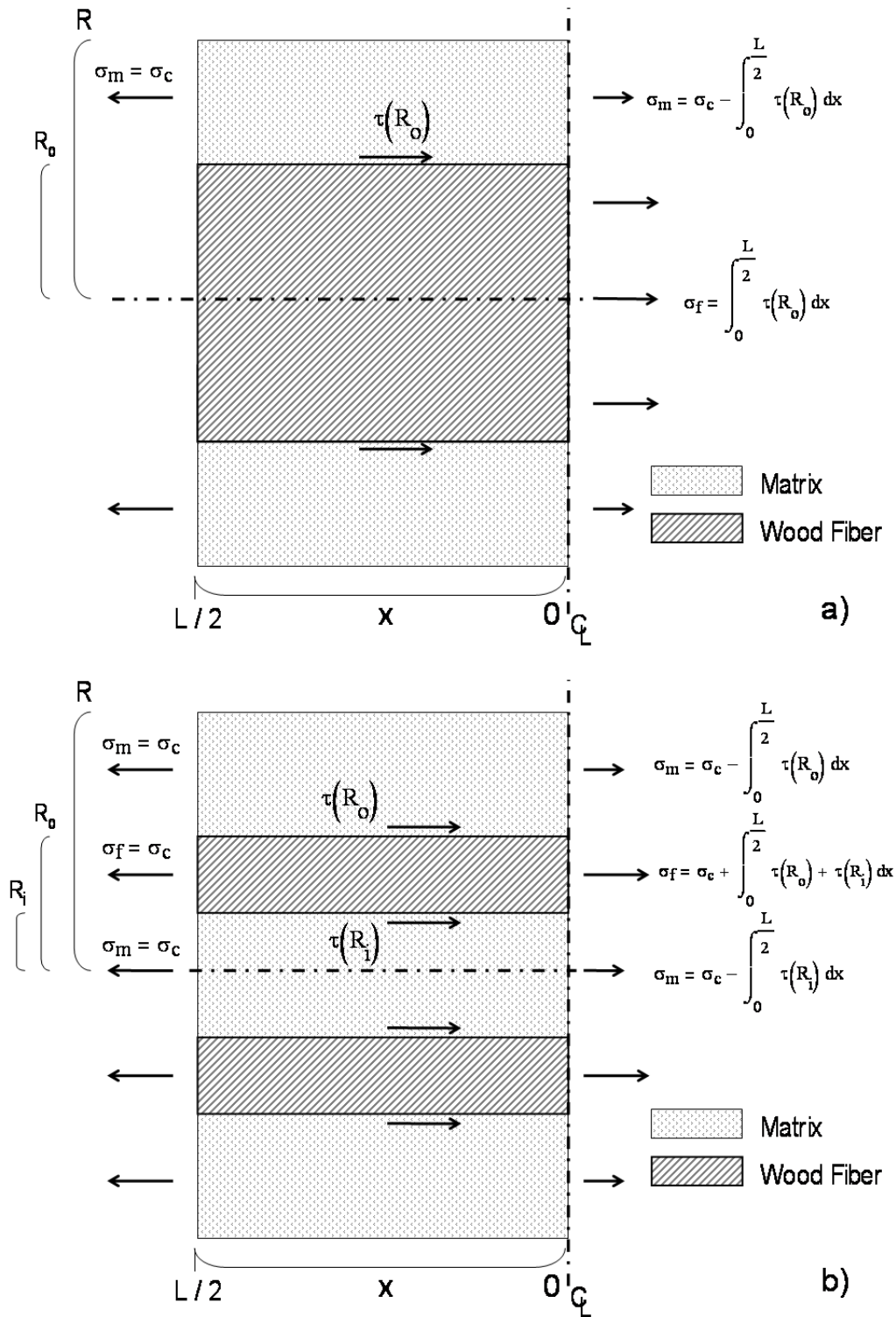


**Figure 4.1.** Cylindrical fiber embedded in polymer matrix with tension stress applied to the polymer matrix @  $x = L/2$  (fiber end) according to a) Cox Shear Lag Theory (Cox, 1952) and b) Double Shear Lag (DSL) model.

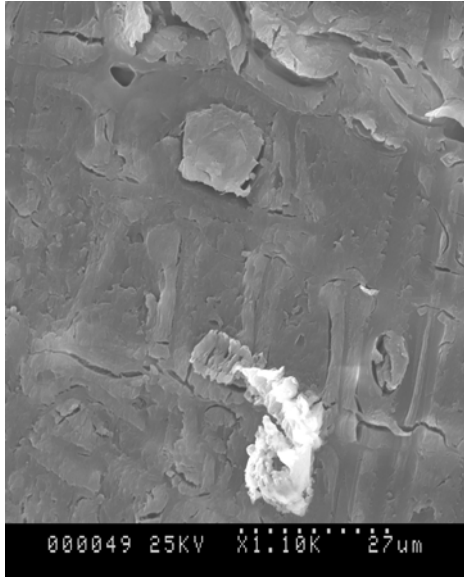


**Figure 4.2.** Scanning electron microscope (SEM) image of TPER WPC.

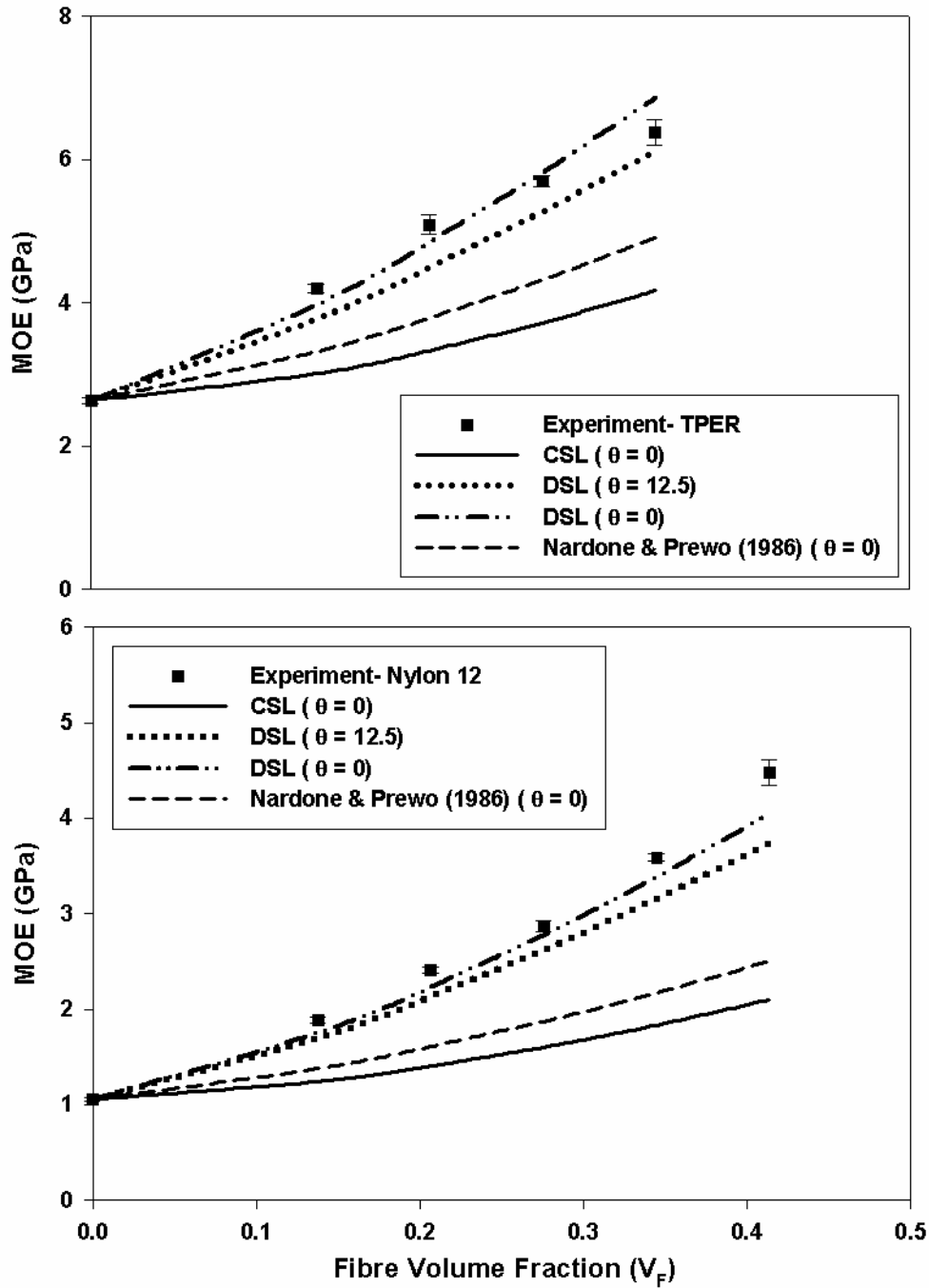


**Figure 4.3.** Comparison of MOE vs. fiber volume fraction for injection molded TPER and nylon 12 WPCs using shear lag and DSL models (Data adapted from Hatch, 2008a).

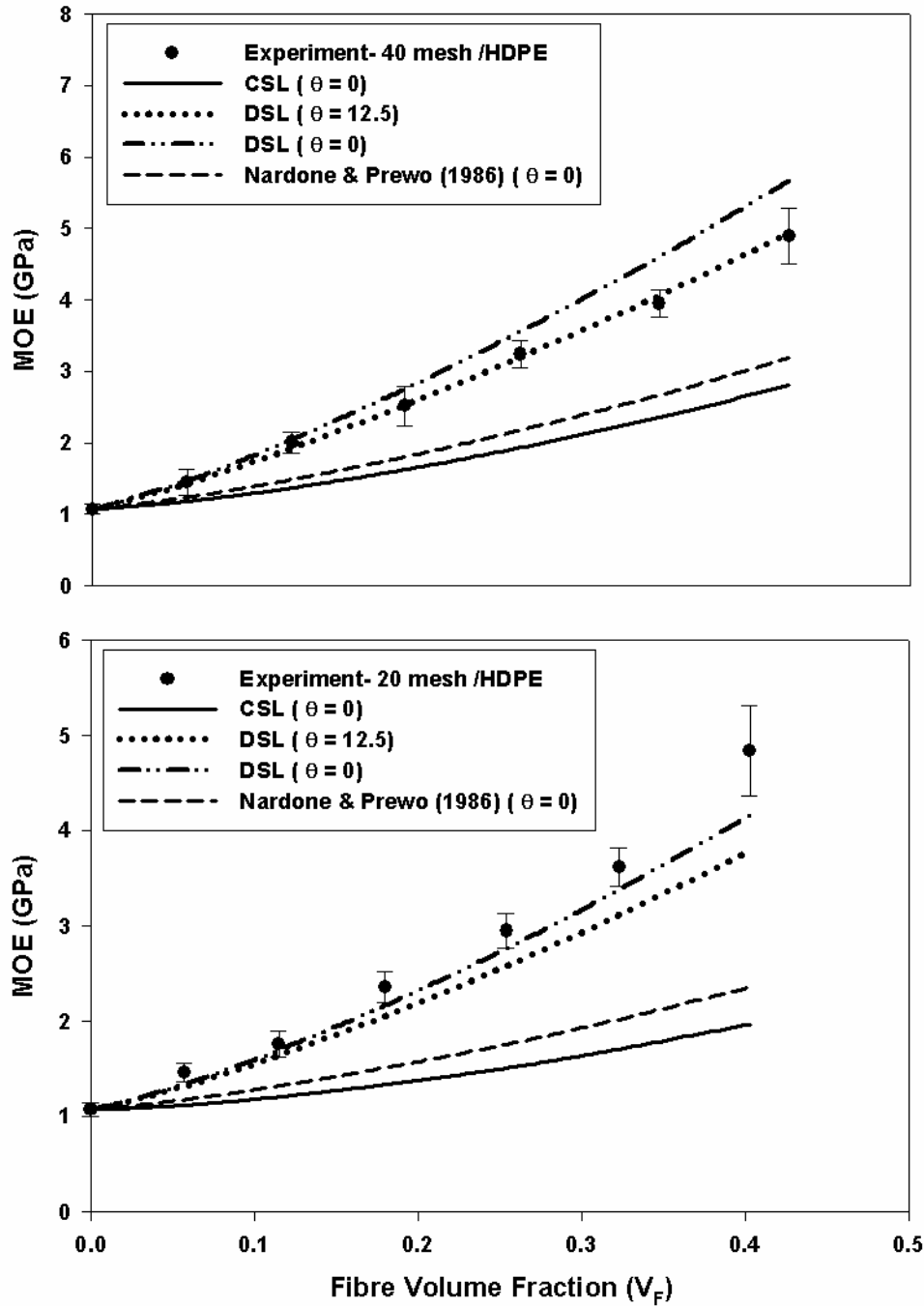


**Figure 4.4.** Comparison of predicted MOE vs. fiber volume fraction for compression molded 20 mesh oak WF/ HDPE and 40 mesh oak WF/HDPE using DSL and shear lag models (Data adapted from Facca, 2006).

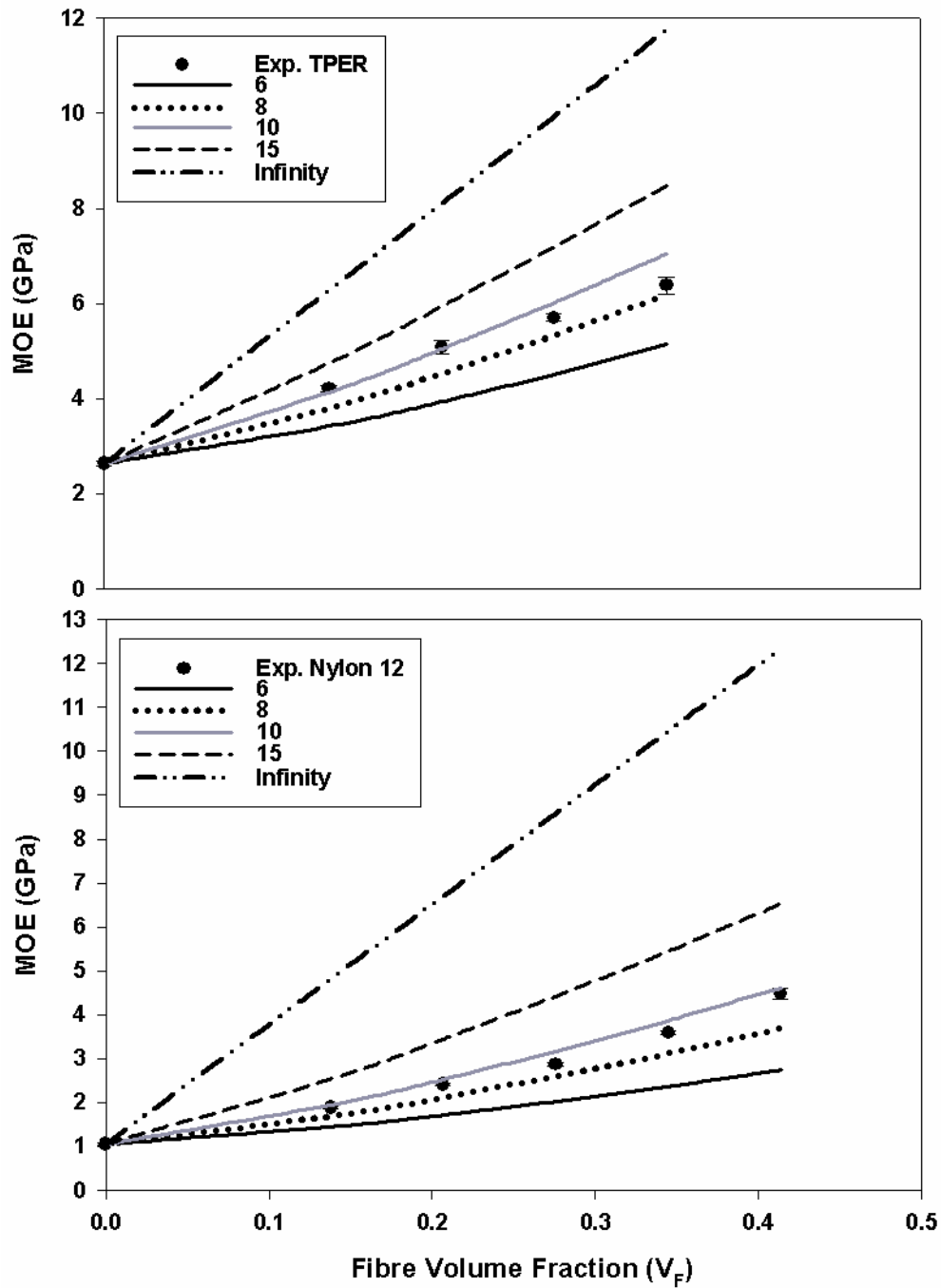


**Figure 4.5.** DSL model ( $\theta = 12.5^\circ$ ) curve predictions for varying fiber aspect ratios ( $L/R_o$ ) from 6 to  $\infty$  for nylon 12 and TPER WPCs (Data adapted from Hatch, 2008a).

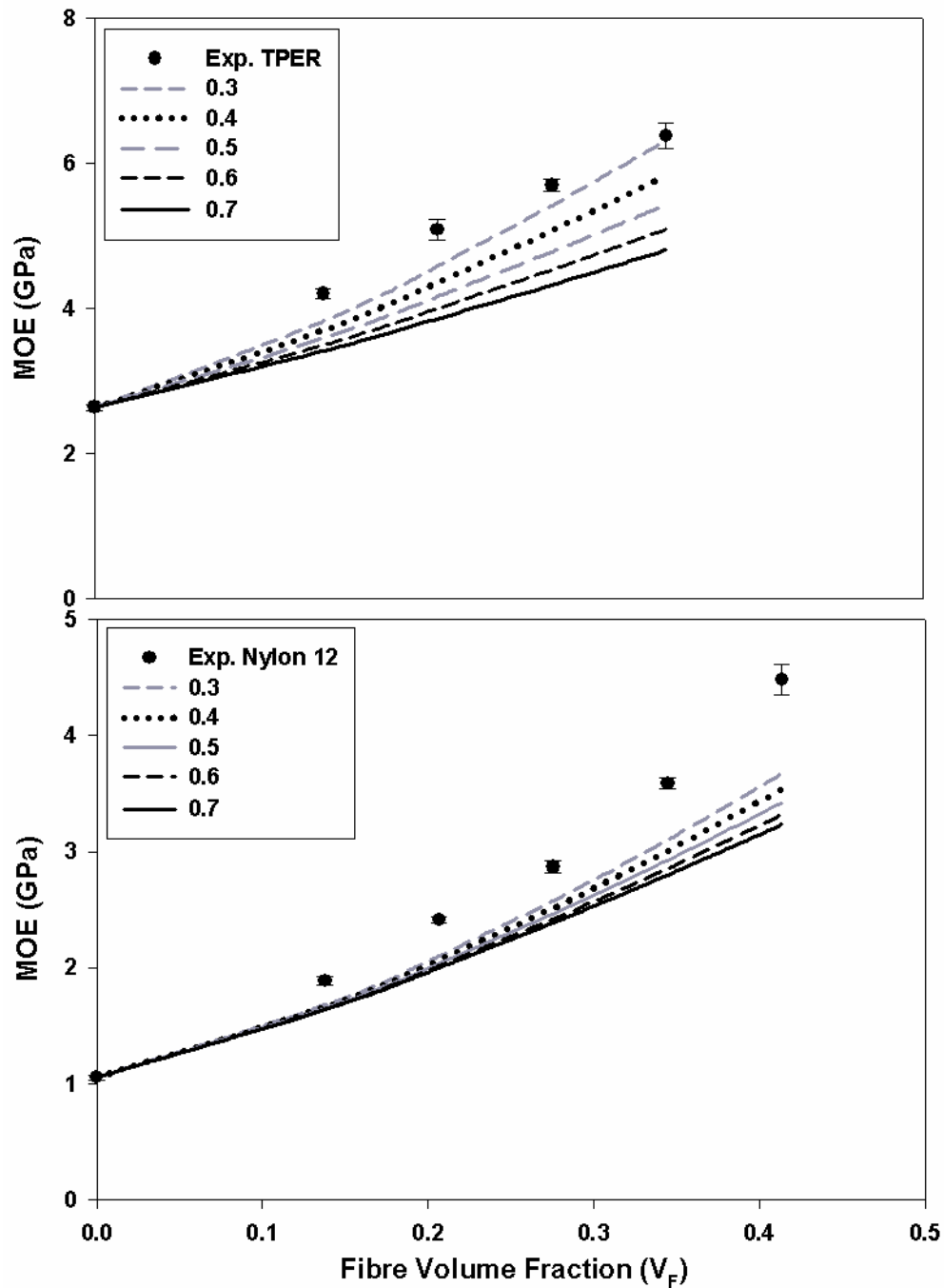


**Figure 4.6.** DSL model ( $\theta = 12.5^\circ$ ) curve predictions for varying fiber bulk specific gravities ( $G_B$ ) from 0.3 to 0.7 for nylon 12 and TPER WPCs (Data adapted from Hatch, 2008a).

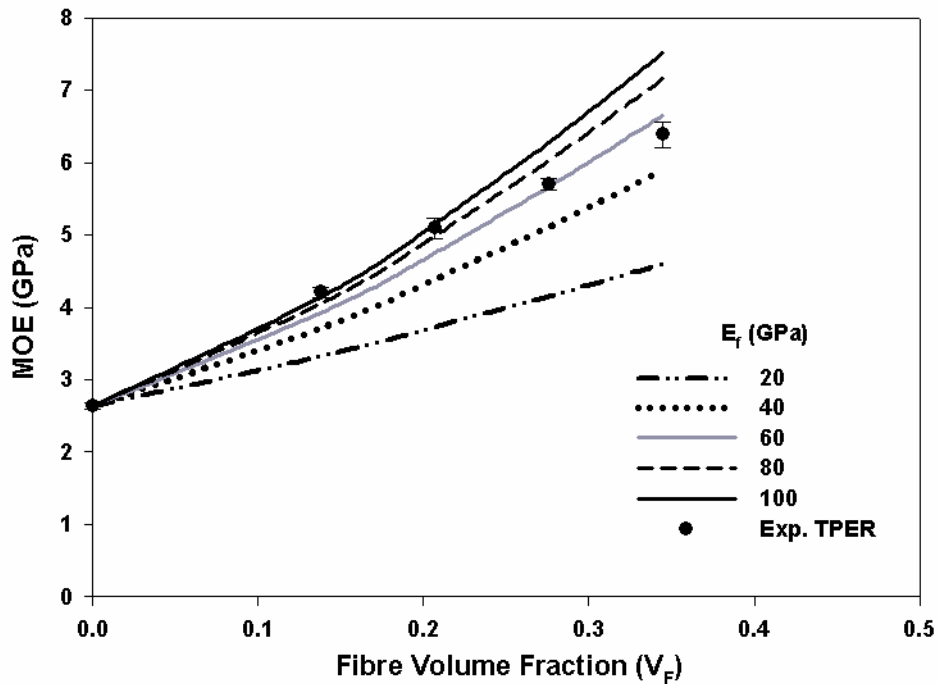
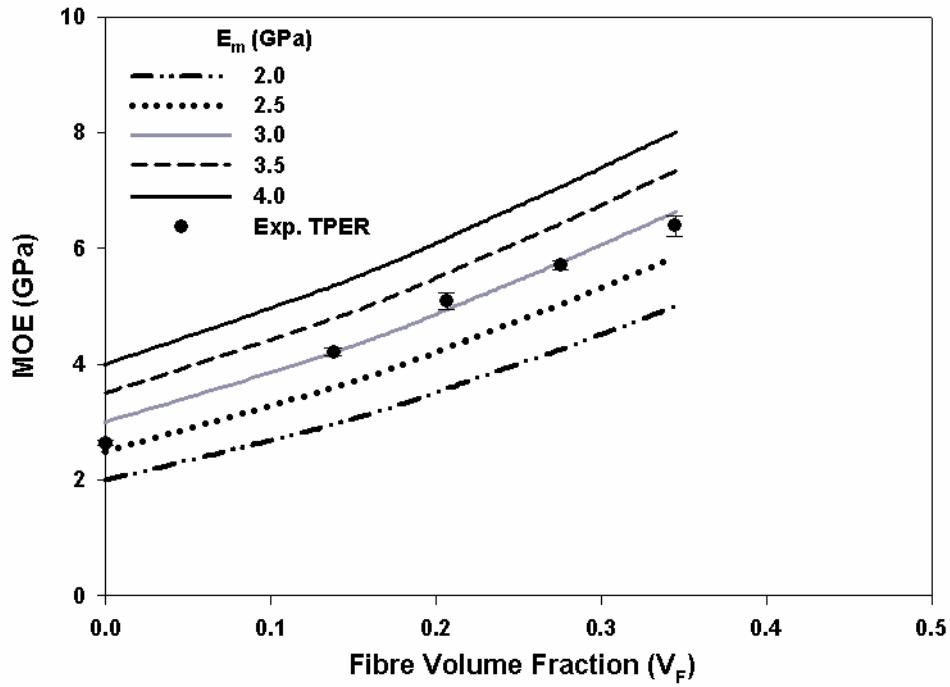


**Figure 4.7.** DSL model ( $\theta = 12.5^\circ$ ) curve predictions for varying matrix moduli ( $E_m$ ) and wood fiber moduli ( $E_f$ ) for TPER WPCs (Data adapted from Hatch, 2008a).

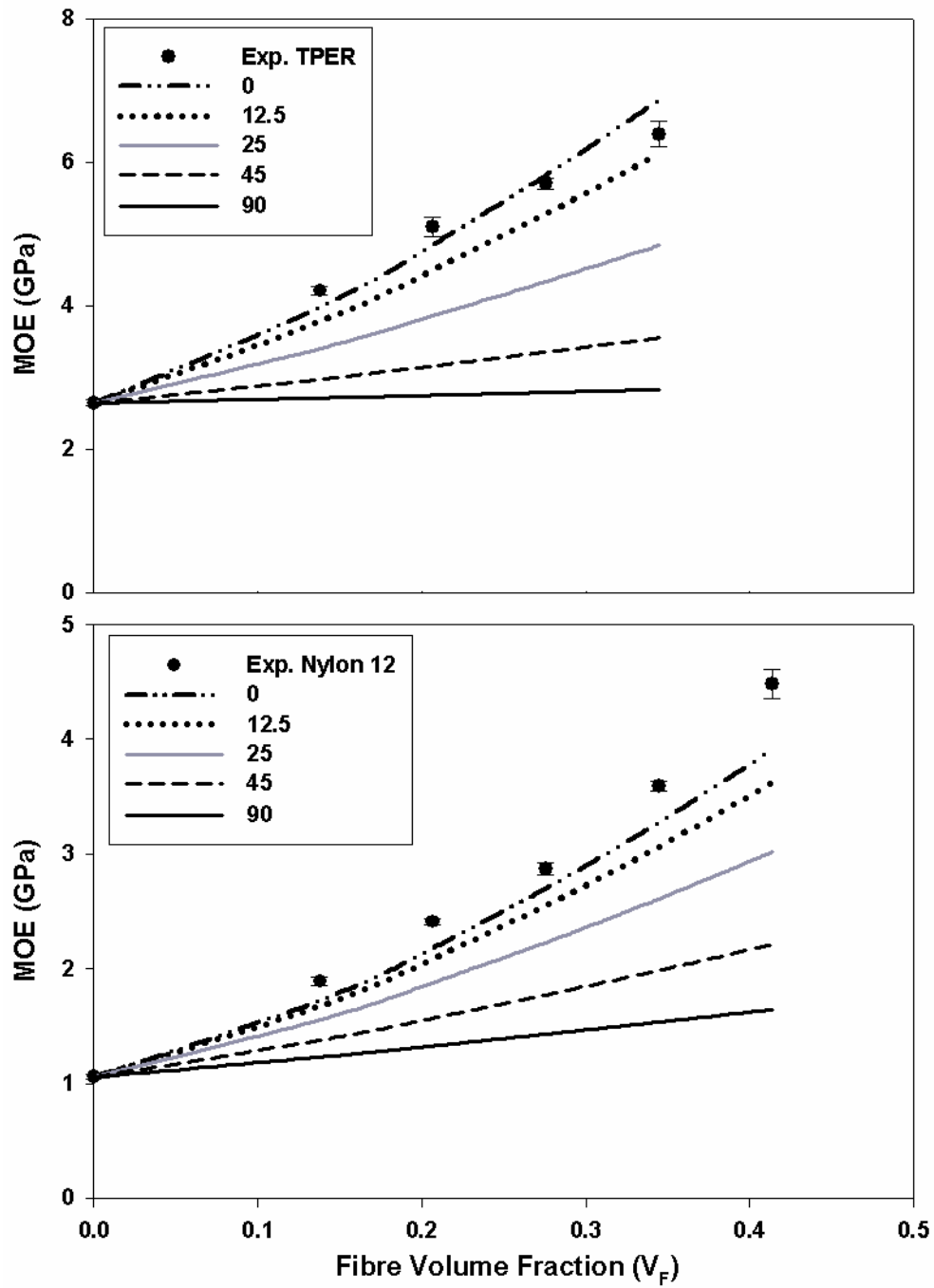


**Figure 4.8.** DSL model curve predictions for  $\theta$  from 0 to 90° for nylon 12 and TPER WPCs (Data adapted from Hatch, 2008a).

## CHAPTER 5 – CONCLUSIONS AND FUTURE WORK

### 5.1 Conclusions

Current extruded wood-plastic composite (WPC) formulations containing polyethylene (PE), polyvinylchloride (PVC), and polypropylene (PP) have been developed for many low strength applications. Future development of structural WPCs requires the development of new, higher strength WPCs. Previous research has found that engineering thermoplastics nylon 12 and thermoplastic epoxy resin (TPER) exhibit superior strength characteristics to traditional polyolefin polymers, and that both polymers show good adhesion to wood fiber. However, extrusion of these composites has been largely ignored due to the high processing temperature of nylon 12 and unfamiliarity with commercial TPER resins. The three primary goals of this research were to; 1) develop an extrusion processing methodology, 2) mechanically characterize and accurately model modulus for each composite with respect to formulation design, and 3) assess the impact of environmental factors including moisture and temperature on performance of TPER and nylon 12 WPCs.

A reverse extrusion profile was selected for nylon 12 and TPER WPCs to ensure adequate melt consolidation of the polymer and wood flour components. Addition of the lubricant OPE629A at 2 and 3-wt% for TPER and nylon 12 composites, respectively, was found to provide the best flow characteristics while minimizing effects on mechanical performance. Although thermal degradation might play a role in nylon 12 WPC performance at processing temperatures reaching 225°C, testing was inconclusive as to the extent of this influence. Increases in wood content improved composite strength and stiffness, indicating good adhesion of nylon 12 and TPER matrices to the wood flour component.

TPER and nylon 12 WPCs exhibited mechanical performance sensitivity to moisture content and environmental temperature changes, so that increases in moisture content or temperature reduced strength and stiffness. TPER composites were the least affected by temperature changes, followed by nylon 12 composites. Nylon 12 composites had the lowest comparative moisture absorption rate, especially using heat treated wood, followed by TPER composites and then traditional high density polyethylene (HDPE) WPCs. However, mechanical properties of both TPER and nylon 12 composites were more sensitive than HDPE to moisture, based on % change.

We developed a double shear-lag (DSL) model, based on a modification of the original shear-lag theory, for use with WPCs by considering a polymer filled hollow fiber encased in a polymer matrix. This improvement takes into account WPCs' fiber structure and composition. Additional corrections were made to consider fiber orientation, wood fiber moisture content, and fiber modulus for hollow fibers. Comparison of several shear lag models showed that the DSL model more accurately and consistently reproduced modulus data as well as trends. Variability between 0.3 – 21% in extreme cases was related to assumptions inherent in the model, such as perfect adhesion of the matrix and fiber interface, no induced transverse stresses, a geometrically symmetric cross section, and negligible processing impacts on material properties. Overall, the DSL model provided a superior prediction method to existing modulus modeling techniques based on shear-lag theory.

This study has provided a better understanding of extruded nylon 12 and TPER WPCs mechanical performance. Determinations were made as to the impact of moisture, temperature, and extrusion processing on MOR, MOE, and strain to failure. Mechanical properties of

extruded nylon 12 and TPER WPCs indicate significant potential in structural composite applications.

## **5.2 Future work**

The scope of this paper addresses only the initial phase of development for extruded TPER and nylon 12 WPCs. More research is needed to investigate the potential of these composites with respect to ultraviolet sensitivity, impact resistance, creep, cyclic weathering, and other factors affecting WPC performance. Further analysis of thermal properties should be performed, since preliminary data was inconclusive regarding molecular influences that affect nylon 12 and TPER WPCs. Heat treatment of wood fibers prior to WPC extrusion may also prove promising for increasing decay resistance, as this study showed that it significantly reduced moisture absorption in WPCs.

## **APPENDIX**

# **APPENDIX A – PROCESSING INFLUENCES ON THERMAL DEGRADATION OF EXTRUDED NYLON 12 COMPOSITES**

## **A.1 Introduction**

In previous research, nylon 12 was shown to have significant potential for use in wood-plastic composites (WPCs) due to its high strength properties (Hatch, 2008). However, processing temperatures above 200°C can produce volatiles from wood degradation, which affects material properties during the extrusion process. Lu et al. (2007) observed through thermo-gravimetric analysis (TGA) that the combination of wood and nylon 12 altered degradation compared to other common thermoplastic WPCs consisting of either polypropylene (PP) or polyethylene (PE). Cozzani et al. (1995) found that rule of mixtures (ROM) modeling was effective for determining fractional components of refuse derived fuels made from polyethylene and wood based materials. However, Rennecker et al. (2004) noted that thermal degradation of WPCs is significantly affected by the proportion of polyolefins present, such as polypropylene and polyethylene.

This study's primary objective is to evaluate wood degradation as it relates to processing of nylon 12 WPCs. Three specific objectives were defined:

1. Evaluate processing and mechanical properties of nylon 12 WPCs utilizing pre-processed/extruded wood flour (PW).
2. Determine the influence of extruder screw speed on mechanical performance of nylon 12 WPCs.
3. Analyze thermal degradation (TGA) behavior of nylon 12 WPCs.

## **A.2 Materials and Methods**

Nylon 12, OPE629A, and wood flour were sourced and blended according to previous studies (Hatch, 2008). Specific formulations are defined in Table A.1 for each extrusion variation. A Cincinatti Milicron CM 35 extruder consisting of two twin counter-rotating screws was used to produce extruded rectangular specimen (3.7 X 0.95-cm). Extrusion processing temperatures were controlled in 3 barrel zones, 2 die zones, and the screw at 225, 225, 205, 190, 190, and 199°C from barrel to screw, respectively. Screw speeds were maintained at 20 revolutions per minute (rpm), unless specifically stated otherwise (i.e. Table A.1 - 10 rpm). Pre-extruded wood flour (PW) was also produced by extruding dried wood flour at processing temperatures described previously, with a screw speed of 30 rpms. Samples were planed on the two wide faces, conditioned, and then tested in flexure according to ASTM D790 standards. Mechanical testing was performed on a screw driven Instron 4466 Standard with 10 kN electronic load cell.

Thermogravimetric analysis (TGA) was performed to determine the influence of specific processing parameters on fiber and polymer thermal degradation. TGA (Rheometric Scientific STA) 9 to 11 mg samples were heated from 50°C to 600°C at 10°C/min.

## **A.3 Results and Discussion**

Pre-extruded wood flour (PW) produced a composite in which the wood flour had already been subjected to the elevated temperatures required for extrusion of nylon 12. Heat treatment of wood at temperatures above 200°C has been proven to decrease equilibrium moisture content, add dimensional stability, improve decay resistance, and increase durability, but also makes the wood more brittle (Rapp et al., 2001). However, all mechanical properties, including strain to failure, of the final composite were apparently unaffected by this pre-

processing step (Table A.1). Coloration of the composite with PW exhibited a very dark brown/black appearance as opposed to the dark brown appearance of the typical nylon 12/WF composite, signifying material degradation.

Mechanical performance of nylon 12 WPCs indicated a very strong association with extruder screw speed. A reduction in screw speed from 20 rpm to 10 rpm reduced the modulus of rupture (MOE) and strain to failure dramatically from 76.05 to 53.56 MPa and 1.81 to 1.15 %, respectively (Table A.1). No significant effect, however, was observed on modulus of elasticity (MOE) or density.

To gain understanding of nylon 12 WPC thermal degradation during processing conditions, TGA was performed on both individual components and the final nylon 12/ WF extruded composites. The following components were analyzed: pure nylon 12 (N12), wood flour (WF), pre-extruded wood flour (PW), and OPE629A (OPE) (Figure A.1). Several composites formulated with 3% OPE were observed, based on variations in processing characteristics, which included: a standard formulation with a screw speed of 20 rpm (60% WF, 37% N12) (Figures A.1-2), 10 rpm (60% WF, 37% N12), and PW at 20 rpm (60% PW, 37% N12) (Figure A.2).

A simple prediction model based on the ROM approach was performed to predict the standard composite degradation with 60% WF, 37% N12, and 3% OPE (Cozzani et al., 1995). This model uses a weighted sum of the individual components:

$$M_T = C_1m_1 + C_2m_2 + C_3m_3 \quad \text{Eq. A.1}$$

Where  $M_T$  is the total residual mass at any given point in the TGA curve for a composite consisting of three components (1 = WF, 2 = N12, 3 = OPE). The coefficient  $C$  is the residual mass fraction of the respective component at a given temperature and  $m$  is the initial mass for

each component. Two critical assumptions are made in this model: 1) no interaction occurs between components and 2) TGA heating rates for components are equal.

According to my prediction model in Figure A.1, the curves for the respective model and experimental data differ dramatically. A deviation from the critical assumption that no interaction is occurring between the WF and nylon 12 components is a primary factor. Some stability appears to be provided by the nylon 12, delaying the thermal decomposition of the wood fraction within the temperature range of 220 – 400 °C (Figure A.1). Inversely the decomposition of the wood fraction appears to cause premature degradation of the nylon. Similar observations were made by Lu et al. (2007) in compression molded nylon 12/WF composites.

#### **A.4 Conclusions**

Evaluation of extrusion processing influences on nylon 12 WPC has yielded some insight into the processing requirements for these composites. Screw speed had significant influence on material strength and strain. In composites with pre-extruded wood flour, the effect on mechanical properties was negligible, while darker coloration appeared to indicate degradation. TGA analysis, however, provided no indication of thermal degradation of components at required processing temperatures for nylon 12 WPCs. From additional analysis, the thermal degradation of nylon 12 WPCs does not follow from a sum of the components, suggesting interactions between nylon 12 and the wood flour. Although no TGA evidence of thermal degradation at processing temperatures is apparent, additional analysis is suggested to determine possible heat-induced chemical reactions.

## A.5 References

- Cozzani, V., Petarca, L., Tognotti, L., “Devolatilization and pyrolysis of refuse derived fuels: characterization and kinetic modeling by a thermogravimetric and calorimetric approach.” *Fuel*, Vol. 74, No. 6, 1995.
- Hatch, M. C., “Processing of Engineering Polymer Wood-Plastic Composites: Thermoplastic Epoxy Resin (TPER) and Nylon 12.” Masters Thesis, Chapter 2, Washington State Univ., Pullman, WA, August 2008.
- Lu, J.Z., Doyle, T.W., Li, K., “Preparation and Characterization of Wood-(Nylon 12) Composites.” *Journal of Applied Polymer Science*, Vol. 103, 270-276, 2007.
- Rapp, R.O., “Review on heat treatments of wood.” The Federal Research Centre for Forestry and Forest Products, Hamburg, Germany, 2001.
- Rennecker, S., Zink-Sharp, A.G., Ward, T.C., Glasser, W.G., “Compositional Analysis of Thermoplastic Wood Composites by TGA.” *Journal of Applied Polymer Science*, Vol. 93, pp. 1484-1492, 2004.

## A.6 Tables

**Table A.1.** Mechanical properties, density, and processing melt pressures of extruded nylon 12/WF formulations at 10 rpms, 20 rpms, and with pre-processed wood flour.

<b>% Wood</b>	<b>% Nylon 12</b>	<b>% OPE</b>	<b>Sample ID:</b>	<b>Modulus of Rupture [MPa]</b>	<b>Modulus of Elasticity [GPa]</b>	<b>Strain @ Failure [%]</b>	<b>Density [g/cm<sup>3</sup>]</b>	<b>Melt Pressure [psi]</b>
60	37	3	<b>20 RPM</b>	76.05 (7.42)	4.207 (0.228)	1.81 (0.21)	1.154 (0.008)	200
60	37	3	<b>10 RPM</b>	53.56 (6.97)	4.362 (0.307)	1.15 (0.15)	1.139 (0.029)	320
60	37	3	<b>Pre-Processed Wood</b>	74.38 (3.11)	4.361 (0.048)	1.69 (0.13)	1.176 (0.010)	360

## A.7 Figures

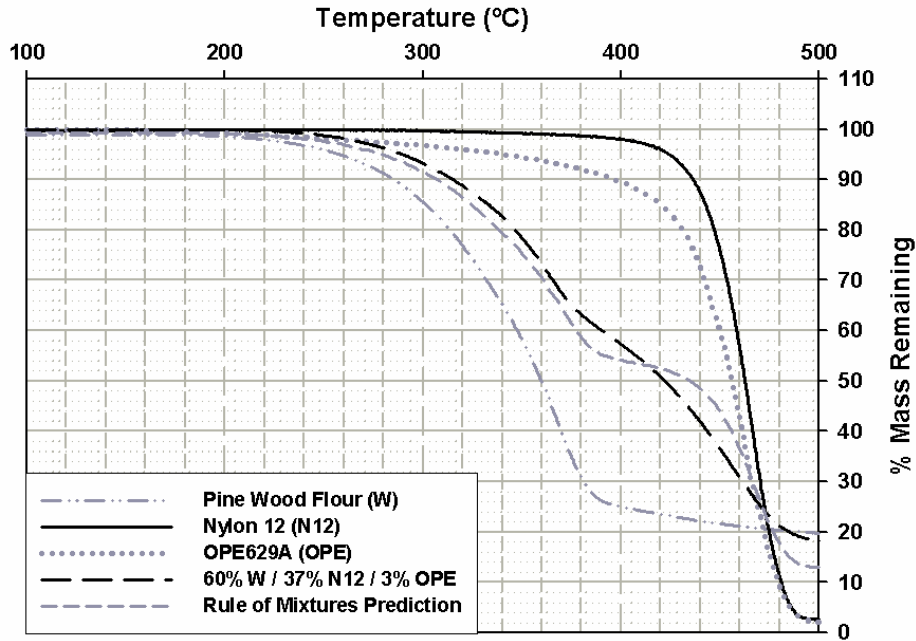


**Figure A.1.** Thermogravimetric curves for nylon 12/WF components, composite, and prediction curve based on rule of mixtures.

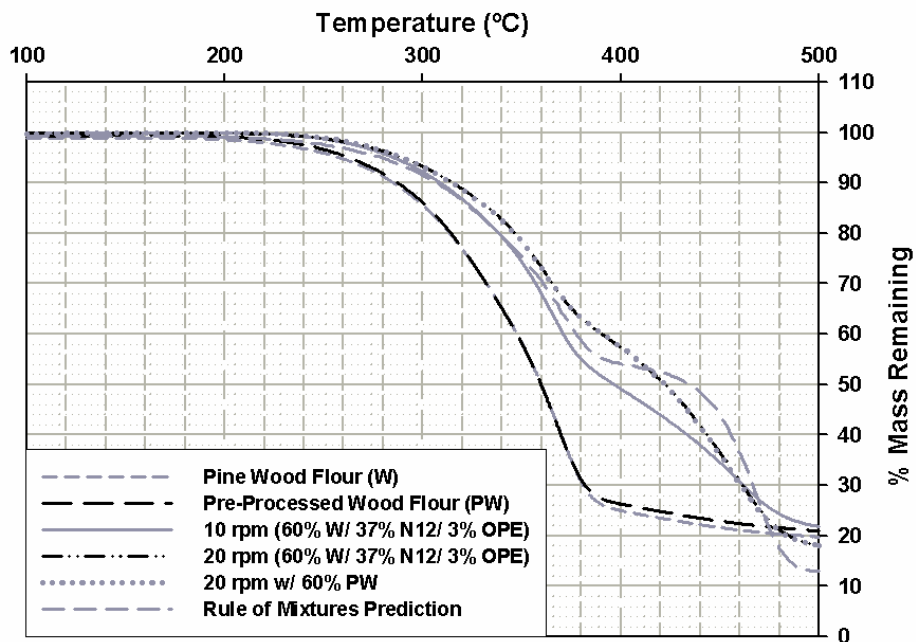


**Figure A.2.** Thermogravimetric curves for nylon 12/WF composites and prediction curve based on rule of mixtures.

## **APPENDIX B – POST EXTRUSION COOLING OF NYLON 12 COMPOSITES**

### **B.1 Introduction**

Processing of extruded wood-plastic composites (WPCs) often concludes with water spray cooling as material exits the extruder die. The importance of cooling rate is often neglected in many WPC studies in which processing temperatures are well below any initiation of wood degradation. However, in nylon 12 WPCs, processing temperatures (max 225°C) are within the onset of wood degradation and volatile formation cited at around 200°C (Hatch, 2008; Saheb and Jog, 1999). This study determines the overall importance of adequate post-extrusion cooling of the composite in regard to mechanical performance of nylon 12 WPCs.

### **B.2 Materials and Methods**

The base formulation for this study consisted of 60% wood flour, 37% nylon 12, and 3% OPE629A, with each material sourced and blended as specified previously (Hatch, 2008). A Cincinatti Milicron CM 35 extruder consisting of two twin counter-rotating screws produced extruded rectangular specimens (3.7 X 0.95-cm). Extrusion processing temperatures were controlled in 3 barrel zones, 2 die zones, and the screw at 225, 225, 205, 190, 190, and 199°C from barrel to screw, respectively. Screw speed was set to 20 revolutions per minute (rpms) and extrudate upon exit was spray cooled 360 degrees with water for 2.44 m. (8 ft.). Samples were planed on the two wide faces, conditioned, and tested in flexure according to ASTM D790 standards. Mechanical testing was performed on a screw driven Instron 4466 Standard with 10 kN electronic load cell.

### **B.3 Results and Discussion**

Standard positioning of the cooling chamber for nylon 12 WPCs is ~0 cm (0 in.) from the extruder die, as observed for this study and others (Hatch, 2008). To evaluate cooling effects on material properties, the position of the cooling chamber from the die was increased from ~0 cm (0 in.) to 7.6 cm (3 in.), and 15.2 cm (6 in.) to obtain three different data sets. Flexure testing of the material showed in Figure C.1 that composite properties were significantly affected by cooling. As cooling was postponed from 0 cm to 15.2 cm, density, modulus of rupture (MOR), and modulus of elasticity (MOE) decreased (Table C.1, Figure C.1). Although this data clearly points to a dependency of composite mechanical properties to density, the cause of this density variation is not yet known. Two possible contributors to density reduction are wood degradation and swell as material exits the extruder die. Further, wood degradation can exacerbate the influence of swell by producing gaseous voids within the composite (Saheb and Jog, 1999).

### **B.4 Conclusions**

Performance of nylon 12 WPCs was significantly influenced by the rate of cooling. Prolonging extrudate water quenching reduced MOR, MOE, and density, while no significant affect was reported for strain to failure. This study indicates the importance of immediate and efficient cooling of nylon 12 WPCs.

### **B.5 References**

- Hatch, M. C., "Processing of Engineering Polymer Wood-Plastic Composites: Thermoplastic Epoxy Resin (TPER) and Nylon 12." Masters Thesis, Chapter 2, Washington State Univ., Pullman, WA, August 2008.
- Saheb, D. N., Jog, J. P., "Natural Fiber Polymer Composites: A Review". *Advanced Polymer Technology*, Vol.18 No. 4: 351-363, 1999.

## B.6 Tables

**Table B.1.** Mechanical properties and density of extruded nylon 12/WF formulations at various distances from extruder die exit to cooling chamber.

% Wood	% Nylon 12	% OPE	Distance to Cooling Chamber [cm]/(in.)	Modulus of Rupture [MPa]	Modulus of Elasticity [GPa]	Strain @ Failure [%]	Density [g/cm <sup>3</sup> ]
60	37	3	0 (0)	65.84 (5.83)	3.905 (0.125)	1.71 (0.2)	1.159 (0.018)
60	37	3	7.6 (3)	57.68 (7.49)	3.493 (0.235)	1.68 (0.18)	1.125 (0.023)
60	37	3	15.2 (6)	50.40 (5.79)	3.200 (0.271)	1.62 (0.21)	1.100 (0.021)

## B.7 Figures

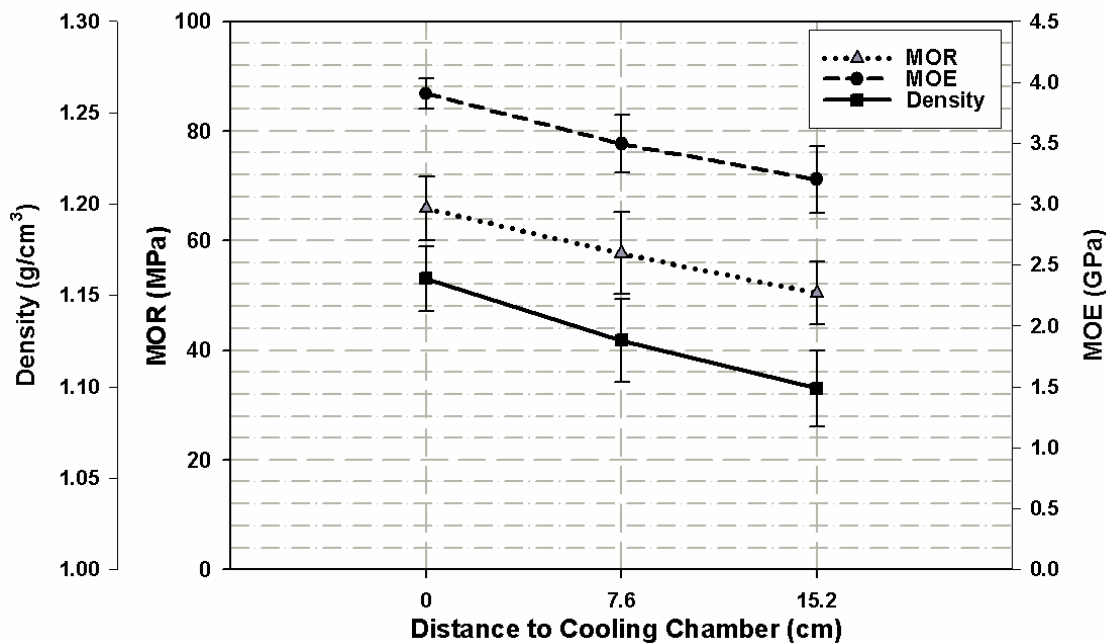


**Figure B.1.** Flexural modulus of rupture and elasticity, and density of nylon 12/WF composite with delayed cooling after die exit: 0, 7.6, and 15.2 cm.

# **APPENDIX C – DYNAMIC MECHANICAL ANALYSIS (DMA) OF THERMOPLASTIC EPOXY RESIN (TPER) COMPOSITES**

## **C.1 Introduction**

The use of thermoplastic epoxy resin (TPER) in wood-plastic composites (WPCs) has shown strong mechanical compatibility with wood flour in previous studies (Hatch, 2008, White et al., 2000). Results of these studies and molecular functionality of both wood flour and TPER has indicated strong adhesion and hydrogen bonding between these two components. This study attempts to determine whether any significant shift in TPER's glass transition ( $T_g \approx \tan \delta \text{ max.}$ ) occurs with increased wood loading, potentially indicating molecular interaction between TPER and wood flour.

## **C.2 Materials and Methods**

WPCs in this study, consisting of TPER, OPE629A, and wood flour, originated from a previous mechanical study of injection molded TPER WPCs (Hatch, 2008). All samples were blended, compounded, processed, and conditioned according to the previous study. Dynamic mechanical analysis (DMA) samples were then milled on a manual milling machine to dimensions of 2 x 4 x 50-mm and analyzed on using a Rheometric Scientific STA II with a dual cantilever configuration. The heating ramp was controlled from 0 to 100°C at a heating rate of 2°C/min.

## **C.3 Results and Discussion**

DMA scans are plotted in Figure B.1 and B.2 for TPER WPCs with wood loadings of 0, 20, and 40% each, containing 2% OPE629A as a lubricant. In addition, pure 100% TPER was

also analyzed for comparison. As evident in both figures, the storage modulus ( $E'$ ) and loss modulus ( $E''$ ) increases with increasing wood content. Surprisingly, 2% OPE629A appears to significantly reduce the peak dampening ( $\tan \delta$ ) or glass transition ( $T_g$ ) temperature of TPER from 80.5°C to 79.5°C. However, the addition of 20% and 40% wood flour raise  $T_g$  to roughly 82°C. Fluctuations in  $T_g$  could possibly indicate interaction between TPER, OPE629A, and wood flour components.

#### **C.4 Conclusions**

Analysis of thermal transitions in TPER WPCs indicated only a slight shift in  $T_g$  of TPER. Increases were clearly evident in both  $E'$  and  $E''$  with increasing wood flour content. It is not clear whether changes in  $T_g$  are indicative of molecular and mechanical performance characteristics of TPER WPCs.

#### **C.5 References**

- Hatch, M. C., "Processing of Engineering Polymer Wood-Plastic Composites: Thermoplastic Epoxy Resin (TPER) and Nylon 12." Masters Thesis, Chapter 2, Washington State Univ., Pullman, WA, August 2008.
- White, J. E., Silvis, H. C., Winkler, M.S., Glass, T. W., Kirkpatrick, D. E., "Poly(hydroxyaminoethers): A New Family of Epoxy-Based Thermoplastics". Journal of Advanced Materials, Vol.12, No. 23, pp. 1791-1800, 2000.

C.6 Figures

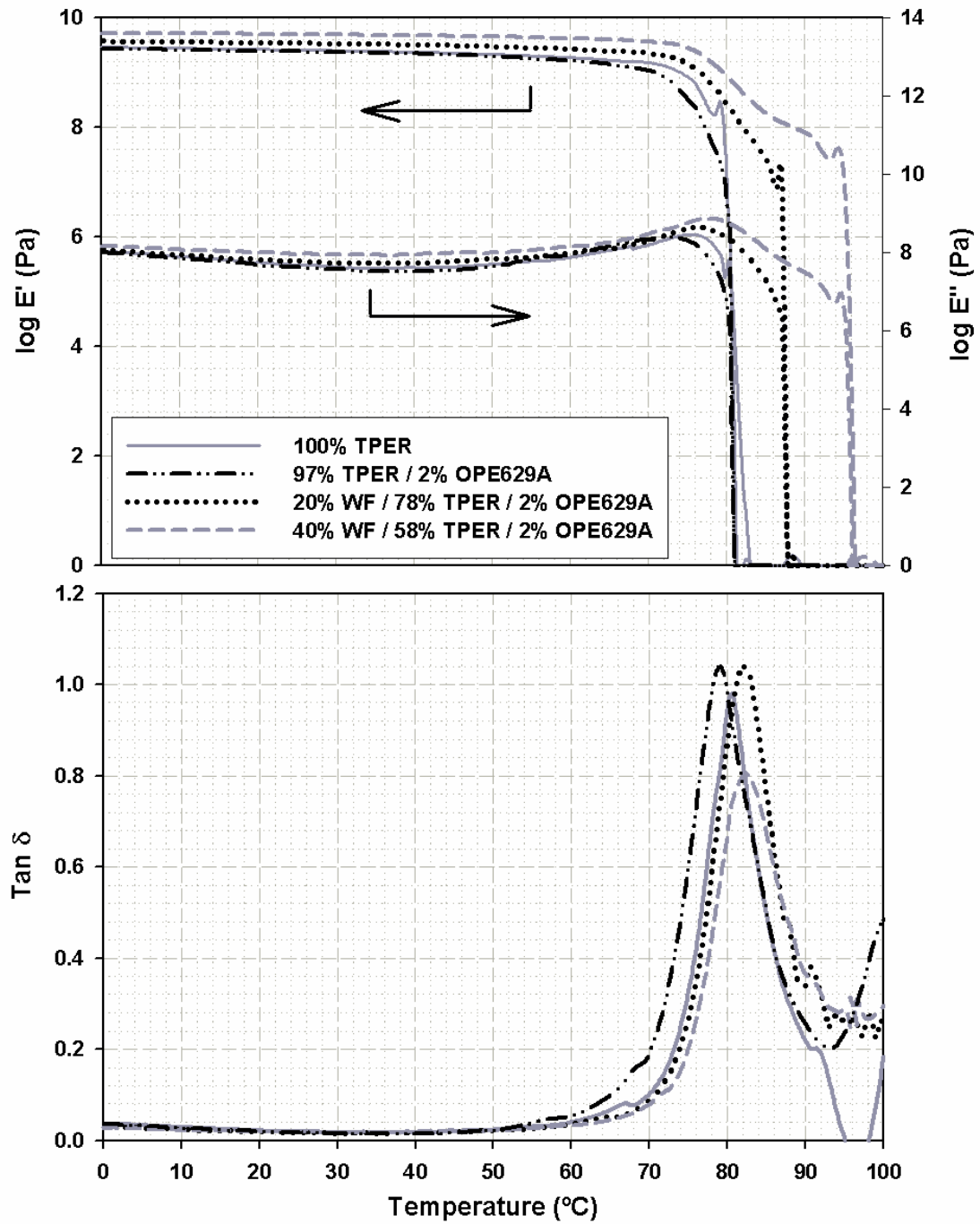


**Figure C.1.** Log E', log E'', and tan  $\delta$  from dynamic mechanical analysis (DMA) of TPER WPCs.

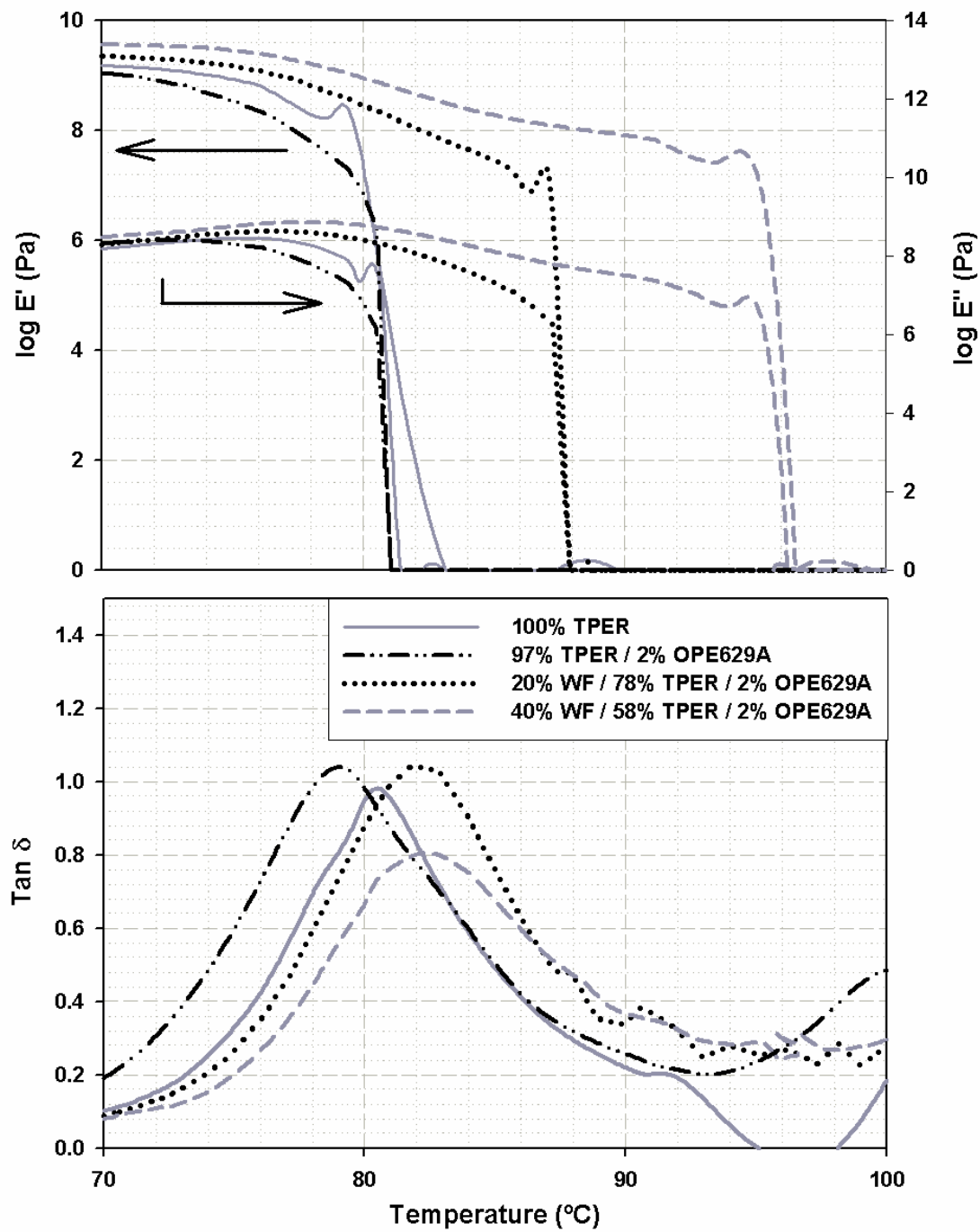


**Figure C.2.**  $\log E'$ ,  $\log E''$ , and  $\tan \delta$  from dynamic mechanical analysis (DMA) of TPER WPCs.

## **APPENDIX D – PHASE TRANSITION BEHAVIOR OF NYLON 12 COMPOSITES**

### **D.1 Introduction**

Nylon 12 wood-plastic composites (WPCs) have been shown to exhibit superior strength to common thermoplastics (Hatch, 2008; Lu et al., 2008). Lu et al. (2007) proposed that the excellent performance of these WPCs was due to an increase in nylon crystallinity. However, no research explains the influence of potential molecular interactions between both nylon 12 and wood flour components. This study evaluates the thermal behavior of nylon 12 in a WPC system.

### **D.2 Materials and Methods**

WPCs in this study consisted of nylon 12, OPE629A (OPE), and wood flour, and originated from a previous mechanical study of injection molded nylon 12 WPCs (Hatch, 2008). All samples were blended, compounded, and processed according to that study. Prior to differential scanning calorimetry (DSC) testing to determine thermal properties, samples were conditioned in an oven for 24 hours at 100°C. DSC (Metler Toledo, DSC 822e) scans were then performed on 4 to 6 mg samples heated from -30°C to 200°C at 20°C/min in hermetically sealed 40- $\mu$ l aluminum crucibles.

### **D.3 Results and Discussion**

The composition and thermal properties of nylon WPC samples tested are shown in Table D.1. It was observed that 60% wood flour reduced the nylon crystallization temperature ( $T_c$ ) from 147.3°C to 143.4°C (Figure D.1). No significant variation in  $\Delta H_c$  or  $\Delta H_m$  was apparent between each WPC. Only a slight reduction in nylon melt temperature ( $T_m$ ) of approximately

one degree was exhibited (Table D.1 & Figure D.2). Therefore, wood fiber does appear to influence the thermal properties of nylon 12.

#### D.4 Conclusions

Nylon 12 thermal properties in nylon 12 WPCs relate to the wood content of the composite. Crystallization and melt temperatures were reduced as wood content was increased. Further investigation is needed to determine the contribution to composite performance.

#### D.5 References

- Hatch, M. C., "Processing of Engineering Polymer Wood-Plastic Composites: Thermoplastic Epoxy Resin (TPER) and Nylon 12." Masters Thesis, Chapter 2, Washington State Univ., Pullman, WA, August 2008.
- Lu, J.Z., Doyle, T.W., Li, K., "Preparation and Characterization of Wood-(Nylon 12) Composites." Journal of Applied Polymer Science, Vol. 103, 270-276, 2007.

#### D.6 Tables

**Table D.1.** Thermal Properties of nylon 12 and nylon 12/WF composites. Heat is measured in J/g of nylon 12.

% Wood	% Nylon 12	% OPE	Melt		Crystallization	
			$T_m$ (°C)	$\Delta H_m$ (J/g)	$T_c$ (°C)	$\Delta H_c$ (J/g)
0	100	0	176.5	40.44	147.3	47.39
0	97	3	176.4	43.13	149.3	51.51
30	67	3	175.5	44.38	146.3	50.04
60	37	3	175.3	42.08	143.4	48.04

## D.7 Figures

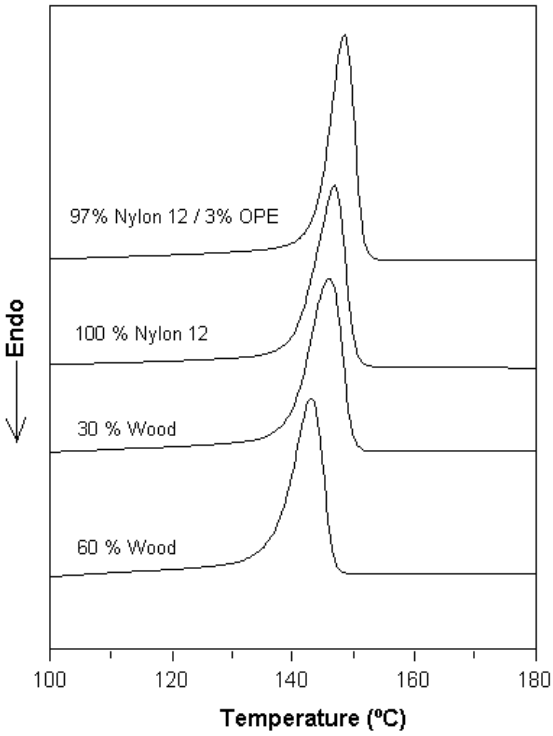


**Figure D.1.** DSC thermograph of cooling for nylon 12 WPCs. Heat is measured in J/g of nylon 12.

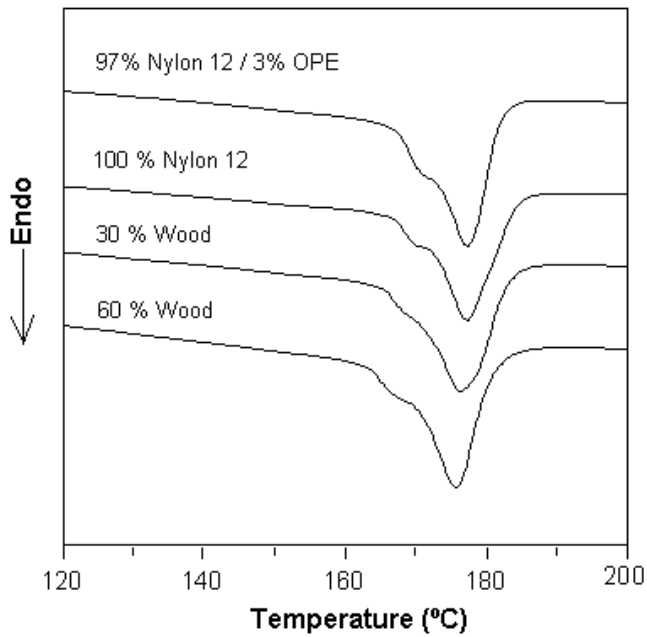


**Figure D.2.** DSC thermograph of second heating for nylon 12 WPCs. Heat is measured in J/g of nylon 12.

## APPENDIX E – DERIVATION OF DOUBLE SHEAR LAG (DSL) MODEL

### E.1 Derivation

The double shear lag (DSL) theory originates from analysis derived based on traditional shear lag theory first proposed by Cox et al. (1952). The following derivation is based closely to a previous derivation of Cox's shear lag theory by Facca (2006). Most assumptions in the derivation remain unchanged. However, two corrections are introduced to account for an additional inner fiber shear surface ( $r_i$ ) and the inclusion of tension at the fiber ends. The initial assumption is that the total shear stresses at any given radius ( $z$ ) from the center of the fiber are equivalent to shear stresses at the fibers inner (i) or outer (o) radius:

$$2 \cdot \pi \cdot z \cdot \tau \cdot dx = 2 \cdot \pi \cdot r_{(i,o)} \cdot \tau_{(i,o)} \cdot dx \quad \text{Eq. E.1}$$

Eliminating  $2\pi dx$  and solving for the shear stress ( $\tau$ ) at any given distance ( $z$ ) yields:

$$\tau = \frac{r_{(i,o)} \cdot \tau_{(i,o)}}{z} \quad \text{Eq. E.2}$$

Next, by relating the shear strain ( $dw/dz$ ) to the shear stress ( $\tau$ ) using the matrix shear modulus ( $G_M$ ), we obtain:

$$\frac{dw}{dz} = \frac{\tau}{G_M} = \frac{r_{(i,o)} \cdot \tau_{(i,o)}}{z \cdot G_M} \quad \text{Eq. E.3}$$

Integration of Eq. E.3 over the shear displacement  $d_R$  and  $d_F$  at radii of  $r$  and  $R$  (Figure

4.1) in the composite provides:

$$\int_{d_F}^{d_R} 1 \, dw = \frac{r_{(i,o)} \cdot \tau_{(i,o)}}{G_M} \cdot \int_r^R \frac{1}{z} \, dz \quad \text{Eq. E.4}$$

$$d_R - d_F = \frac{r_{(i,o)} \cdot \tau_{(i,o)}}{G_M} \cdot \ln\left(\frac{R}{r}\right) \quad \text{Eq. E.5}$$

Thus, it can be assumed that Eq. E.5 ( $d_R - d_F$ ) for both (i) and (o) are equivalent from Eq. E.2 given by:

$$r_i \cdot \tau_i = r_o \cdot \tau_o \quad \text{Eq. E.6}$$

In addition, Eq. E.5 can be further modified by making the common substitution of  $0.5 \ln(P_F/V_f)$  for  $\ln(R/r)$  to account for fiber packing interactions ( $P_F$ ) and volume fraction ( $V_f$ ) within the composite (Facca, 2006). If radius  $R$  is assumed to be much larger than radii  $r_i$  and  $r_o$ , then it can be assumed the ratio  $R/r_i \approx R/r_o$ . Based on these assumptions,  $\ln(R/r)$  is given by:

$$\ln\left(\frac{R}{r_i}\right) = \ln\left(\frac{R}{r_o}\right) = 0.5 \cdot \ln\left(\frac{P_F}{V_f}\right) \quad \text{Eq. E.7}$$

If we consider that the normal tensile stresses ( $\sigma_f$ ) along the fiber at position ( $x$ ) are induced by shear stresses contributed by two shear planes (i and o) with shears ( $\tau_i$ ,  $\tau_o$ ), and radius ( $r_i$ ,  $r_o$ ) then:

$$\frac{d}{dx} \sigma_f = \frac{-2 \cdot \tau_i}{R_i} + \frac{-2 \cdot \tau_o}{R_o} = \frac{-2 \cdot (d_R - d_F) \cdot G_M}{r_i^2 \cdot \ln\left(\frac{R}{r_i}\right)} + \frac{-2 \cdot (d_R - d_F) \cdot G_M}{r_o^2 \cdot \ln\left(\frac{R}{r_o}\right)} = \left(\frac{1}{r_i^2} + \frac{1}{r_o^2}\right) \cdot \frac{-4 \cdot (d_R - d_F) \cdot G_M}{\ln\left(\frac{P_F}{V_f}\right)} \quad \text{Eq. E.8}$$

From the common isotropic relation  $G_m = E_m/2(1+\mu_m)$ , where  $\mu_m$  gives the Poisson's ratio, Eq. E.8 converts to:

$$\frac{d}{dx}\sigma_f = \left( \frac{1}{r_i^2} + \frac{1}{r_o^2} \right) \cdot \frac{-2 \cdot (d_R - d_F) \cdot E_m}{\ln\left(\frac{P_F}{V_f}\right)(1 + \mu_m)} \quad \text{Eq. E.9}$$

Utilizing Hooke's law displacement and strain ( $\varepsilon$ ) are related for the matrix (m) and fibre (f) by:

$$\frac{dd_F}{dx} = \frac{\sigma_f}{E_f} = \varepsilon_f \quad \text{Eq. E.10}$$

$$\frac{dd_R}{dx} = \frac{\sigma_m}{E_m} = \varepsilon_m = \varepsilon_c \quad \text{Eq. E.11}$$

Substitution of strain terms ( $dd_F/dx$ ) and ( $dd_R/dx$ ) for ( $d_R$ ) and ( $d_F$ ) in Eq. E.9 provides:

$$\frac{d\sigma_f^2}{d^2x} = \left( \frac{1}{r_i^2} + \frac{1}{r_o^2} \right) \cdot \frac{-2 \cdot \left( \frac{dd_R}{dx} - \frac{dd_F}{dx} \right) \cdot E_m}{\ln\left(\frac{P_F}{V_f}\right)(1 + \mu_m)} = \left( \frac{1}{r_i^2} + \frac{1}{r_o^2} \right) \cdot \frac{-2 \cdot \left( \varepsilon_c - \frac{\sigma_f}{E_f} \right) \cdot E_m}{\ln\left(\frac{P_F}{V_f}\right)(1 + \mu_m)} = \left( \frac{1}{r_i^2} + \frac{1}{r_o^2} \right) \cdot \frac{-2 \cdot \left( \frac{-\varepsilon_c \cdot E_f + \sigma_f}{E_f} \right) \cdot E_m}{\ln\left(\frac{P_F}{V_f}\right)(1 + \mu_m)} \quad \text{Eq. E.12}$$

By integration of Eq. E.12 the following solution is developed for the variation of stress with respect to position (x) along the fiber:

$$\sigma_f = E_f \varepsilon_c + R \cdot \sinh(\beta_{i+o} \cdot x) + S \cdot \cosh(\beta_{i+o} \cdot x) \quad \text{Eq. E.13}$$

where:

$$\beta_{i+o} = \left[ \left( \frac{1}{r_i^2} + \frac{1}{r_o^2} \right) \cdot \frac{2 \cdot E_m}{E_f (1 + \mu_m) \cdot \ln \left( \frac{P_F}{V_f} \right)} \right]^{\frac{1}{2}} \quad \text{Eq. E.14}$$

The standard derivation to determine the constants of integration, R and S, for Cox's shear lag theory assumes that the tensile stresses at the fiber ends are equal to zero. ( $\sigma_f = 0$  at  $x = \pm L/2$ ). Nardone and Prewo (1986), however, considered tension stresses in the fiber ends to equal composite stress,  $\sigma_c$ . Incorporation of the boundary conditions,  $\sigma_f = \sigma_c$  at  $x = \pm L/2$ ) into Eq. E.13 gives two equations with two unknowns which yields the solution:

$$R = 0 \quad S = \frac{\sigma_c - E_f \varepsilon_c}{\cosh \left[ (\beta_{i+o}) \cdot \frac{L}{2} \right]} \quad \text{Eq. E.15}$$

Solving Eq. E.13 with solutions for R and S provides:

$$\sigma_f = E_f \varepsilon_c + (\sigma_c - E_f \varepsilon_c) \cdot \left[ \frac{\cosh \left[ (\beta_{i+o}) \cdot x \right]}{\cosh \left[ \frac{(\beta_{i+o}) \cdot L}{2} \right]} \right] = E_f \varepsilon_c \cdot \left[ 1 + \left( \frac{\sigma_c}{E_f \varepsilon_c} - 1 \right) \cdot \frac{\cosh \left[ (\beta_{i+o}) \cdot x \right]}{\cosh \left[ \frac{(\beta_{i+o}) \cdot L}{2} \right]} \right] \quad \text{Eq. E.16}$$

To determine the average fiber stress ( $\sigma_{f,avg}$ ), integration over half the fiber length is necessary, since the stress distribution is symmetric from  $x = 0 \rightarrow \pm L/2$  (Figure 4.1).

$$\sigma_{f,avg} = \frac{E_f \varepsilon_c}{\frac{L}{2}} \cdot \int_0^{\frac{L}{2}} \left[ 1 + \left( \frac{\sigma_c}{E_f \varepsilon_c} - 1 \right) \cdot \frac{\cosh \left[ (\beta_{i+o}) \cdot x \right]}{\cosh \left[ \frac{(\beta_{i+o}) \cdot L}{2} \right]} \right] dx = E_f \varepsilon_c \cdot \left[ 1 + \left( \frac{E_f}{E_f} - 1 \right) \cdot \frac{\tanh \left[ (\beta_{i+o}) \cdot \frac{L}{2} \right]}{\frac{(\beta_{i+o}) \cdot L}{2}} \right] \quad \text{Eq. E.17}$$

where:

$$\sigma_c = \sigma_m = E_m \cdot \varepsilon_c$$

Next, the relationship for stress to strain of the composite can be calculated by substituting Eq. E.17 into the following equation, based on the rule of mixtures (ROM).

$$\sigma_c = E_f \varepsilon_c \left[ 1 + \left( \frac{E_m}{E_f} - 1 \right) \cdot \frac{\tanh\left[\frac{(\beta_{i+o}) \cdot L}{2}\right]}{\frac{(\beta_{i+o}) \cdot L}{2}} \right] \cdot V_f + E_m \cdot \varepsilon_c \cdot V_m \quad \text{Eq. E.18}$$

Assuming an elastic response of the composite system ( $\sigma_c = E_c \cdot \varepsilon_c$ ), Eq. E.18 is reduced to the final formal of the DSL model:

$$E_c = E_f \left[ 1 + \left( \frac{E_m}{E_f} - 1 \right) \cdot \frac{\tanh\left[\frac{(\beta_{i+o}) \cdot L}{2}\right]}{\frac{(\beta_{i+o}) \cdot L}{2}} \right] \cdot V_f + E_m \cdot V_m \quad \text{Eq. E.19}$$

It is important to note that Eq. E.19 follows a similar form to that derived by Zhao and Ji (1997); however, the derived  $\beta$  is different. To solve for the composite modulus, substitute,  $\beta_{i+o}$ , from eq. E.14 into eq. E.19.

## E.2 References

- Cox, H.L., "The elasticity and strength of paper and other fibrous materials." *British Journal of Applied Physics*, Vol. 3, pp. 72-79, 1952.
- Facca, A.G., "Predicting Tensile Strength and Modulus of Single and Hybrid Natural Fibre Reinforced Thermoplastic Composites." *Doctoral Thesis, University of Toronto, Toronto, Canada, 2006.*
- Hatch, M. C., "Application of Elasticity Shear-Lag Models to Wood-Plastic Composites." *Masters Thesis, Chpt. 4, Washington State Univ., Pullman, WA, August 2008.*
- Nardone, V.C., Prewo, K.M., "The Strength of Discontinuous Silicon Carbide Reinforced Aluminum Composites." *Scripta Metallurgica*, Vol. 20, pp. 43-48, 1986.
- Zhao, P., Ji, S., "Refinements of shear-lag model and its applications." *Tectonophysics*, Vol. 279, pp 37-53, 1997.